CERGE - EI
Center for Economic Research and Graduate Education –
Economics Institute

Essays in Energy Economics

Dali Tsintskiladze Laxton

Dissertation

Prague 2025

Dissertation Committee:
Krešimir Žigić (CERGE-EI, Chair)
Milan Ščasný (Charles University Environment Centre)
Randall K. Filer (The City University of New York)
Silvester van Koten (CERGE-EI)

Referees:
Karel Janda (Prague University of Economics and Business)
David Vavra (OGResearch)

Table of Contents

Acknowledgements

I would like to express my deepest gratitude to Prof. Krešimir Žigić for his kind and unwavering support. He treated my dissertation with great seriousness even during challenging personal times, and I sincerely wish him health and happiness in the years to come.

I thank Prof. Randall Filer for consistently supporting and encouraging me through many of the milestones inherent to completing a PhD. I am also very thankful to his wife, Barbara Forbes, whose kindness and empathy made me feel like she was looking after me as if I were her own daughter, a gesture that meant a great deal to me.

I am also very grateful to Prof. Byeongju Jeong, whose demanding yet flexible mentorship was invaluable at the beginning of my doctoral journey. Despite his high expectations, I could always reach out to him at any hour with questions or concerns, and I deeply appreciated our diverse conversations beyond the thesis that nourished my intellectual curiosity.

I extend my thanks to Milan Ščasný, one of my co-authors and a generous mentor who supported me through a difficult period by offering employment that allowed me to continue to focus on energy and environmental research. This continuity has helped make the transition from PhD work to my future path both smooth and meaningful.

My special thanks go to Silvester van Koten for generously sharing a grant that supported one of my chapters, which was crucial for the completion of this work. Through teaching and collaborative work, he significantly deepened my understanding of energy economics. His support, both practical and intellectual, has been instrumental in shaping my development as an energy economist.

I would also like to thank ISET (International School of Economics at Tbilisi State University), without which I would not have had the opportunity to come to the Czech Republic. It was there that I first discovered my passion for energy economics and was inspired to pursue it as my area of expertise. Their rigorous training and mentorship laid the essential foundations for everything that followed.

I am deeply grateful to my dissertation referees, Prof. Karel Janda and David Vavra, for their kind and constructive feedback. My thanks also go to the CERGE-EI Academic Skills Center and the broader CERGE-EI community for building a family-like environment where support and care were always present.

To my husband, Jared Laxton, without whom I might never have finished this PhD, in particular, the third chapter would not exist without his patience and support. He generously gave me the space and time necessary to make progress, and his steady presence made all the difference.

I owe immense gratitude to my mother, Manana Sirabidze, who pushed me to seize the opportunity to study in the Czech Republic. Though she believed I had already achieved enough education and hoped I would remain in Georgia, she pragmatically convinced me that this chance was rare and not to be missed. Most of my major academic paths were paved by her persistent, clear-headed encouragement.

Finally, my daughters deserve my heartfelt thanks. There were moments when I seriously considered quitting, not because I am a quitter, but because the PhD journey pushes one's

limits and can feel overwhelming. They changed everything. For a mother of young children wanting to be present as much as possible, the flexibility that academia offers was a lifeline. Their presence helped me alleviate anxiety and focus on what truly matters. Through them, I learned to manage my time better, to value every moment, and to find deeper meaning and joy in both my life and work.

All remaining errors are my own.

Prague, Czech Republic — Dali Tsintskiladze Laxton

November, 2025

Abstract

This dissertation explores strategies to support a sustainable energy transition, focusing on the economic, technological, and ecological challenges of decarbonization. While fossil fuels remain cheaper in the short term, renewable energy technologies offer long-term advantages through lower emissions and innovation-driven cost reductions. The three chapters provide complementary insights from technological, system-level, and macroeconomic perspectives. The first paper introduces a new engineering-based method to measure innovation in wind energy. It isolates material-based costs to assess learning over time. It shows that onshore wind may become cost-competitive without subsidies under continued technological progress. The second paper examines the role of biomass in decarbonization using a spatially disaggregated TIMES-CZ model. It incorporates ecological constraints, including bark beetle infestations, to evaluate biomass availability and identify the least-cost renewable energy pathways for the Czech Republic. The third paper analyzes the macroeconomic implications of oil price shocks, emphasizing the need for expert-level thinking when interpreting market dynamics. Despite a growing shift to cleaner energy, oil remains crucial, and its price fluctuations continue to have significant macroeconomic impacts. A realistic approach is needed to navigate the complexities of oil price dynamics and their broader economic consequences. Together, the papers offer practical tools and insights for designing resilient, innovation-focused energy policies that are aligned with climate goals.

Introduction

The path toward a sustainable energy future requires navigating a complex trade-off between the desire for economic development and the necessity to decarbonize. This tension is particularly evident in decisions involving energy production: while fossil fuels are typically cheaper and more readily deployable, renewable energy technologies offer long-term benefits through lower carbon emissions and potential for cost reductions via innovation. In practice, policymakers must simultaneously consider energy independence, energy security, and environmental sustainability: an analytical space too vast for any single thesis to fully address. This dissertation contributes to this effort by examining a range of strategies, including innovation measurement, system optimization, and macroeconomic risk analysis, that can support decarbonization, especially within the real-world constraints faced by both renewable and conventional energy sources.

What binds the three papers in this dissertation is a common objective: to improve our understanding of the variables and trade-offs that must be considered to guide effective and feasible decarbonization strategies. While much of the academic literature tends to treat energy technologies in isolation or assume away difficult structural constraints, this research attempts to offer more grounded, transparent, and practically implementable tools and perspectives. Each chapter contributes a different lens: technological, systems-level, and macroeconomic, through which to examine energy transition strategies, and together they form a comprehensive picture of the analytical support needed for a sustainable energy future.

The first chapter focuses on onshore wind technology and aims to derive a clearer, more accurate measure of innovation. While renewable technologies often receive support due to their low carbon footprint, a common criticism is that they remain uncompetitive without subsidies. This paper investigates the learning potential of wind energy technology and proposes a novel strategy for measuring it. Using a bottom-up engineering-based approach, it constructs a time series of unit production costs for US wind turbines from 1998 to 2017, where the costs are derived exclusively from material inputs and turbine specifications, excluding confounding variables such as fluctuations in interest rates, wind speed, and exchange rates. By isolating cost reductions due purely to technological improvements, the paper offers a more robust metric for assessing innovation over time. The results strengthen the case that wind technology can become competitive with conventional energy sources, reinforcing the potential for subsidy-free deployment under the right conditions. The methodological care taken in constructing this innovation measure is the paper's core contribution. The paper also delves into the details of how greater penetration of intermittent renewable energy resources, such as wind, may become problematic from a system-wide perspective, and how it could affect so-called integration costs.

The second chapter shifts attention to another net-zero carbon fuel, biomass, which plays a dominant role in the renewable energy mix of many countries, including the Czech Republic. This chapter uses a spatially enriched energy system optimization model (TIMES-CZ) to evaluate the role of forest biomass in supporting long-term climate targets. A distinguishing feature of the paper is its integration of ecological risks, particularly the widespread bark beetle infestation affecting Czech forests, into the assessment of biomass availability and

cost. By modelling regional biomass potentials under several forest development scenarios, and exploring the implications of subsidies and ecological constraints, the paper identifies least-cost pathways to decarbonization. It reveals that while biomass can remain a reliable component of the energy mix, relying on it too heavily, especially under ecological stress, can raise system-wide costs and risk falling short of EU renewable energy targets. The study thus contributes both methodologically and substantively to the design of realistic, regionally grounded energy policies.

In the third chapter, the focus turns to a non-renewable energy resource: oil. Despite international commitments to climate goals, oil remains a foundational energy source in the global economy. The motivation for this paper stems from a critical gap in macroeconomic analysis among prominent institutions that publish oil price forecasts, such as the Energy Information Administration (EIA). Specifically, these forecasts often overlook the underlying demand and supply fundamentals that drive oil prices. Central banks, which typically base their macroeconomic projections on EIA forecasts, therefore inherit this same limitation, relying on projections that are not grounded in a structural understanding of the oil market. We, therefore, introduce **OILMOD**, a semi-structural model of the oil market that captures both demand- and supply-side dynamics, with emphasis on OPEC spare capacity. Using OILMOD, we generate oil price scenarios and embed a high oil price trajectory into a monetary policy model (ENDOCRED) to examine the trade-offs that monetary policymakers face in a post-COVID inflationary environment. In such a setting, inflation expectations may no longer be well anchored if the global economy were to experience another major supply shock. The results highlight the danger of overreliance on third-party institutions for such a critical variable as oil prices and urge central banks to undertake more in-house analysis. This would enable them to develop more robust, forward-looking strategies for managing the output-inflation trade-off under a stagflationary scenario.

Together, these three papers offer a layered approach to supporting the energy transition: from identifying innovation trajectories and planning resilient, cost-effective systems, to managing the macroeconomic risks of remaining fossil dependencies. While the global shift away from carbon-intensive energy will not occur overnight, and no clean technology is without trade-offs, this dissertation argues that better data, more realistic models, and nuanced risk assessments can significantly enhance our ability to chart a sustainable and economically viable energy future.

Chapter 1

Innovations in the Wind Energy Sector

The original version of this paper was published as a working paper by CERGE-EI.[1] *An updated version, reflecting revisions made during the peer-review process, was later published in the Journal of Energy Engineering.*[2]

1.1 Introduction

Technological innovations can reduce the costs of electricity production in the wind energy sector. Despite the achieved reduction in costs, many producers still receive subsidies to allow them to compete with conventional power producers. Understanding the drivers of technological innovation is a first step towards constructing effective policies to accelerate the innovation process to an extent that the subsidies are no longer required. However, we cannot fully understand the drivers of innovation without an accurate measure of innovation itself. This paper focuses on generating a more accurate innovation measure for wind energy technologies, which the current literature does not provide. We illustrate the importance of our data by conducting a learning curve analysis - a widely applied method in the energy literature to predict reductions in the costs of electricity production.

Innovation in this paper refers to any type of wind turbine modification which produces electricity at a lower cost than its predecessor. If we directly use production cost reductions as the measure for innovation, we will obtain biased results because production costs can also change due to factors unrelated to technological innovation, such as interest rates, material prices, exchange rates, and wind speed fluctuations.

In order to derive an accurate measure of innovation, we apply an engineering model (Malcolm & Hansen, 2002; Poore & Lettenmaier, 2000-2002) and estimate the cost of the wind electricity

[1] Laxton, D. T. (2019). *Innovations in the Wind Energy Sector* (CERGE-EI Working Paper No. 647). Charles University – CERGE-EI. Retrieved from https://www.cerge-ei.cz/pdf/wp/Wp647.pdf

[2] Laxton, D. T. (2023). Novel Measure of Innovation: Application to the Onshore Wind Energy Sector in the US. *Journal of Energy Engineering*, *149*(2), 04023002. https://doi.org/10.1061/(ASCE)EY.1943-7897.0000838

production of wind turbines installed each year in the US from 1998 to 2017. The engineering model calculates the costs of electricity production based on the engineering properties of installed turbines, their material composition and the corresponding material prices in the selected year. This approach can effectively exclude from the estimated production cost the factors unrelated to technological innovation, such as interest rate, material price and exchange rate fluctuations. This is the major motivation for using the engineering model in this paper. We refer to our production cost data as an "innovation measure" or levelized engineering cost of energy ($LECOE$) series.

We illustrate the usefulness of our measure of innovation by conducting a learning curve analysis. A learning curve measures the correlation between the deployment of wind technology and electricity production cost reduction. Using our levelized engineering cost of energy measure delivers an improved fit of the learning curve in comparison to alternative data. This is crucial as the learning curve is a popular tool in the energy literature to measure technological innovation. In addition, learning rates are frequently used in other electricity market modelling practices, which influence policy decisions. Therefore, learning rates inferred from improved data should be more reliable for informing successful policies.

The paper is organized in the following way: section 1.2 describes the process of generating our innovation data for wind technology in the US and compares it with other studies; section 1.3 summarizes and analyzes wind technology support policies in the US; section 1.4 evaluates these policies in the context of learning curve literature, and section 1.5 concludes.

1.2 Measuring Innovation in Wind Energy Technologies

1.2.1 Defining the Levelized Cost of Energy ($LCOE$)

Technological innovations are reflected in cost reductions in energy production. Other, non-innovative factors may also contribute, and we aim to eliminate these. To describe how we accomplish this, it is helpful to define the terminologies used in the study. In this section, we define the components of production cost.

Traditionally, the production cost of electricity is assessed using the levelized cost of energy ($LCOE$) (e.g., McKenna, Hollnaicher, & Fichtner, 2014). $LCOE$ includes all capital and operating costs throughout the useful life of a wind turbine. A simple formula for calculating $LCOE$ is the following (Ramadhan & Naseeb, 2011):

$$LCOE = \frac{CRF \times CapEx + O\&M}{AEP} \tag{1.1}$$

Capital Cost ($CapEx$). Capital cost includes: (i) the cost of a turbine, (ii) the balance of system cost (BOS), which includes development costs of the wind farm, permits, engineering and management, roads for site access, foundation, transportation, assembly, installation and electrical infrastructure costs. Investment costs are expressed in \$/MW, where MW measures the turbine capacity. Turbine capacity is the maximum amount of electricity that a particular wind turbine can generate in an hour. Generated electricity depends on the wind

speed. The maximum amount can be reached above some threshold wind speed. We denote the capital cost of a turbine as $CapEx$ and

$$CapEx = \frac{\text{Turbine Cost} + BOS}{\text{Turbine Capacity}} \tag{1.2}$$

Capital Recovery Factor *(CRF).* We can represent capital cost as a discounted sum of annual fixed payments throughout a wind turbine's useful life. These fixed payments, or the rental rate of capital, are a product of capital cost and a capital recovery factor (CRF), where CRF equals $\frac{i(1+i)^n}{(1+i)^n-1}$ (Chabot & Saulnier, 2001). In this formula, n is the expected useful life of a turbine and i is the discount rate. The rental rate is measured in \$/MW/year.

Operations and Maintenance Costs *(O&M).* Operations and maintenance costs (O&M) include replacement of wind turbine components, insurance, land lease and all other costs that occur from the time the wind farm starts operation. Some of these costs are fixed each year and do not depend on the amount of electricity produced, and some are variable. However, for convenience, we convert this cost to \$/MW/year.

Annual Energy Production *(AEP).* Wind turbines can reach maximum turbine capacity at a certain wind speed. However, wind speed varies throughout a day, at various seasons and across geographic locations. In fact, wind turbines rarely produce at their maximum capacity. Therefore, in order to calculate the production costs of a unit of electricity, we need to know the electricity production per MW of turbine capacity per year. The unit of measurement is MWh/MW/year, which can be phrased as effective hours in operation annually.

1.2.2 Identifying Gaps in the Literature

Before describing the process used to generate our measure of innovation, we explain why we did not rely on measurements from prior studies. Firstly, the vast majority of papers on innovation in wind energy technology (e.g., Hayward & Graham, 2013; Grafström & Lindman, 2017; Yu, Li, Che, & Zheng, 2017; Huenteler, Schmidt, Ossenbrink, & Hoffmann, 2016; Wiebe & Lutz, 2016) use changes in average capital expenditures or average turbine price per unit capacity as the measure of innovation. Using only capital expenditures in the literature may be a result of a lack of production cost data. This approach is problematic because, as turbines become larger, capital expenditures per unit capacity may rise[3]. Considering only capital expenditures as the measure of innovation in this case would suggest technological decay. However, as turbines become taller, effective hours in operation also increase, and this may compensate for rises in the capital costs.

Another problem is that the most frequently cited International Energy Agency's (1991-2018) capital expenditure data is not of equal quality across countries. In this source, some countries report all components of capital costs, while others only report parts of them. For example, for some countries, the BOS cost component is missing. In addition, capital expenditure

[3]The reason for the rising capital expenditures is that wind speed rises as it reaches higher altitudes. Stronger wind exerts more force on the turbine, requiring heavier materials to withstand these forces (Hemami, 2012)

data or turbine price data reflect the exchange rate, material prices, and/or interest rate fluctuations, none of which contribute to technological innovation (Bolinger & Wiser, 2012). Thus, these factors should be eliminated when deriving measurements of innovation.

McKenna et al. (2014) uses the same wind turbine component-cost-scaling model (Fingersh, Hand, & Laxson, 2006) as we do, in order to calculate the LCOE across various wind turbine designs that are matched with a particular wind resource and the terrain of a geographic location in Germany. However, McKenna et al. (2014) does not attempt to produce series that describe trends in technological development. Instead, the authors try to produce a high-resolution image of the theoretical cost potential of wind energy across different locations. In contrast, we only identify technological innovation trends where small site-specific variations are not of crucial importance.

Several papers use a different approach to measure innovation. Qiu and Anadon (2012) measure production costs using average tariffs that potential wind farm developers were bidding to receive in the Chinese wind energy concession program of 2003-2007. Tang and Popp (2016) criticizes the approach of Qiu and Anadon (2012) arguing that wind farm investors are inclined to underbid their costs in order to win auctions. Instead, Tang and Popp (2016) uses the levelized cost of energy data from Chinese wind energy subsidy project that covers 2002-2009. Their data represents the expected levelized cost of energy estimated by eligible investors. Even if truthfully reported, this data is likely to reflect fluctuations in the factors that do not contribute to technological innovation, such as material price, exchange rates, and interest rate fluctuations. This is due to the fact that investors' expectations are most likely based on actual turbine prices.

We found only one source (Wiser & Bolinger, 2018), which delivers an innovation measure that follows $LCOE$ notion from equation 1.1, in which the series are sufficiently long, and comparable to our innovation data. Wiser and Bolinger (2018) measure the capital cost ($CapEx$) component of $LCOE$ based on the average investment cost of newly installed turbines each year. In addition, they compute the AEP component based on the empirical data of the actual average production of these turbines. Similarly to the papers mentioned above, the problem with this approach is that wind farm investment costs may reflect interest rates, material prices, and exchange rate fluctuations. In addition, historical electricity production data may reflect variations in geographical, annual, seasonal and daily wind resources. Our paper estimates both $CapEx$ and AEP components of $LCOE$ using an engineering model. We will discuss this in more detail in section 1.2.5.

To summarize, many papers do not rely on the traditional notion of $LCOE$ and measure innovation by using capital expenditures or turbine prices. Several papers proxy $LCOE$ using other methods. Nevertheless, the estimated values are likely to reflect fluctuations of variables unrelated to technological innovation. Furthermore, the data series of these papers is quite short and may not represent actual innovation trends.

1.2.3 Deriving Our Innovation Measure

In this section we derive our innovation measure, discuss the strengths and the weaknesses of our method and compare our $LECOE$ data to alternative series.

Each year, new wind turbines are installed in the US. The average characteristics of the turbines installed change annually due to innovation. Key characteristics, including turbine capacity, rotor diameter, and hub height, are the major determinants of the technological progress of wind turbines. The fact that production rates improve at higher altitudes and that stronger wind exerts more force on wind turbines implies that the major innovation in wind technology has to come from increases in the size of turbines. Figure 1.1 confirms that the wind turbines have been persistently increasing in size.

Figure 1.1: Distribution of wind turbine *vintage* characteristics

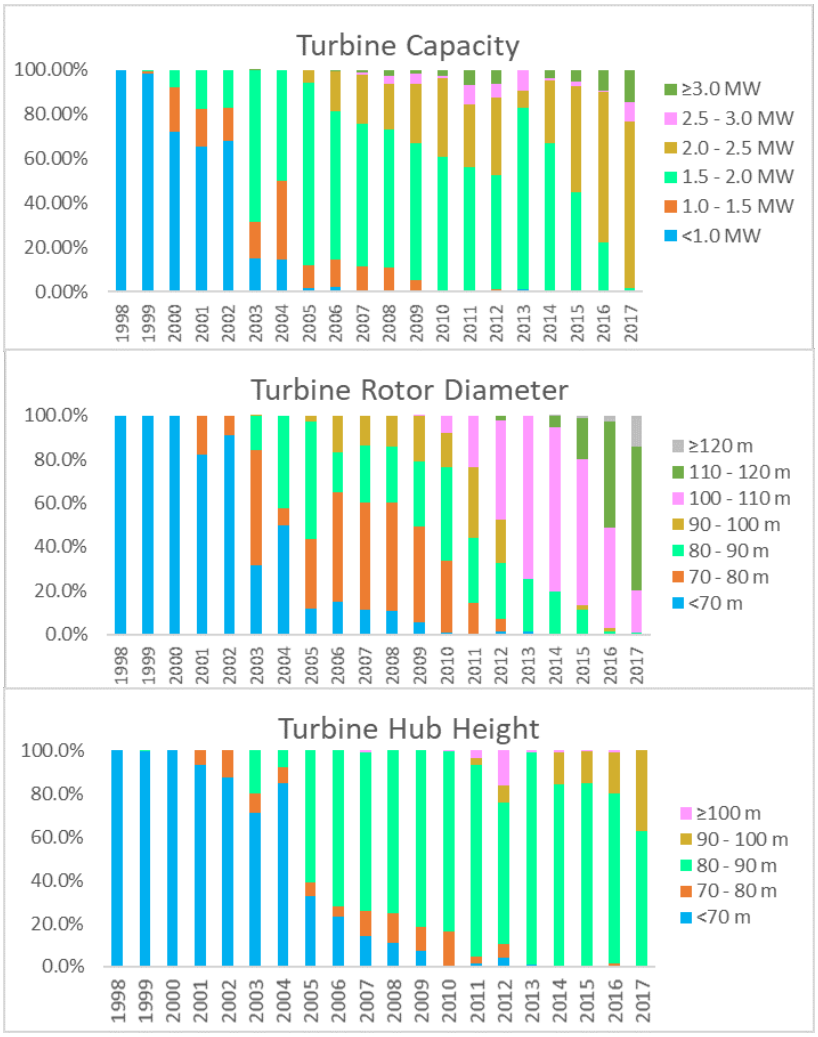

Source: Wiser and Bolinger (2018). Notes: The figure shows that the key wind turbine vintage characteristics have been gradually updated. Therefore, we argue that the average characteristics of wind turbines installed annually represent the frontier technology in the year of installation.

The figure shows the distribution of key turbine characteristics by year of installation. According to the figure, on average, older turbine models are gradually replaced by new ones. Therefore, we argue that the frontier technology is advancing. For these reasons, we use the average key characteristics of turbines installed in a particular year as a representative of

frontier technology in that year. For convenience, we refer to the hypothetical wind turbine model possessing the key characteristics of turbines installed in a particular year as *vintage*.

Several studies, which we characterize as engineering models, use the key turbine characteristics as inputs to derive the mass of turbine components (Malcolm & Hansen, 2002; Poore & Lettenmaier, 2000-2002). Once the turbine mass is properly estimated and the material composition of the turbine is known, we can use material prices to calculate the cost of turbine components. Similarly, these key turbine characteristics can be used to assess the productivity of the turbines. Hence, we can exploit engineering models to estimate $LCOE$ in equation 1.1. We refer to $LCOE$ estimated using engineering models as levelized engineering cost of energy ($LECOE$).

We calculate the $LECOE$ of each wind turbine vintage installed in the US from 1998 to 2017. The data for average key characteristics is taken from Wiser and Bolinger (2018) and is documented in the Appendix table 1.A. Below, we begin calculating $LECOE$ from the simplest components of equation 1.1.

Capital Recovery Factor ***(CRF).*** CRF is a function of the useful life of a wind turbine and a discount rate. In the literature, the discount rate is calculated as a weighted interest rate to finance capital[4] (e.g Mone, Smith, Maples, & Hand, 2015). Certainly, the discount rate may differ across vintages due to the fact that the set of firms installing new wind farms in a particular year face different market-specific and company-specific conditions, which affect the interest rate. We abstract from these short-run interest rate fluctuations to focus only on engineering factors affecting the costs of electricity production. Therefore, we use the same discount rate across the vintages.

Our data is expressed in 2015 dollars because the engineering cost model is expressed in 2015 dollars (Dykes, K, personal communication, January 29, 2019). Taking the discount rate of 7% is appropriate during this period (Mone et al., 2017). In fact, the magnitude of the discount rate is not crucial. As long as we fix the discount rate across vintages, changing it affects the level, but not the trend, of our $LECOE$ data. The purpose of our analysis is to identify the trends in innovation correctly. Figure 1.2 illustrates this point and shows our $LECOE$ data measured using 7% and 1% discount rates, respectively.

Regarding the useful life of the wind turbines, we do not have empirical evidence about the improvement of wind turbines' useful life with technological innovation. In fact, wind farms installed in 1998, when our dataset starts, are expected to still be in operation. Therefore, we do not vary *useful life* across vintages. Manufacturers typically assign 20 years of useful life to wind turbines, so the literature frequently assumes the same (Mone et al., 2017). We follow this practice, and it delivers a CRF of approximately 9.5% for each vintage.

Annual Energy Production ***(AEP).*** As mentioned earlier, AEP measures the annual

[4]The weighted interest rate calculates the rate to be paid as the interest on debt and the rate of return on equity, depending on the proportion of the debt and equity in the total investment cost. The formula is the following: rate of return on equity $\times$ equity share in the portfolio $+$ interest on debt $\times$ debt share in the portfolio $\times$ $(1 -$ income tax rate$)$. The argument against using weighted interest rates is that individual firms usually face increasing marginal interest rates to finance new projects. However, we do not focus on firm-level differences; instead, we depict an industry-level picture. When many wind farms enter the market, it is reasonable to assume that the interest rates remain constant, because not all owners of new wind farms face financial limitations. In addition, using a weighted interest rate is a common practice in the energy literature.

Figure 1.2: Impact of discount rates on the levelized engineering cost of energy

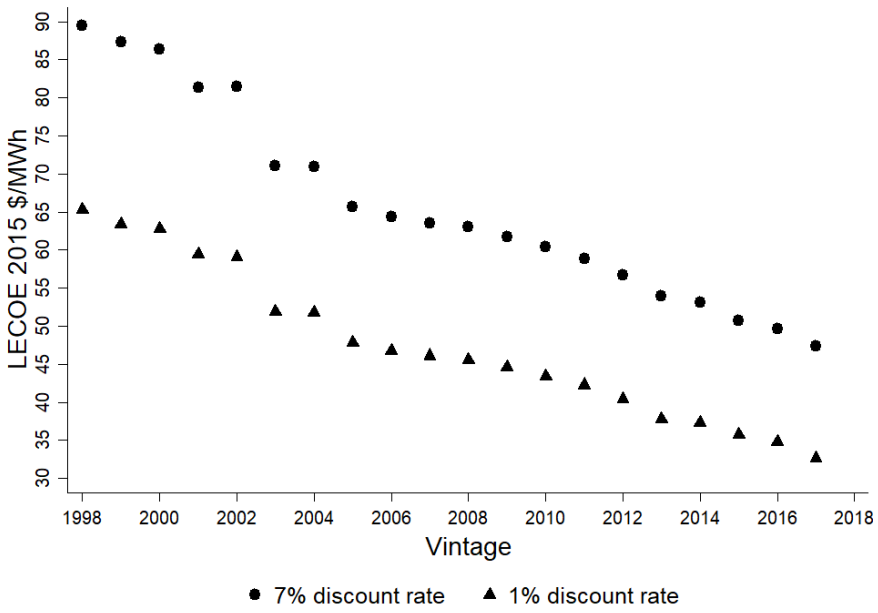

Notes: The figure plots our *LECOE* data calculated using 7% and 1% discount rates. This illustrates that changing the discount rate for all vintages does not affect the trend of the data.

effective operational hours of a wind turbine. Calculating the *AEP* of a wind turbine depends on the wind speed distribution at the site and the power curve of the turbine. Wind speed density reflects the probabilities of various wind speeds occurring in an hour at a site at a certain altitude. The power curve measures the amount of electricity generated at each wind speed bar, based on the turbine characteristics. Multiplying the probability of each wind speed bar by the corresponding power expected to be produced and summing these products delivers the *AEP* of a wind turbine.

Hence, calculating *AEP* partly depends on turbine characteristics and partly on wind conditions and geographic location. Since we want to capture productivity changes due solely to technological innovation, we do not vary the wind speed distribution and other location-specific parameters across the vintages. The idea is to measure the improvement in the productivity of a new wind turbine if we put it in exactly the same location as the old one.[5]

To measure the *AEP*[6], we estimate the power curve of each vintage using the vintage characteristics documented in table 1.A as inputs. In addition, we fix wind and location-specific parameters across vintages at the levels recommended in Mone et al. (2017). The recommended wind and location-specific parameters reflect the average wind conditions

[5]Fixing the wind resource parameters might be questionable if wind turbines were increasingly installed in areas with lower wind speed due to geographic constraints. In this case, we would suspect that the wind turbines were specifically designed for these locations and do not necessarily represent the frontier technologies. However, we show in figure 1.D that such crowding out of new wind farms has not occurred so far.

[6]In this paper, we estimate *AEP* for each vintage using the Plant-EnergySE plug-in of the WISDEM software by NREL available on GitHub (NREL, 2015a). Specifically, we use the nrel-csm-aep script.

and the altitude of a representative site in the interior of the US, where most wind farms are located. To understand the theoretical model behind the AEP estimation, readers are referred to Fingersh et al. (2006). The estimated AEP for each vintage is documented in table 1.C.

Capital Cost (CapEx). Deriving $CapEx$ accurately is the most challenging of the $LECOE$ components. Below, we derive capital costs for each vintage using engineering wind turbine component-mass scaling models. The National Renewable Energy Laboratory (NREL) provides the most extensive engineering turbine-scaling studies. The WindPACT project (Malcolm & Hansen, 2002; Poore & Lettenmaier, 2000-2002) represents NREL's first attempt to measure the scaling of the mass of a turbine with its key characteristics.

There are approximately twenty major components which make up a turbine, including blades, hub, low-speed shaft, tower, generator and gearbox. The WindPACT studies take a baseline wind turbine and project how the mass of each component has to scale when blades become longer, hubs increase in height, and capacity grows. Hence, the WindPACT studies build component-mass scaling models which represent the mass of each turbine component as a function of the key turbine characteristics.

A WindPACT model first simulates wind turbines of various sizes and parameters. Second, it calculates the stress on turbine components under certain wind distributions and parameters. The underlying stress has to be within predetermined limits for the wind turbine to withstand the wind forces for a desired period of time.

For many component-mass scaling models, the arguments have power functions with exponents ranging from 2 to 3. This implies a non-linear increase in turbine mass with turbine characteristics. Certainly, technological innovation can reduce the exponents on the power functions. Some of this type of innovation may be anticipated by the engineering model, while others may not. For this reason, the engineering component-mass-scaling models may become outdated. The WindPACT studies were conducted between 2000 and 2002. During that time, turbines were significantly smaller than today. As the large-sized turbines entered the market, a discrepancy arose between the predicted and the actual mass of these turbines. To account for this, NREL produced new component mass-scaling models[7] in 2015. In the rest of the paper, we frequently refer to the engineering component-mass-scaling models presented in the WindPACT studies as the "old model" and the new component-mass-scaling models as the "new model".

The new model uses a different approach to projecting the mass of turbine components. The authors first collect data about various wind turbines, their key characteristics, and the mass of their components. Then, they regress the values of the turbine characteristics on the mass of turbine components and identify a polynomial fit to the data. The resulting polynomial functions are the new component-mass-scaling models. Although the new model does not rely on a pure engineering estimation technique, it is based on the engineering parameters of turbines.

[7]The new model has not been published officially (Stehly, Beiter, Heimiller, & Scott, 2018), however, the Turbine-CostsSE plug-in is available on GitHub (Dykes, 2015) as a part of WISDEM software, which is programmed to calculate the mass of each turbine component based on key turbine characteristics. Specifically, we use the nrel-csm-tcc-2015 and the turbine-costsse-2015 scripts.

According to equation 1.2, $CapEx$ includes turbine cost and BOS cost. We will first derive the turbine cost based on each model:

Turbine Cost - Old Model

Fingersh et al. (2006) uses the old component-mass-scaling models, the material composition of components and material prices to offer component-cost-scaling models. Component cost-scaling models express the costs of turbine components as a function of their key characteristics. The procedure that the authors use to derive these models is the following:

step 1: Convert the turbine component-mass vector into the component-material-mass vector. For most turbine components, only one material is used, and they do not require assembly[8]. For the components that consist of several materials, the WindPACT studies assume that the proportion of materials in the component remains the same when turbine components scale.

step 2: Apply material prices to compute the component-material-cost vector. Material prices in Fingersh et al. (2006) are given as producer price indices of these materials (PPIs). We are flexible in choosing the material prices of a particular year and expressing all the costs in that year.

step 3: Compute labor costs for turbine components. As mentioned, most turbine components consist of only one material and do not require assembly by the manufacturer. Labor costs are already reflected in the PPI of such materials. The same is true for several more complex components, such as generators. In Fingersh et al. (2006), a generator is treated as a single material to which a single PPI applies, which includes the labor costs. Only three turbine components: blades, nacelle cover, and the electrical connections require labor by manufacturers, according to Fingersh et al. (2006). The labor costs are assumed to amount to fifteen percent of the total cost of the nacelle cover and the electrical connections. For the blade, labor costs scale with the rotor radius. Certainly, there are labor costs associated with the assembly and installation of a turbine itself. However, these are included in the balance of system (BOS) cost.

step 4: Summing the material and labor costs of components yields the component costs. Component costs can be expressed in 2015 US dollars by applying the PPIs of 2015.

We use the component-cost-scaling models in Fingersh et al. (2006) to derive the turbine cost for each vintage. To do this, we plug the key vintage characteristics from table 1.A and the PPIs[9] of 2015 into the component-cost-scaling models and calculate component costs in 2015 dollars[10] for each vintage. The sum of component costs yields the turbine cost in 2015 dollars for each vintage.

[8]These components are readily available in the market and turbine manufacturers do not produce them separately

[9]Producer price indices can be selected based on the NAICS codes suggested in Fingersh et al. (2006). PPIs are available from the Bureau of Labor Statistics web-page.

[10]Using the PPIs of 2015 for materials would be wrong if the material composition of vintages changed frequently; however, Fingersh et al. (2006) assumes a fixed proportion of materials in each component based

Turbine Cost - New Model

The new model does not explicitly provide either the composition or the proportion of materials in each component. Therefore, we cannot apply producer price indices in order to calculate the cost of each turbine component as we did based on the old model. However, Dykes (2015) provides the costs per kilogram of each component in 2015 dollars. These costs are likely computed with similar steps as in Fingersh et al. (2006). In order to compare the old and the new *LECOE* series, we express both in 2015 dollars.

To calculate the turbine cost for each vintage based on the new model, we use *nrel-csm-tcc-2015* and *turbine-costsse-2015* python scripts, which contain the turbine component-mass-scaling models[11]. The calculation procedure is the following:

step 1: Calculate the mass of each wind turbine component for each vintage given the key vintage characteristics from table 1.A. The new model offers four alternative component-mass-scaling functions for blade mass depending on the type of blade used. Hence, blade type is an additional input variable for the blade-scaling model. Blades differ based on whether they have carbon content and whether the turbine is class I or class II/III. Carbon content makes the blade lighter; however, according to Fingersh et al. (2006), carbon should not be used for blades with rotor diameters of less than 100 meters in size. The average rotor diameter for the vintages 1998-2014 is less than 100 meters (See table 1.A). Hence, we calculate the blade mass for these vintages using "no carbon" as input. For all other vintages, we assume carbon content.

The prevailing wind conditions in a location determine which class of turbine should be installed. The literature distinguishes at least five classes of turbines (Wiser & Bolinger, 2018), however, the new model divides these classes in two groups: class I and class II/III turbines. The reason for the division into two groups is that the second group is designed for particularly low-wind-speed areas. The first group includes turbine classes up to class II/III, these are: class I, class I/II and class II. The second group includes turbine classes II/III and III. According to Wiser and Bolinger (2018), since 2012, there has been a greater tendency to install group two turbines (II/III and III), although wind conditions have not changed (See figure 1.B). Because more of the second group turbines have been installed since 2012, we calculate the blade mass by using the "class I" group as input in the blade-scaling model for vintages 1998-2011. We calculate the blade mass by using "class II/III" group as input for vintages installed in 2012 and afterwards.

step 2: Calculate cost per component in 2015 dollars for each vintage. As we mentioned, we are given the cost per kilogram of each component in 2015 dollars. Therefore, we multiply the cost per kilogram of a particular component by its mass calculated in the previous step.

on WindPACT studies. This can be explained by the fact that the industry has significantly converged to three-bladed tubular horizontal axes wind turbines due to their efficiency and, therefore, material composition usually does not substantially differ across vintages (Hemami, 2012).

[11]These scripts are available as a part of Turbine-CostsSE plug-in on GitHub (Dykes, 2015).

step 3: The sum of all turbine component costs is the turbine cost for each vintage in 2015 dollars.

Balance of System Costs

Both the old and the new models offer models for BOS cost-scaling with turbine characteristics. The old BOS cost-scaling models are linear in the number of turbines. This implies that installing a second turbine in an existing wind farm adds exactly the same amount of BOS cost as the first turbine. The new BOS model takes the number of turbines as an additional input variable. This implies that adding a turbine to an existing wind farm saves some part of the BOS costs. However, there is a trade-off between the number and the size of turbines. With larger turbines, fewer can be installed per area for efficiency and security reasons (Hemami, 2012).

We plug the key turbine characteristics from table 1.A and 2015 PPIs into the BOS cost-scaling models documented in Fingersh et al. (2006) to generate the old BOS cost series for each vintage in 2015 dollars.

As we mentioned, in the new BOS model[12], the number of turbines is an additional input variable. The number of turbines multiplied by turbine capacity is referred to as farm size. A common practice is to fix the farm size and calculate the number of turbines installed per wind farm. We follow this practice and fix the farm size for each vintage at 200 MW, which is a typical farm size according to Mone et al. (2017). Subsequently, together with the number of turbines, we input the key vintage characteristics in the new BOS model, which is expressed in 2015 dollars, to compute the new BOS cost series for each vintage in 2015 dollars.

The sum of turbine and BOS cost divided by turbine capacity is $CapEx$ in 2015 US $/MW for each vintage. The estimated $CapEx$ for each vintage using both models is documented in table 1.C.

Operations and Maintenance Costs (O&M). $O\&M$ costs can also be modelled as a function of turbine characteristics. However, the $O\&M$ cost-scaling-models which the old model proposes are not accurate, partly because there are insufficient empirical observations of the frequency at which the turbine parts are replaced in order to validate the model. Public data on $O\&M$ costs that wind electricity producers incur is typically unavailable. Wiser and Bolinger (2008-2018) collect limited and mostly confidential empirical data about $O\&M$ costs annually. This data may not be representative, but could be informative of the trend of $O\&M$ costs across the vintages. According to the plot of $O\&M$ data in Wiser and Bolinger (2018), long-run $O\&M$ costs are generally declining.

Since 2010, NREL has published Costs of Wind Energy Reviews (2011-2018), in which $O\&M$ costs are reported in nominal values. They infer $O\&M$ costs from expert opinions combined with the $O\&M$ data from Wiser and Bolinger (2008-2018). For vintages installed between 2010 and 2017, we use their reported values of $O\&M$ cost and convert them to 2015 dollars using the GDP deflator[13] (Fingersh et al., 2006). In addition, Wiser and Bolinger (2018)

[12]The new BOS model is available as a part of the Plant-CostsSE plug-in on Github (NREL, 2015b).
[13]We extracted the GDP deflator from the U.S. Bureau of Economic Analysis

reports the value of $O\&M$ costs for vintage 1998 at 80 \$/kW/year in 2017 dollars based on expert opinions. We take this value, convert it to 2015 dollars and use linear interpolation to proxy the $O\&M$ costs for vintages 1998-2009. When we calculate $LECOE$ based on the old and the new engineering models, we use this $O\&M$ data in both calculations. The estimated $O\&M$ costs for each vintage are documented in table 1.C.

The $O\&M$ cost component is the weakest in our estimation of $LECOE$. However, its share of the total costs is not significant and it is also unlikely to vary significantly with engineering improvements and hence, across vintages. As a result, we do not expect that it would markedly influence the trend of the $LECOE$ data.

1.2.4 Comparing the Results from the New and the Old Engineering Models and the Lessons Learned

According to the procedure described above, we derived the $LECOE$ components for vintages 1998-2017 using the old and the new engineering models (see table 1.C in the appendix). Figure 1.3 shows the $LECOE$ derived using the two alternative models. The new model produces a steeper series. The series starts to significantly diverge from the 2005 vintage. We can suggest several explanations for these differences: an unanticipated technological innovation occurred, the old model required a correction, or both. If the old model was correct, then an unanticipated technological innovation alone would deliver a different picture: the new series would precisely follow the old series until the technological switch occurred. Figure 1.3 rules out that the old model was correct, since the series follow different paths from the beginning of the period.

To repeat, in the old model, the component-mass-scaling relationships are derived based on simulated conceptual wind turbines. In contrast, in the new model, the same relationships are fitted curves given the data on the actual key characteristics of the turbines and the mass of their components.

Hence, the old model identifies technological trends from simulated wind turbines, while the new model uses actual wind turbine data on units installed in the US. When the original engineering study was undertaken, the turbines on the market were small in size. Figure 1.3 implies that the old model significantly mismeasured the mass of the turbines that were not available on the market at the time.

The comparison of the two $LECOE$ series provides information on the margin of error that an application of the engineering estimation method can produce. The new engineering model may require further improvement as new turbines enter the market. Therefore, caution must be taken when predicting $LECOE$ for future wind turbine vintages using this model. Nevertheless, we can rely on the new model to calculate $LECOE$ for the vintages installed during the period under review. This is due to the fact that the new engineering model already incorporates the data of turbines installed in this period.

Hence, in the rest of the paper, we consider our $LECOE$ series generated based on the new model as the innovation measure. We argue that our innovation measure reflects the engineering improvement of the vintages and is not influenced by interest rates, material

Figure 1.3: Levelized engineering cost of energy

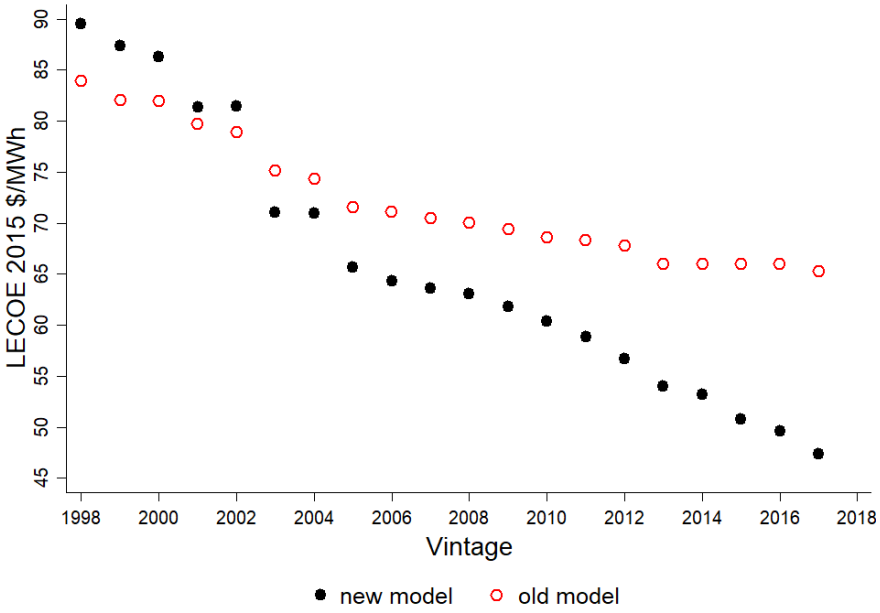

Notes: The figure plots our *LECOE* series calculated based on the old and the new engineering models. We use a 7% discount rate. The figure illustrates the margin of error that using the engineering method may produce.

prices or wind resource variations. In order to illustrate how the influence of these factors can impair innovation measures, in what follows, we compare our *LECOE* series to an alternative measure.

1.2.5 Comparing Our Innovation Data with Alternative Series

We compare our *LECOE* data with alternative series from Wiser and Bolinger (2018). The procedure for calculating *LCOE* in Wiser and Bolinger (2018) is the following:

step 1: Calculate *CapEx* for each vintage based on the empirical data about capital expenditures of wind farms installed in the US. Wiser and Bolinger (2018) have compiled capital expenditure and performance data on approximately 86% of such wind farms. The *CapEx* data typically includes turbine and *BOS* cost. The authors note that, due to the diversity of sources, the available data is not of equal quality; therefore, they warn readers to rely only on the general trends in the data, not on the individual. Using empirical *CapEx* data to measure innovation is problematic in several ways. First, its major component is the price of a turbine. Turbine prices may vary due to temporary shocks such as fluctuations in the exchange rates, material prices or interest rates. We do not consider that these temporary shocks contribute to technological innovation. Second, *CapEx* represents the largest part of the lifetime cost of a wind farm. Investors are likely to react to the temporary market shocks or

technology-related policy changes and shift their investment decision to a different period. Therefore, using empirical $CapEx$ data may represent a distorted view of the actual trend of the capital cost. In contrast, using engineering properties of newly installed turbines to measure the $CapEx$ avoids these issues.

step 2: Unlike this study, the authors do not fix the value of the discount rate across vintages when calculating CRF. In particular, they vary the interest on debt throughout the period with respect to the changes in the twenty-year swap rate and bank spread. The fact that two vintages are charged different interest rates should not be the reason for the difference in the production costs if our goal is to measure changes in the production costs due to innovation.

step 3: The authors calculate AEP based on the actual performance of the vintages installed. AEP estimated in this manner will reflect annual, seasonal and locational wind resource variations. We instead calculate AEP for each vintage using an engineering model and by fixing wind resource parameters across the vintages.

step 4: For $O\&M$ costs Wiser and Bolinger (2018) rely on their own compiled data and the expert opinions to assign the value in 1998 \$80/kW/year, in 2003 - \$60/kW/year, in 2010 - \$51/kW/year and in 2017 \$44/kW/year.

Figure 1.4 compares our $LECOE$ data with the series from Wiser and Bolinger (2018). First, we notice that the Wiser and Bolinger (2018) data is very volatile. Our $LECOE$ measure represents the production costs of energy, which is free from market-driven temporary shocks such as material costs, interest rates, and exchange rate fluctuations, while the Wiser and Bolinger (2018) data reflects such fluctuations. For example, their data reflects an abnormal period between 2006 and 2011 when the production cost was rising. Certainly, this was not due to technological decay but because $CapEx$ largely reflected increases in turbine prices during this period. Bolinger and Wiser (2012) explained the rise of turbine prices in this period: first, many turbines were imported into the US from abroad, and during this period, the US currency was depreciating against the importing country currencies. Second, demand for turbines increased significantly, and the supply side could not catch up with this trend immediately. For this reason, manufacturers started to face labor supply issues, which increased labor costs. In addition, manufacturers increased their profit margins, given the supply deficit. Finally, the rise in wind turbine material prices also contributed to the increase in turbine prices.

If we omit the abnormal period, we notice that both series show similar trends and that our data series are slightly above the ones from Wiser and Bolinger (2018). This is a good indicator that the engineering costs quite realistically reflect the empirical cost of the turbines. One reason our $LECOE$ series is slightly above the alternative ones, omitting the abnormal period, is that we may be using a higher discount rate on average. Another reason could be that we fix wind resource parameters and distribution to calculate turbine productivity, while actual productivity might have been higher on average during this period.

Hence, in this section, we have illustrated the advantage of using the engineering method to calculate the production costs of wind turbines. The engineering model more realistically reflects production cost reductions driven by innovation.

Figure 1.4: Visualizing the advantage of our innovation data

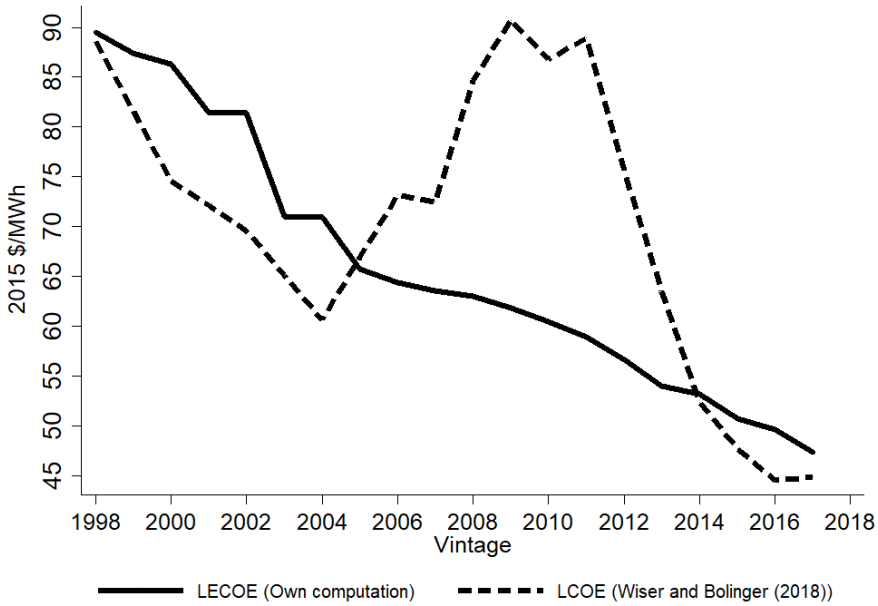

Notes: The figure contrasts our innovation data with the alternative series from Wiser and Bolinger (2018). Because the alternative $LCOE$ data was not directly accessible, we measured it from the bar chart produced in the 2017 Wind Technologies Market Report (Wiser & Bolinger, 2018). We used the WebPlotDigitizer tool to measure the bars.

1.3 The US Wind Energy Policy Environment

In order to discuss potential applications of our measure of innovation, we first study the current wind technology market structure and policy environment in the US. For this reason, we explore the supply and demand sides of wind electricity producers and the prevailing equilibrium outcomes given the current government policy instruments.

1.3.1 The Cost Side of Wind Electricity Producers

In the previous section, we found that the long-run marginal cost curve (the supply curve) of wind electricity is downward sloping due to innovation. We now observe that the electricity supply curve for each vintage is horizontal (see figure 1.5). On the maps in figure 1.D in the appendix, we see that the majority of wind farms have been built in densely populated areas and close to one another. This indicates that geographic constraints have not crowded out the wind farms to less windy areas. The crowding out of wind farms would imply an upward sloping electricity supply curve for each vintage. The upward sloping curve would reflect an increase in the marginal costs due to poorer wind resources, which electricity producers would face in remaining wind farm sites. To reinforce the claim that geographic constraints have not yet become binding in the US, we check the changes in the average wind speed across various vintages at the wind farm cluster level. Figure 1.E in the appendix shows that wind quality has not worsened for newer vintages at the location level.

Figure 1.5: Long-run and short-run electricity supply curves

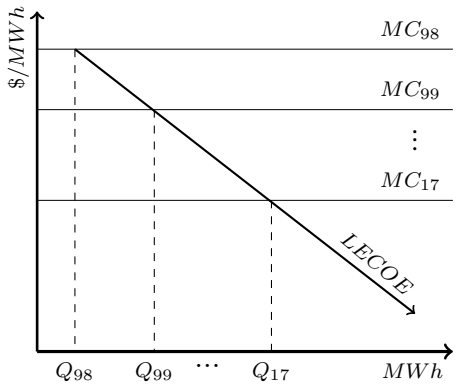

Notes: The LECOE curve represents the long-run marginal cost curve of wind electricity producers, while MC curves illustrate short-run marginal costs of electricity production by each vintage 1998-2017. Q denotes cumulative production.

1.3.2 The Revenue Side of Wind Electricity Producers

Wind electricity producers receive income from selling electricity and from subsidies. Electricity sales are usually established through long-term power purchasing agreements (PPAs). The most significant subsidies producers receive are federal production tax credits and depreciation benefits. Before we summarize these sources of income and provide some statistical data, it is crucial to introduce the market players and to review the US electricity market structure. What follows is mostly based on the handbook of Federal Energy Regulatory Commission (2015).

Many types of players participate in the complex electricity markets, so we introduce only the core players. Electricity producers, electricity generators and wind farm owners own a generation facility and produce electricity. Utilities own transmission and distribution lines and are regulated by the government. Electricity suppliers deliver electricity to the final consumers. A supplier may be a utility or a non-utility company. We will frequently refer to a non-utility electricity supplier as a retail electricity provider (REP). Electricity suppliers, unless they own generation facilities, purchase electricity from generators; therefore, we will also refer to them as wholesale electricity purchasers when needed.

Utilities have interconnected their transmission lines in the US, and this has formed several electricity markets. Transmission capacity between these markets is usually limited. Figure 1.6 displays the markets. Market structure determines the predominant nature of trade in these markets - bilateral or wholesale. Independent system operators (ISO) run the wholesale markets. The ISOs are non-profit organizations, and they enforce efficient and non-discriminatory trade between participants.

Three types of market structures are prevalent in the US: vertically integrated markets (VIM), partially deregulated markets (PDM) and fully deregulated markets (FDM). In VIMs utilities own generation facilities and also supply electricity to final consumers. Utilities enter into bilateral trade in VIMs. In PDMs utilities are unlikely to own generation facilities, but they

still supply electricity to final consumers. Electricity producers participate in the wholesale markets and compete to sell electricity to utilities.

Figure 1.6: US electric power markets

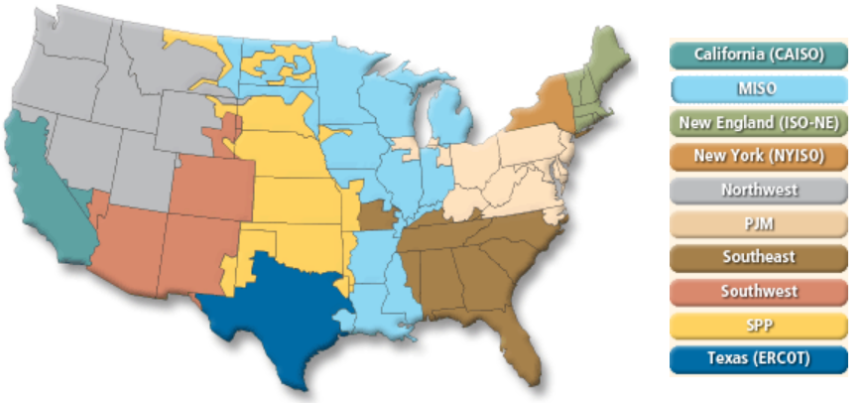

Notes: The figure shows deregulated and vertically integrated electricity markets in the US. The Northwest, Southeast and Southwest regions are vertically integrated, while the rest are operated as wholesale markets by independent system operators. Source. Federal Energy Regulatory Commission (2019).

FDMs are similar to PDM, however, competition is established not only at the generation level but also at the supply level. By default, in FDMs, utilities purchase electricity in the wholesale market and supply electricity to consumers in the areas where they own transmission and distribution lines. Nevertheless, final electricity consumers have the option to switch to REPs. The reason for the switch could be due to a cheaper electricity package or a green electricity option. If a consumer chooses a REP as a supplier, then the REP is responsible for purchasing electricity from generators and scheduling it for transmission and distribution. Transmission and distribution fees will be included in the final electricity bills. The fees are very small in comparison to the cost of energy.

Figure 1.6 shows that the markets referred to as Southeast, Southwest and Northwest are VIMs (Federal Energy Regulatory Commission, 2019). The rest of the markets are either PDM or FDM. Comparing figures 1.D and 1.6 suggests that the majority of wind farms operate in the interior region of the US, where electricity markets are at least partially deregulated. This implies that utilities in these regions are unlikely to own wind farms and that most wind farms operate in the wholesale markets. However, participation in the wholesale markets is not mandatory for wind electricity producers. To hedge against market price fluctuations, they can enter into long-term power-purchasing agreements (PPAs) with electricity suppliers.

Statistically, utilities own only fifteen percent of the cumulative wind generation capacity installed between 1998 and 2017. In addition, only 23% of the cumulative capacity participates in the wholesale markets (Wiser & Bolinger, 2018). Therefore, we argue that PPAs are the most common source of revenue for wind electricity producers in the US. Hence, PPA is the best measure of revenue. We summarize the average PPA rates across vintages below as the revenue source, and judge whether they are set competitively. Assessing the degree

of competitiveness between wind farms is necessary for analyzing wind technology support policies.

Income From Power Purchasing Agreements

A power purchasing agreement is the negotiated price per unit of electricity between a wind electricity producer and an electricity supplier. A typical PPA specifies the price of unit electricity, annual escalation of this tariff, and the duration of the contract. The duration of approximately 60% of contracts is 20 years, and about 90% of contracts are 15-25 years (Wiser & Bolinger, 2018). Therefore, the vast majority of wind electricity generators are locked in at a specified price throughout the useful life of a wind farm project. As a result, electricity producers are protected from wholesale market price fluctuations.

The wholesale markets are competitive because all technology generators compete with each other. However, it may not always be the case that PPAs are set competitively. If there are too few wind farms and the utilities or REPs have an obligation to supply a certain portion of electricity from renewable sources[14], then wind electricity generators will have incentives to set premiums on their electricity prices.

We investigated the number of wind electricity generating firms that have entered each electricity market annually to assess potential competition levels between them. We first obtained data on all operating wind farms since 1998 in the US. The US Geological Survey, the Berkeley Lab, and the American Wind Energy Association (2016) compile such data in the United States Wind Turbine Database. The database provides the names of each wind farm, the years the farms were installed, and the locations and technical parameters of installed turbines. We then identified the wind farm owners and the electricity suppliers which purchase electricity from these wind farms[15]

We removed all observations when a wind farm owner and a corresponding electricity purchaser were the same entity, or one was a subsidiary of the other. Such firms would not be appropriate to analyze competition. Furthermore, we disregarded the Southeast market because there are few wind farms and the majority are owned by utilities (refer to the map in figure 1.D)

Using the locations of wind farms, we assigned each of them to the electricity markets in figure 1.6, where they most likely sell electricity. Table 1.F in the appendix shows the cumulative number of wind farm owners in each market each year. The table suggests that there has been a reasonable level of competition between wind farms since the mid- 2000s. However, in the beginning of the period under review, wind farms were less competitive. To verify whether there is sufficient competition between probable electricity purchasers, we found information on the number of utilities and REPs participating in each electricity market. Table 1.G demonstrates a reasonable level of competition between probable electricity purchasers as

[14]Renewable portfolio standards represent state-specific targets for the share of electricity that suppliers are obliged to procure from renewable sources, cumulatively in a particular state by a certain date. Some states may have high targets and implement penalties for non-compliers, while others require only goals and apply no penalties. The targets can be subject to change. (DSIRE, 2019b)

[15]Information on wind farm owners and corresponding electricity purchasers was mostly taken from the American Wind Energy Association (2013-2017), the Open Energy Information Database (2019) and the Wind Power database (2019). Information on electricity purchasers was confidential in only about one percent of cases.

well.

Data series regarding the levelized PPA are documented by Wiser and Bolinger (2018). We convert the values into 2015 dollars using the GDP deflator[16] The authors generate levelized PPA series using the steps described below. The unit of measurement of levelized PPA is $/MWh:

step 1: Group individual power purchasing agreements by their execution date. PPAs are usually executed one or two years before wind farms are installed. Therefore, the PPA execution date and vintage launching date are different.

step 2: If an individual PPA involves annual price escalation, levelize it using a 7% discount rate, which implies making the negotiated price constant each year.

step 3: Assign weights to individual PPAs based on the generation capability of wind farms by PPA execution date. This implies that the authors assign bigger weights to wind farm projects which produce more, instead of simply averaging individual PPA prices by their execution date.

step 4: Derive levelized PPA by their execution date, i.e. sum the generation-weighted individual PPAs by their execution date.

The "Revenue + Subsidy" curve in figure 1.7 is the sum of levelized PPA prices and levelized subsidies. Levelized PPA represents approximately 70% of the total income of the vintages. We should note that wind farm investors negotiate PPAs one or two years before installing the wind farms. Levelized PPA data is grouped by the year when these PPAs were executed, not by the year when the corresponding wind farms were installed (Wiser & Bolinger, 2018). For example, PPAs executed in 2010 primarily denote the vintages installed between 2011 and 2012. According to Wiser and Bolinger (2018), PPAs that are executed in a particular year effectively reflect the market conditions for the vintage that was installed in the same year. Following this argument, when we plot figure 1.7, we assign to each vintage the levelized PPA which was executed in the year of installation.

The revenue side of the wind electricity producers can be affected by the integration costs as well. Integration costs are those that wind technology brings to the power system due to the intermittent nature of wind resources (Milligan & Kirby, 2009). When the share of intermittent generation rises in the system, it becomes more challenging to balance electricity supply and demand. In many cases, oversupply incidents rise, which is sometimes addressed by forced curtailment of wind technologies, which in turn implies lost producer revenues (unless losses are compensated). Figure 1.H in the appendix shows the estimated average capacity factors of wind generation in the US if curtailment had not occurred and compares them with the actual average capacity factors. The figure shows no curtailment before 2007. After 2007, capacity factors declined by 0.1-1 percent due to curtailment[17]. This reduction in capacity factors and hence, wind electricity generation, would not significantly affect the levelized PPAs. Therefore, we omit the curtailment factor from our discussion. Moreover,

[16]The data can be extracted from Wiser and Bolinger's (2018) data file.

[17]Only in 2009 did the average capacity factor decline by two percent due to curtailment.

Figure 1.7: Costs and revenues

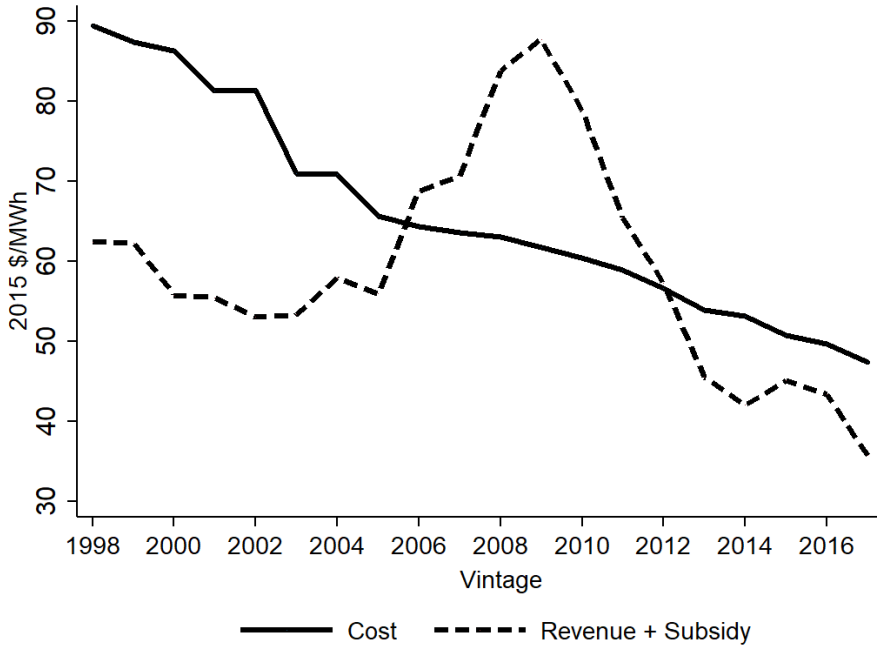

Notes: The figure plots the cost and income sides of each vintage, where income includes revenues from PPAs and subsidies. The cost side is calculated using an engineering model, while the income data is primarily empirical. Therefore, caution should be taken when inferring information from these curves.

we use only the revenue side of the wind electricity producers for qualitative analysis, and a slight reduction in levelized PPA after 2007 will not impact our results.

Production Tax Credits

Wind electricity producers receive subsidies per MWh of production in their first 10 years of operation as a production tax credit (PTC). The amount of PTC is determined at 15 $/MWh, which is the value in 1993 dollars and needs to be adjusted for inflation using the adjustment factor released annually by the US Internal Revenue Service[18] (Internal Revenue Code, Sec.45(e)). The adjustment factor for each year is the ratio of the most recently revised GDP implicit price deflator for the preceding year and the GDP implicit price deflator for 1993.

We derived the levelized value of PTC received for twenty years instead of ten years in order to distribute its value throughout the useful life of the wind farms. The process of calculating levelized 20-year PTC is written out in steps below. The brackets indicate the units of measure in each step:

step 1: Find the value of a ten-year PTC subsidy in 2015 dollars. To be consistent with our cost data, we want to convert everything into 2015 dollars. The value of a PTC

[18]The PTC policy has been stated to expire 10 times since its implementation but has been extended retroactively each time. Currently, wind energy technologies that were in construction prior to 2019 will still receive PTC.

subsidy in 2015 dollars is the ratio of the GDP deflator in 2015 and 1993 multiplied by 15 \$/MWh. As a result, we obtain the value of a ten-year PTC subsidy in 2015 dollars 21.5\$/MWh. (\$/MWh).

step 2: Derive the annual PTC subsidy per vintage capacity. The value of PTC is independent of the productivity of a vintage as it is calculated per unit of electricity. Therefore, we imagine a wind turbine that works effectively for only one hour per year. In addition, we assume that the annual productivity of vintages does not change through their useful life. Given these assumptions, the calculation is simple: we multiply the value of a ten-year PTC subsidy 21.5\$/MWh by 1 h/year. (\$/MW/year).

step 3: Derive the present value of the annual PTC subsidy calculated in the previous step. We use a 7% discount rate to be consistent with our innovation data. (\$/MW).

step 4: Given the present value of a ten-year PTC subsidy, the annual amount of PTC subsidy per vintage capacity for 20 years would be a constant annuity. The constant annuity is the product of the present value calculated in the previous step and the fraction $\frac{i(1+i)^n}{(1+i)^n-1}$, where $i = 7\%$ and $n = 20$. (\$/MW/year).

step 5: Find the levelized value of a twenty-year PTC subsidy for each vintage by dividing the annuity calculated in the previous step by 1 h/year. We obtain a levelized value of a twenty-year PTC subsidy in 2015 dollars to be 15 \$/MWh. (\$/MWh).

Depreciation Benefits

The Modified Accelerated Cost Recovery System (MACRS) allows wind generators to depreciate their turbines within 5 years[19] (Internal Revenue Code, Sec.168 (e)(3)(B)). The Federal Economic Stimulus Act of 2008 added a 50% bonus depreciation for wind technologies placed in operation in 2008 (Internal Revenue Code, Sec.168 (k)), which was retroactively extended several times and included all later vintages, including 2014. In addition, the Tax Relief, Unemployment Insurance Reauthorization, and Job Creation Act of 2010 allowed a 100% bonus depreciation for the 2011 vintage (DSIRE, 2019a). The depreciation rates are listed in table 1.1.

In a similar manner to how we derived PTC, we calculate the levelized value of net depreciation benefit per MWh. Net depreciation benefit refers to the amount that is obtained after subtracting the benefit that wind electricity producers would have received if their capital were not treated as a five-year property. For simplicity, we assume that the 5-year depreciation schedule applies to full capital expenditures because a wind turbine represents the most significant part of the capital expenditure, and because most of the *BOS* costs are also depreciated based on the 5-year depreciation schedule. The derivation steps follow:

step 1: Calculate the annual depreciation expense of each vintage. This will be the product of the $CapEx$ of a vintage and the MACRS depreciation schedule from table 1.1. For

[19]The depreciation schedule actually extends six years because of the so-called "half-year convention" (Internal Revenue Code, Sec.168(d)). This means that the law treats properties as being placed into operation in the middle of the year. Hence, in the first year, taxpayers are only allowed six months of depreciation, and any remaining amount is transferred to the sixth year.

Table 1.1: Depreciation schedule

Year	1	2	3	4	5	6
MACRS	20%	32%	19.20%	11.52%	11.52%	5.76%
MACRS+50% bonus	60%	16%	9.60%	5.75%	5.75%	2.90%

Notes. We use a 12-year linear depreciation schedule as a counterfactual. The schedule depreciates 4.17% of the capital expenditure in the first and the last years of operation and 8.33% in the remaining years.

vintages 2008-2014 the fifty percent bonus depreciation schedule applies, except for the 2011 vintage, for which a 100% bonus depreciation applies. ($/MW/year)

step 2: Calculate the annual depreciation benefit for each vintage by multiplying the depreciation expense above by the federal corporate income tax rate - 0.35% (Mone et al., 2017). This is the amount that would have been paid in taxes if the depreciation expense were not available. ($/MW/year).

step 3: Compute the present value of the five-year depreciation benefit for each vintage using a 7% discount rate. ($/MW)

step 4: Calculate the annual depreciation benefit for each vintage for 20 years, which is a constant annuity. Constant annuity is the product of the present value calculated in the previous step and the fraction $\frac{i(1+i)^n}{(1+i)^n-1}$, where $i = 7\%$ and $n = 20$. ($/MW/year).

step 5: Find the levelized depreciation benefit for each vintage by dividing the annuity calculated in the previous step with the AEP of each vintage from table 1.C. ($/MWh).

step 6: Calculate the levelized net depreciation benefit. We need to subtract the levelized depreciation benefit that each vintage would have obtained if it were not treated as a 5-year property from the previous step. Bolinger (2014) suggests using a 12-year linear depreciation schedule as the counterfactual. Hence, we also compute the levelized value of linear depreciation benefit for each vintage following the previous steps, and subtract it from the levelized depreciation benefit in *step 5*. ($/MW).

Thus, we have calculated the levelized PTC and levelized net depreciation benefit for each vintage. The sum of these two values we refer to as the subsidies per MWh of electricity. We add these subsidies to the levelized PPA price data and plot it as the "Revenue + Subsidy" curve in figure 1.7.

1.3.3 Analysis of the US Wind Energy Sector

In figure 1.7 we present historical income and cost figures for vintages. We emphasize that we calculate the cost side using an engineering model as described in the previous section. In contrast, the income side is primarily based on empirical data. However, we can still compare the trends in the data.

In figure 1.7, we first notice an abnormal increase in the income side between 2004 and 2009. This abnormality is primarily caused by increased turbine prices and is well-documented by Bolinger and Wiser (2012). Certainly, wind farm investors take the capital costs into account when negotiating PPAs. According to Bolinger and Wiser (2012), the US imports most wind turbines from abroad and the US dollar was becoming weaker in relation to the currencies of the largest importing countries during this abnormal period. Furthermore, the US substantially increased wind turbine installation, and high demand increased turbine prices. Hence, wind electricity producers required higher PPAs to compensate for rises in capital costs. Finally, in order to fully monetize production tax credits, wind farm investors typically cooperate with tax equity investors. During the 2008-09 global financial crisis, access to tax equity substantially declined and raised the discount rate in equation 1.1. In contrast, we fix the discount rate across vintages in our computation. Similar factors on a smaller scale could explain other minor variability in the income side.

We also notice that, omitting the abnormal period, the cost curve is above the income curve. This is due to the fact that when calculating the engineering cost, we fix the wind resource parameters and distribution nationwide and compute production using only the key turbine characteristics as inputs. In contrast, levelized PPAs are based on the expected production estimated by the wind farm investors. We know that PPAs are not negotiated for all wind farms installed each year and that most PPA contracts are signed for farms in the interior of the US because these markets are deregulated[20] (Federal Energy Regulatory Commission, 2019). The interior region has the most favorable wind resources (Wiser & Bolinger, 2018), hence, PPAs in this region should be lower on average than nationwide. In addition, a smaller discount rate in equation 1.1 would shift the $LECOE$ curve down.

If we omit the abnormal period, we can argue that costs and income follow similar patterns. However, the ratio between costs and revenues is larger in the beginning of the period under review. This is consistent with our earlier observation that competition between wind farm owners before the mid 2000s may have been low. This does not imply that the firms were monopolistic, but they were probably obtaining more markups, possibly as a return for the risk that they were taking for entering a relatively immature industry.

Based on the observations above, we developed an intuition into how wind energy support policies function in the US. The government first determines wind technology deployment targets. Then, it anticipates the average wholesale market price of electricity[21], which in turn determines the demand for wind electricity. The wind electricity demand curve is horizontal for each vintage, as is the marginal cost curve. In order to achieve an equilibrium, the government provides sufficient production subsidies to align the demand and supply curves: producers cover their production costs and obtain some markups using PPAs and subsidies. This provides investors with sufficient incentives to enter the market. However, due to the fact that both demand and supply curves are horizontal given the vintages, multiple equilibrium outcomes are possible. To avoid this, the government applies quantitative instruments to promote the deployment of sufficient wind turbines to reach the targeted capacity.

[20] In the vertically integrated markets utilities typically own the wind farms, and hence, do not make PPA contracts.

[21] Wind energy currently satisfies only seven percent of the total market demand in the US; therefore, it cannot influence the average market price of electricity

According to this logic, government deployment targets, combined with subsidies, determine the wind technology deployment rate. Government subsidies alone would not determine the deployment rate because of the horizontal marginal cost curves that wind electricity producers face. In addition, if the wind farm owners were monopolistic, and the demand for wind electricity were not horizontal, the firms would choose sub-optimal production. This would imply deployment below the targeted amount. Therefore, given sufficient competition, the government can determine deployment rates using quantity-based policies.

The ability of the government to determine deployment rates may translate into its ability to influence the rate of wind technology innovation. A simple guess would be that wind turbine manufacturers would innovate as a response to anticipated deployment rates. The relationship between increased deployment and production cost reduction is the subject of learning curve literature (e.g. Ibenholt, 2002; Junginger, Faaij, & Turkenburg, 2005; Kobos, Erickson, & Drennen, 2006). In the following section, we will briefly summarize the learning curve method and evaluate it using our innovation measure. Later, we will also discuss a possible causal relationship between government deployment targets and innovation.

1.4 Outcomes of the Learning Curve

In this section, we illustrate the use of our innovation measure in the learning curve analysis. Analysis of learning curve is the most widely applied method in the energy literature of predicting future unit cost reductions. An accurate innovation measure, would make learning curve analysis more reliable, which we will show by comparing the performance of our data with alternatives.

The traditional meaning of "learning curve" in this sense is that electricity production costs are reduced with increased production because of learning by production (Arrow, 1962). However, learning can be a result of innovative activities not related to production. For example, R&D investments in wind technology may lead to innovation, but this innovation is not related to production. We refer to this type of learning as learning by investing. Our analysis of the learning curve combines both types of learning.

To obtain the learning curve, we express the unit cost of energy at time t as C_t, cumulative installed wind generation capacity at time t as Y_t^C, the cost of energy at initial capacity as C_0, and learning elasticity as α in the equation below. We treat the year 1998 as period zero in our dataset. In addition, since the cumulative installed generating capacity before 1998 was very small, we assume it to be zero:

$$C_t = C_0(1 + AY_{t-1}^C)^{-\alpha} \quad \text{for} \quad t = (0, ..., T) \tag{1.3}$$

The majority of the learning curve papers use $CapEx$ or turbine prices per MW as the measure of unit cost (e.g., Hayward & Graham, 2013; Grafström & Lindman, 2017; Yu et al., 2017; Wiebe & Lutz, 2016). We consider that this approach underestimates the learning effect. As turbines become larger, $CapEx$ per MW may rise; however, effective hours of operation also rise, which compensates for the increase in $CapEx$. Therefore, if we measure innovation using $CapEx$ only, it is highly likely to underestimate the learning effect. In

contrast, measuring the unit cost using $LECOE$ takes into account increases in effective operating hours. For these reasons, in our learning curve analysis, $LECOE$ data represents the unit cost of electricity for each vintage.

The time lag on the cumulative capacity in equation 1.3 takes into account the fact that learning does not occur instantly, given the deployed capacity. Figure 1.I in the appendix plots our $LECOE$ and wind capacity deployment data. The following observations help us verify that the learning curve can deliver an unbiased measure of correlation between deployment targets and innovation:

Observation 1 - Wind electricity producers face horizontal marginal cost curves

If the marginal cost curves were not horizontal, then applying the learning curve method would deliver a biased measure of correlation without further assumptions. The bias would be present due to the omission of the geographic factor. Figure 1.8 illustrates the point: when the marginal cost curves are horizontal, the entire cost reduction is attributed to increased deployment (the segment A on the left graph); when the marginal cost curves are upward sloping, some cost reduction is not achieved due to geographic constraints, i.e. due to crowding out of new wind farms from high-wind-speed areas (the segment B on the right graph). Therefore, the correlation between increased deployment and technological innovation would be underestimated.

Figure 1.8: Illustration of potential supply curves

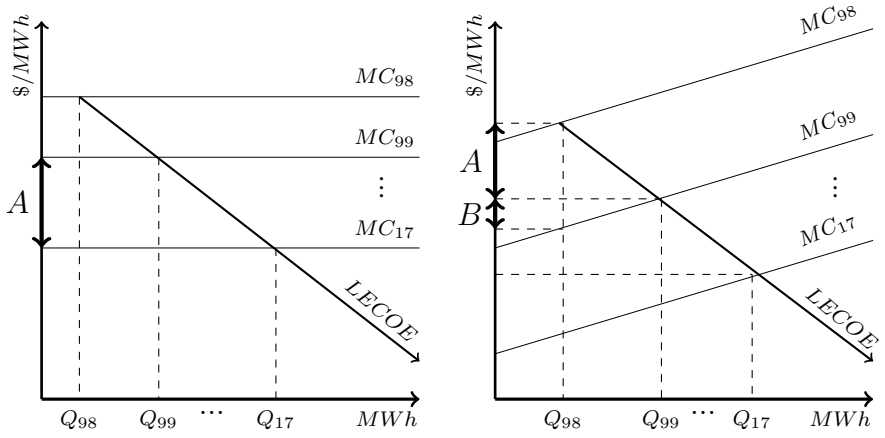

Notes: The left graph shows that when short-run electricity supply curves given each vintage are horizontal, we should attribute all reductions in production costs to increased deployment (segment A). However, if the curves are upward sloping, we cannot attribute all reductions in production costs to increased deployment; otherwise, we will miss the impact of geographic factors (segment B on the right graph).

Observation 2 - Cumulative production may be a better explanatory variable than cumulative capacity.

We argued in the previous section that government deployment targets influence the deployment rates. If the manufacturing sector anticipates deployment rates and innovates as a

response, then we may wonder why the government would not set higher targets in order to increase their incentive to innovate. On one hand, the required subsidy budget increases with installed generation capacity, which might become unaffordable. On the other hand, short-run marginal costs of innovating increase with R&D. This implies that it is costly to speed up the innovation process.

For these reasons, we use cumulative production instead of cumulative capacity as an explanatory variable in the learning curve. A substantial increase in generation capacity in a particular year will substantially increase cumulative capacity, while it will not increase cumulative production as much. Therefore, cumulative production will have a smoother reaction to changes in the installed generation capacity, and this will justify the slower response of innovation.

1.4.1 Learning Curve with Cumulative Production

In this subsection, we conduct a learning curve analysis using cumulative production as an explanatory to the reductions in the production costs, and compare it with the original specification in equation 1.3. We run both specifications of the learning curve using three sets of alternative innovation data: our innovation data generated using the new and the old engineering models, and the innovation data of Wiser and Bolinger (2018).

In order to derive the time-t cumulative production variable, we first derive the time-t production Q_t^N. Not all turbines that are installed in a particular year start production immediately. In fact, some turbines may be installed at the end of each period. To account for this, we assume that only half of the newly installed wind generation capacity in year t produces electricity in year t. The rest starts in the next period. Taking this into account and denoting time-t capacity by Y_t^N delivers:

$$Q_t^N = \sum_{s=0}^{t} Y_s^N AEP_s + \frac{1}{2} Y_t^N AEP_t \quad \text{for} \quad t = (0, ..., T) \tag{1.4}$$

Where AEP_t is the effective annual hours in operation for each vintage installed in year t from table 1.C. The cumulative production Q_t^C will simply be:

$$Q_t^C = \sum_{s=0}^{t} Q_s^N \quad \text{for} \quad t = (0, ..., T) \tag{1.5}$$

Therefore, the learning curve model with cumulative production is the following:

$$C_t = C_0(1 + AQ_{t-1}^C)^{-\alpha} \quad \text{for} \quad t = (0, ..., T) \tag{1.6}$$

Production before 1998 is assumed to be zero because it is relatively insignificant. We run a non-linear regression on both equations 1.3 and 1.6 to find the parameters C_0, A, and α. We consider three time series as input to the production cost. The first and second are our innovation measure generated based on the new and old engineering models, respectively, and the third is the $LCOE$ data of Wiser and Bolinger (2018).

Figure 1.9: Estimation of the learning curve

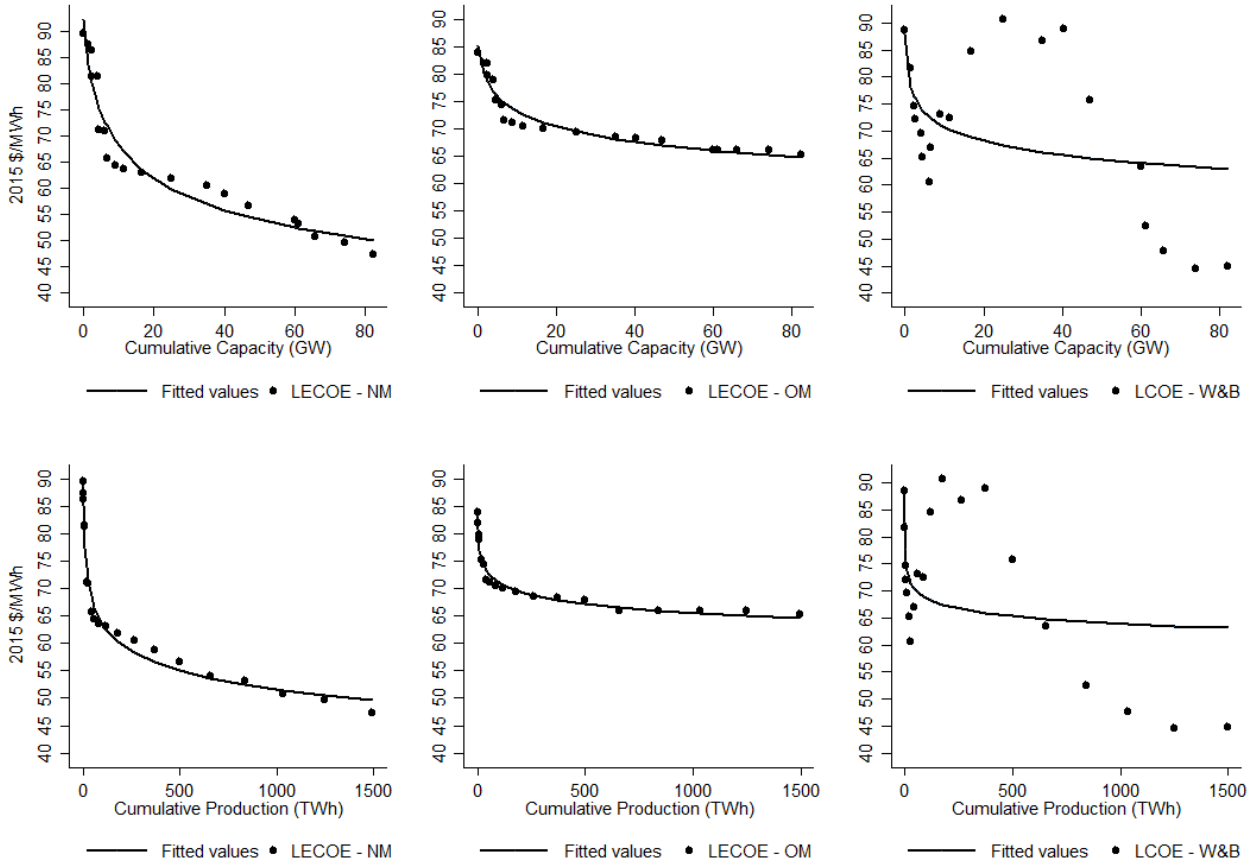

Notes: Abbreviations NM, OM and W&B, refer to the innovation measures obtained from the new model, old model, and Wiser and Bolinger (2018), respectively.

Regression tables 1.J and 1.K can be found in the Appendix. In figure 1.9, we notice that using cumulative production instead of cumulative capacity in the learning curve estimation arranges the data cloud more smoothly. However, it does not deliver significantly different estimation results (compare tables 1.J and 1.K).

A noticeable difference arises when different innovation data are used. The learning curve is steeper when an innovation measure based on the new model is used instead of the measure based on the old model. A steeper learning curve implies a higher rate of learning. Both innovation measures confirm a correlation between cumulative production and production cost reductions, since the estimated parameters are statistically significant. In contrast, for the *LCOE* data of Wiser and Bolinger (2018), the learning parameter is very small and statistically insignificant.

Also, notice that the data cloud is not smooth for Wiser and Bolinger (2018) and the deviation from the fitted line is substantial. In tables 1.J and 1.K, we can see that the innovation data of Wiser and Bolinger (2018) delivers a larger root mean square error in comparison to our data. This indicates a weak fit. Hence, we have illustrated how we could improve the

fit of the learning curve by supplying our improved measure of innovation. Our measure of innovation shows a strong correlation between wind technology deployment and innovation.

1.4.2 Effects of Policy on Innovation

In the above learning curve analysis, we show a strong correlation between the wind technology deployment rate and innovation in the US. In this section, we discuss possible causality. In particular, it is not unreasonable to conjecture that when the government sets wind technology deployment targets, which determine the deployment rate, the incentive of wind turbine manufacturers to innovate is likely to increase.

Certainly, we cannot rule out reverse causality, i.e., increased deployment of wind turbines as a response to reduced production costs. In addition, we do not argue that the US wind technology deployment targets are the only instruments that could influence wind technology innovation. For example, R&D spending in wind technology and other countries' wind technology support policies also contribute to innovation. However, it is still our conjecture that the US deployment targets influence innovation.

It is a fact that most countries aim to support clean technologies, particularly, solar and wind, in order to reduce greenhouse gas emissions and to limit climate change. For this reason, we consider that innovation is not the main driver of government policies, or at least policy is an important factor affecting innovation.

Suppose that the US deployment target does not drive innovation. Instead, suppose that costs would decline regardless of any intervention. We construct a simple optimization problem to show optimal wind technology deployment in this case. The government tries to maximize the social surplus. A positive surplus is delivered by exploiting a cheaper technology, i.e. a technology with lower marginal costs. We can assume that the long-run marginal cost curve of an alternative technology is horizontal because conventional technologies do not experience technological innovation. The long-run marginal cost curve of wind technology is downward sloping, according to figure 1.2.

In equation 1.7 below, MC_t is the marginal cost of production using wind turbines at time t, MC^A is the marginal cost of production using an alternative source, Q_t is wind electricity production at time t, and Q_T is the final deployment target:

$$\max_{Q_t} \quad \sum_{t=0}^{T} Q_t(MC^A - MC_t) \qquad \text{s.t.} \quad \begin{array}{l} Q_0 \;\leq\; Q_t \;\leq\; Q_T \\ Q_T \quad \text{given} \end{array} \tag{1.7}$$

The solution to the optimization problem is:

$$Q_t = \begin{cases} Q_0 & \text{if} \quad MC^A < MC_t \quad \text{for} \quad t \in [0, T-1] \\ \text{Any } Q \in [Q_{t-1}, Q_T] & \text{if} \quad MC^A = MC_t \quad \text{for} \quad t \in [1, T-1] \\ Q_T & \text{if} \quad MC^A > MC_t \quad \text{for} \quad t \in [1, T] \end{cases}$$

The logic of this result is quite simple: the government will obtain the maximum social surplus if conventional sources produce electricity until innovation in wind technology makes it

competitive with conventional sources. Once the wind farm investors do not require subsidies, they will install the needed amount of generation capacity without government intervention. This is not, however, what we observe in the data. The US government has been supporting wind technologies for decades, and as a result, it has deployed the second largest amount of capacity in the world after China (Global Wind Energy Council, 2019).

The fact that the US government deploys a significant amount of wind technology implies that by supporting wind technology, either it delivers social benefits different from least-cost generation, or it actually tries to impact the pace of innovation. Other benefits of promoting wind technology may include environmental benefits, developing the domestic wind technology manufacturing sector and creating new jobs (EWEA, 2012).

1.5 Conclusion

Supporting faster innovation in wind energy technology requires an understanding of the drivers of technological innovation. However, this is not feasible without an accurate measure for innovation itself. This paper generates such data and thus fills a gap in the wind energy technology innovation literature. Our innovation data represents production cost reductions of wind turbine vintages installed in the US between 1998 and 2017. Computations of production costs are based on an engineering model, which allows us to exclude factors that can change production costs, but which do not contribute to technological innovation.

After generating our more accurate innovation measure for wind energy technology, we illustrate its potential use. We analyze the learning curve, which measures correlations between the wind energy technology deployment rate and innovation. Our innovation measure improves the fit of the learning curve in comparison to alternative measures. The results show strong correlations between the wind energy technology deployment rate and innovation.

Abbreviations Used

AEP	Annual Energy Production
BOS	Balance of System
CRF	Capital Recovery Factor
FDM	Fully Deregulated Market
ISO	Independent System Operator
LCOE	Levelized Cost of Energy
LECOE	Levelized Engineering Cost of Energy
NREL	National Renewable Energy Laboratory
O&M	Operations and Maintenance
PDM	Partially Deregulated Market
PPA	Power Purchasing Agreement
PPI	Producer Price Index
PTC	Production Tax Credit
REP	Retail Electricity Provider
RPS	Renewable Portfolio Standards
VIM	Vertically Integrated Market

Appendix 1. Supplementary Materials

1.A. Wind Turbine Vintage Characteristics

Vintage	CAP (kW)	RD (m)	HH (m)
1998	710	47.2	52.3
1999	720	48.2	56.6
2000	800	49.4	58.7
2001	890	53.1	58.2
2002	890	52.8	62.9
2003	1370	67.8	67.4
2004	1220	65.1	66
2005	1500	75.3	75.7
2006	1610	77.9	76.2
2007	1650	79	78.2
2008	1670	79.3	78.5
2009	1740	81.5	78.8
2010	1800	84.2	79.8
2011	1970	89	81
2012	1950	93.4	83.8
2013	1860	96.9	80.5
2014	1940	99.5	82.7
2015	2010	102.4	82.4
2016	2150	108.2	83
2017	2320	113	86

Notes: CAP - Turbine capacity; RD - Rotor diameter; HH - Hub height; all values are average characteristics of newly installed turbines. Units in the brackets. The data are borrowed from (Wiser & Bolinger, 2018) data-file.

1.B. Distribution of Wind Turbine Class

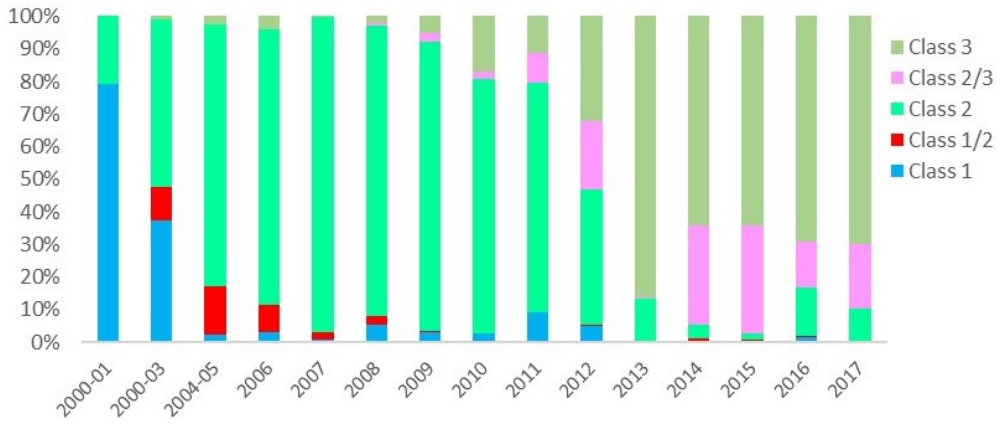

Notes: The figure shows that wind electricity producers have increasingly favored class 2/3 and 3 turbines, which are more suitable for lower wind-speed areas since 2012. Source: The data are borrowed from Wiser and Bolinger (2018).

1.C. *LECOE* and Its Components

Vintage	Turbine Cost^{new} ($/kW)	BOS^{new} ($/kW)	Turbine Cost^{old} ($/kW)	BOS^{old} ($/kW)	O&M ($/kW/yr)	AEP (h/yr)	LECOE^{new} ($/MWh)	LECOE^{old} ($/MWh)
1998	985	584	922	498	77	2520	89	84
1999	1030	579	943	506	76	2608	87	82
2000	994	537	922	493	75	2538	86	82
2001	962	502	938	481	73	2596	81	80
2002	1001	501	943	488	72	2620	81	79
2003	927	391	1007	449	70	2762	71	75
2004	959	419	1016	462	69	2801	71	74
2005	1005	378	1111	458	67	3009	66	72
2006	990	365	1118	452	66	3008	64	71
2007	998	361	1128	452	64	3028	64	70
2008	995	358	1127	451	63	3023	63	70
2009	994	352	1143	449	61	3047	62	69
2010	1006	348	1173	450	60	3106	60	69
2011	1004	336	1205	447	59	3143	59	68
2012	1032	343	1306	458	58	3305	57	68
2013	1084	353	1409	465	51	3466	54	66
2014	1074	350	1437	466	52	3498	53	66
2015	1011	344	1468	465	51	3527	51	66
2016	1025	339	1537	466	49	3581	50	66
2017	1033	331	1581	470	42	3611	47	65

Notes: Costs are expressed in 2015 US dollars. Source: Author's own computations.

1.D. Deployment of the Wind Technology in the US

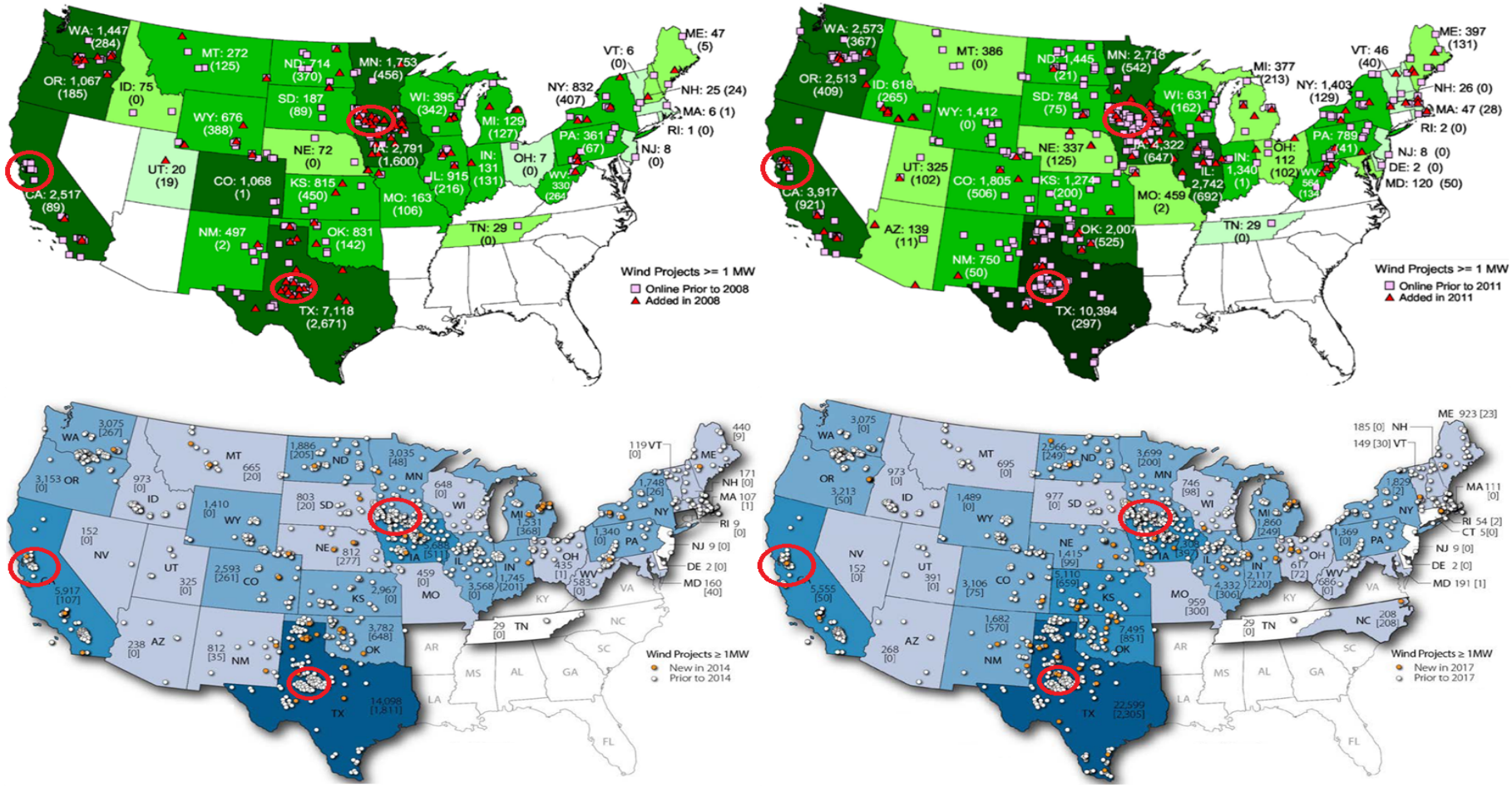

Notes: The numbers displayed within states with and without brackets represent cumulative and annual installed wind capacities, respectively in megawatts. The figure shows that new wind turbines have mostly been installed near exploited wind farm areas and in densely populated locations. This implies that geographic constraints have not crowded out new wind vintages to worse wind resource areas. The red circles show clusters of wind farms, for which we analyzed the changes in the wind quality in the following figure.

Source: The maps are borrowed from (Wiser & Bolinger, 2008-2018)

1.E. Distribution of Wind Speed Across Vintages

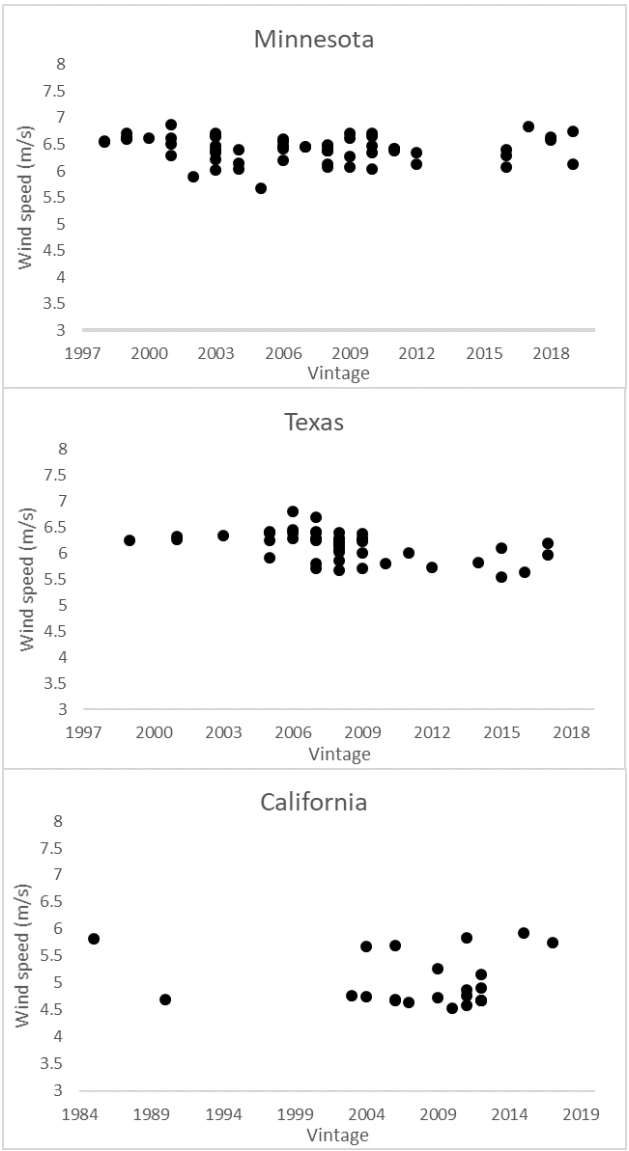

Notes: The following figure shows the wind speed distribution across various vintages for three clusters of wind farms in Minnesota, Texas and California. The wind speed data is taken from the global wind atlas (Technical University of Denmark, 2017) at 50 meters altitude in the exact location of chosen wind farms. For the analysis, we picked a reference wind farm in each of the three states and collected the wind speed information for all operational wind farms within a hundred-kilometre distance from the reference wind farms. The reference wind farms are the Stoneray Wind Farm in Minnesota, the Loraine Wind Farm in Texas and the Solano Wind Project in California. The clusters of wind farms are circled on maps in Figure 1.D. We chose a hundred-kilometre distance in order to have sufficient wind farms to reveal any trend in the wind speed distributions across vintages. The graphs do not reveal a downward trend in wind speed at the cluster level. This indicates that the marginal costs have not been increasing due to the crowding out of wind farms to less windy areas, given the location.

1.F. Cumulative Number of Wind Electricity Generating Firms on the US Electricity Markets

Year	CAISO	ERCOT	ISO-NE	MISO	NYISO	Northwest	PJM	SPP	Southwest
1998	0	0	0	2	0	1	0	0	0
1999	5	2	0	6	0	2	0	4	0
2000	5	2	0	7	2	2	1	4	0
2001	6	4	1	13	2	5	1	6	1
2002	8	4	1	16	2	5	1	6	1
2003	9	8	1	20	2	7	2	7	4
2004	10	8	1	22	2	7	2	7	6
2005	13	10	1	24	3	11	3	9	6
2006	13	11	2	27	3	17	4	11	8
2007	13	18	3	35	6	19	5	11	10
2008	15	27	4	45	7	23	8	15	11
2009	16	31	6	53	9	24	14	21	14
2010	17	33	8	60	10	28	16	23	14
2011	19	36	12	69	11	32	19	27	17
2012	24	44	24	89	13	42	29	35	20
2013	24	44	24	89	13	42	29	36	21
2014	26	47	24	93	13	45	31	40	21
2015	26	55	27	96	14	45	33	48	22
2016	26	59	33	100	14	48	36	50	23
2017	26	62	34	107	14	53	37	53	23

Notes: The table shows the number of wind electricity generating firms which has entered each US electricity market in 1998-2017. Since we have counted the number of firms based on the owners of the operating wind farms, the table may be omitting those wind farm owners who installed turbines during this period, decommissioned them and exited the market. However, such cases are extremely small, because the expected useful life of wind farms is at least twenty years. Therefore, the proportion of decommissioned farms is very small (U.S. Energy Information Administration, 1998-2017). In addition, it is highly likely that such firms owned some other operating wind farms, and hence, they are still included in the table.

1.G. Number of Potential Power Purchasers in US Electricity Markets

Markets	Purchasers	Covered States	Source
CAISO	About 60 utilities	Covers California	https://www.energy.ca.gov/almanac/electricity_data/utilities.html#iou
ERCOT	More than 100 utilities. At least 40 REPs	Texas	https://callmepower.com/tx/utility
ISO-NE	More than 15 utilities	Connecticut, Maine, New Hampshire, Massachusetts, Rhode Island and Vermont	http://www.bestenergynews.com/solar/utility_co/utility_companies.php
MISO	More than 80 utilities. More than 50 REPs	Arkansas, Luisiana, Michigan, Minnesota, Wisconsin, parts of Illinois, Indiana, Iowa, Mississippi and Missouri	https://www.misoenergy.org/stakeholder-engagement/members/
NYISO	7 large utilities and many small ones	New-York	http://www.bestenergynews.com/solar/utility_co/utility_companies.php
Northwest	About 20 utilities	Idaho, Nevada, Oregon, Washington, Parts of Montana and Wyoming	http://www.bestenergynews.com/solar/utility_co/utility_companies.php
PJM	About 50 utilities and about 85 REPs.	Delaware, Meriland, New Jersey, Ohio, Pennsilvania, Virginia, West Virginia, Part of Indiana and part of Kentucky	https://www.pjm.com/about-pjm/member-services/member-list.aspx
SPP	More than 60 utilities	Kansas, Nebraska, Oklahoma, South Dakota, and small parts of contiguous states	https://www.spp.org/about-us/members-market-participants/
Southwest	About 10 utilities	Arizona, New Mexico, Colorado and small parts of contiguous states	http://www.bestenergynews.com/solar/utility_co/utility_companies.php

Notes: The table shows the number of potential electricity purchasers: utilities and REPs in each electricity market. The list omits some of the potential electricity purchasers, such as end-use consumers who directly purchase electricity and the power marketers who engage in the resale of electricity.

1.H. Impact of Curtailment on Capacity Factors

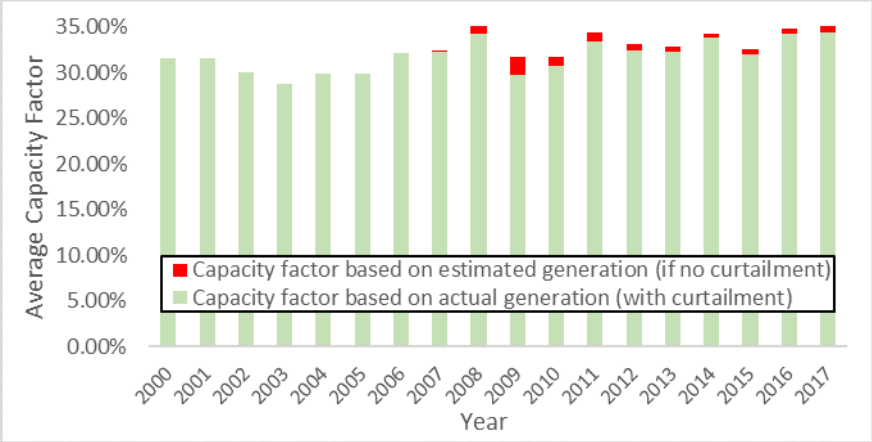

Notes: The figure shows the impact of curtailment on average capacity factors of wind generation in the US. Since curtailment has affected 0.1-1 percent of total generation each year, the revenues of the producers are unlikely to be significantly affected. In addition, forced curtailment is usually compensated. Source: Wiser and Bolinger (2018) data file.

1.I. Relationship Between LECOE and Cumulative Capacity

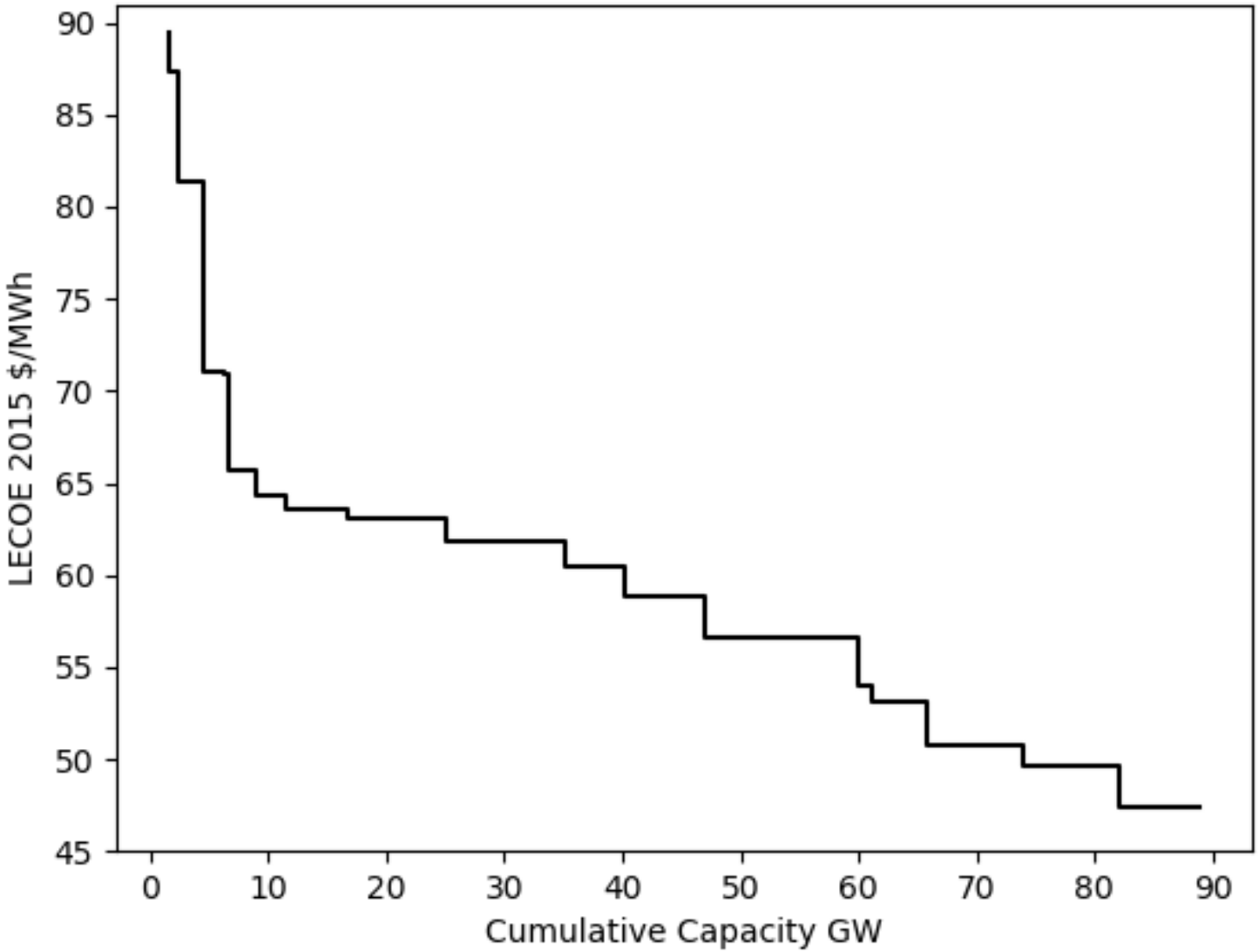

Source: LECOE - Author's own computations; cumulative capacity - Wiser and Bolinger (2018) data file

1.J. Estimation of Learning Curve with Cumulative Capacity

Parameters	(1) LECOE - NM	(2) LECOE - OM	(3) LCOE - W&B
c_0	92.274***	85.114***	88.082***
	(3.40)	(1.66)	(13.89)
A	0.584	1.146	5.242
	(0.32)	(0.68)	(24.31)
α	0.157***	0.060***	0.055
	(0.02)	(0.01)	(0.04)
Root MSE	3.626	1.710	13.908

Notes: Standard errors in parentheses. * $p < 0.05$, ** $p < 0.01$, *** $p < 0.001$. The table reports estimation results of the learning curve model in equation 1.6 using three alternative sets of innovation measures. Abbreviations NM, OM and W&B, relate to the innovation measures obtained from the new model, old model, and Wiser and Bolinger (2018), respectively. The explanatory variable is cumulative capacity.

1.K. Estimation of Learning Curve with Cumulative Quantity

Parameters	(1) LECOE - NM	(2) LECOE - OM	(3) LCOE - W&B
c_0	89.247***	83.626***	88.358***
	(1.37)	(0.74)	(13.69)
A	0.407*	0.986*	40.606
	(0.15)	(0.44)	(306.68)
α	0.091***	0.035***	0.030
	(0.01)	(0.00)	(0.02)
Root MSE	1.970	0.975	13.734

Notes: Standard errors in parentheses. * $p < 0.05$, ** $p < 0.01$, *** $p < 0.001$. The table reports estimation results of the learning curve model in equation 1.6 using three alternative sets of innovation measures. Abbreviations NM, OM and W&B, relate to the innovation measures obtained from the new model, old model, and Wiser and Bolinger (2018), respectively. The explanatory variable is the cumulative quantity.

Chapter 2

The Role of Biomass in Decarbonization Efforts: Spatially Enriched Energy System Optimization Modelling

---

Originally published as:
Rečka, L., Ščasný, M., & Laxton, D. T. (2023). The Role of Biomass in Decarbonization Efforts: Spatially Enriched Energy System Optimization Modelling. *Energies*, 16(21), 7380.

2.1 Introduction

One way to combat climate change is to promote renewable energy sources (RESs). Most countries worldwide support RES investment and have set targets to increase their share of total energy consumption. On 17 September 2023, the European Parliament agreed to boost the deployment of renewable energy in line with the European Green Deal and REPowerEU plans. This update of the Renewable Energy Directive (RED) increases the share of renewables in EU final energy consumption to 42.5% by 2030, whilst the EU Member States should strive to achieve 45%.

Following this legislation, in September 2023, the Czech government prepared the actualization of its National Energy and Climate Plan, which relies heavily on combining renewable and nuclear energy sources. To date, biomass has been the most crucial source of clean energy in Czechia, as has been the case in most central European countries. Due to the limited capacity of biomass, other renewable energy sources—wind and, in particular, solar energy—will become more important sources of clean energy in the future energy mix. However, biomass has the potential to be a flexible source, unlike many other RESs, because it can be burned in conventional power plants. One drawback, though, is that forests can be some distance from power plants, and transporting biomass can be costly (Stolarski, Stachowicz, Sieniawski,

Krzyżaniak, & Olba-Zięty, 2021), limiting its economic potential.

Moreover, the central European region has recently experienced a spruce bark beetle infestation (Hlásny, König, et al., 2021), which has cast doubt on the medium and long-term accessibility of forest biomass for energy production. This paper analyzes the role of forest biomass in the decarbonization of the Czech energy system, considering the EU requirements, ecological constraints, and economic limitations, by using a spatially enriched energy system model.

The need to practice reliable and science-based energy system modelling (ESM) has been growing as a direct response to policymakers' calls for strategies and plans to reach a carbon-neutral future. Although many such models have been built and applied for decades, they still face multiple modelling challenges to providing realistic and effective energy transition plans. Energy system optimization models search to identify cost-minimal pathways, assuming perfect behaviour from a central planner's perspective and neglecting decision making under uncertainties or biased perceptions and behaviour. This modelling feature often leads to inaccurate assumptions regarding the requirements of a successful energy transition. As a result, ESM underestimates the required capacities for power generation, storage, and transmission compared with real-world energy systems, which is a phenomenon known as the "economic granularity gap" (Sarfarazi, Sasanpour, & Cao, 2023). Furthermore, a review by Fodstad et al. (2022) identifies four main challenges in ESM: the handling of several energy carriers within the system analyzed, how uncertainty is dealt with, the integration of energy transition dynamics and energy behaviour, and the integration of different scales regarding time and space; the latter aspect has also been most frequently identified as the main modelling challenge in previous reviews.

The first contribution of our paper is to enrich the literature that deals with spatial resolution in cost-optimization ESM. In principle, the spatial granularity of the model can be improved by linking ESM to a Geographic Information System (GIS) or by increasing the resolution of the model with respect to space. While the former involves an assessment of meteorological conditions, and the deployment and expansion of energy infrastructure or land availability, the latter modifies model granularity to realistically map the potential and availability of RESs or to analyze optimal power-plant siting (see more in ref. Martínez-Gordón, Morales-España, Sijm, and Faaij (2021)). Because transporting biomass to a power/heat plant can entail considerable costs, GIS linkage or finer spatial granularity allows the model to consider distances directly in energy system cost optimization.

There are several examples of studies that have implemented regional aggregation of electricity and climate data: see, for instance, refs. Carpio (2021); Castillo, e Silva, and Lavalle (2016); Holttinen et al. (2011); Monforti et al. (2014); Pfenninger and Staffell (2016); Roques, Hiroux, and Saguan (2010); Yang et al. (2019). Maimó-Far, Homar, Tantet, and Drobinski (2022) analyze the effects of spatial granularity on an optimal renewable (wind and solar) energy portfolio in Spain. However, literature on spatially enriched ESM is relatively recent and sparse (Martínez-Gordón et al., 2021). Resch et al. (2014) and Ramirez Camargo and Stoeglehner (2018) discuss the integration of spatial resolution and ESM but mainly focus on GIS applications, while other studies have aimed to investigate how spatial data aggregation improves the precision of results (e.g., Hörsch and Brown (2017)). A very recent review by Martínez-Gordón et al. (2021) identifies several ESM applications based on a

finer spatial resolution in biomass energy; however, the majority of the applications aim to analyze optimal locations of biomass power plants based on proximity to biomass sources, including transportation costs. Three other studies have aimed to calculate the potential and availability of certain types of biomass; however, these studies have focused only on limited biomass sources, such as residual biomass (Lozano-García, Santibañez-Aguilar, Lozano, & Flores-Tlacuahuac, 2020), biomass from agricultural land (Knápek, Králík, Vávrová, & Weger, 2020), or biomass planted on marginal lands (Zhang, Hastings, Clifton-Brown, Jiang, & Faaij, 2020).

We enrich the TIMES (Rečka & Ščasnỳ, 2016, 2018, 2017) energy system optimization model by splitting three components of the otherwise country-wide ESM—forest biomass availability, power and heat, and industry production and energy services consumption—into 14 relatively small sub-systems (≈3000-11,000 km^2) defined by EUROSTAT's NUTS3 regions. This allows us to vary the transportation costs of biomass by distance from the sources to the generation units (grouped into 14 sub-systems) and, hence, to evaluate the economic costs of biomass more precisely. The level of granularity in the TIMES-CZ model is beneficial in a number of ways. Because forest biomass is not evenly distributed throughout the country, a regionalized model more accurately reflects the costs associated with transporting forest biomass. For example, forest biomass is abundant in southwestern Czechia. As the cost of transporting biomass increases with distance, a regionalized TIMES-CZ model can make more informed decisions on where to establish new biomass-burning or co-burning facilities. Increasing spatial granularity also brings our TIMES-CZ model closer to the real-world energy system. To the best of our knowledge, no comprehensive regionalization of any optimization ESM has been conducted prior to this study.

The second contribution of this paper is its evaluation of the potential impact of the spruce bark beetle infestation on the Czech energy system until 2050. Before the infestation, spruce trees made up roughly half of Czech forests (Lorenc, 2022). Prolonged periods of drought and increased temperatures, together with bark beetles, have been quickly destroying spruce trees since 2012. The paths through which the spruce bark beetle infestation may evolve up to 2070 have recently been conceptualized by the Institute for Forest Ecosystem Research (IFER), which built four possible scenarios on the availability of forest biomass given the spread of spruce beetles and the Land Use, Land Use Change, and Forestry (LULUCF) (Cienciala & Melichar, 2023). Based on these scenarios, we quantify the potential availability of forest biomass for energy purposes. Because forest biomass is unequally distributed across regions and the spruce beetle infestation is not uniform (Hlásny, Zimová, et al., 2021), our regionalization of forest and energy system modelling was performed using the same spatial granularity.

Applying our spatially enriched TIMES-CZ model, we analyze impacts on the energy mix, decarbonization efforts, and final allocation of forest biomass resources up to 2050. Specifically, we incorporate forest biomass projections, based on Cienciala and Melichar (2023), into our regionalized TIMES-CZ model. The previous version of the TIMES-CZ model (Rečka, Máca, & Ščasnỳ, 2023) had limited ability to distinguish energy production and demand technologies by location. The model employed in this paper offers a spatial resolution that more effectively accounts for potential transportation costs. It identifies a more realistic allocation of final energy resources and the decisions on where to install new heat and power plants.

Third, our paper contributes to the current literature by examining the role of forest biomass in achieving greenhouse gas emission (GHG) reduction targets in Czechia, considering that forests have become heavily infested with spruce bark beetles in the last ten years. We analyze energy system pathways, GHG emissions, and RES targets for four main 'ecological' scenarios on forest development in Czechia: RED anticipates that the spruce beetle infestation will subside, GREEN assumes the infestation will end soon, and 6% more timber can be harvested. In BLACK, the infestation will continue to spread in Western regions, and in BLACK-REP, it will resurge every ten years. We then change policy measures and GHG emissions targets in the following three RED scenarios: RED-P50 assumes a 50% production cost subsidy on wood pellets, RED-HH requires the exclusive use of biomass in households, starting from 2035 in accordance with ecological requirements, in order to maximize biomass remaining in forests, and RED-0 is the only scenario in which GHG emissions are set to be reduced to near-zero, reaching a maximum emission balance of 2.2 Mt by 2050. Our main research question is whether the availability of forest biomass affected by the bark beetle infestation and biomass costs could pose challenges for Czechia to contribute sufficiently to the EU's 2030 RES target and to achieve climate neutrality by 2050.

The rest of this paper is structured as follows. Section 2.2 describes the model and data. The next section describes the scenarios and the key assumptions. Section 2.4 presents and discusses the results of the modelling. Section 2.5 concludes.

2.2 The Regionalized TIMES-CZ Model and Biomass Availability

TIMES is an energy system optimization model that operates from a bottom-up perspective. It seeks the most cost-effective path to fulfil energy service demands under given constraints. The TIMES is developed and maintained as part of the Energy Technology System Analyses Program (ETSAP) by the International Energy Agency (IEA) (Loulou, Goldstein, & Noble, 2004). Originally, the TIMES-CZ model was based on the Czech region of the pan-European TIMES PanEu model, which was developed by the Institute of Energy Economics and Rational Energy Use at the University of Stuttgart (Capros et al., 2014). Since the introduction of the initial version, the TIMES-CZ model has undergone enhancements, including the incorporation of individual facilities operating within the scope of the EU Emission Trading System (EU ETS) (Rečka & Ščasnỳ, 2016, 2018) and the inclusion of a comprehensive transportation module (Rečka et al., 2023).

In this paper, we update and extend the TIMES-CZ model considerably in several ways. We update the base year of the model to 2019. Although data for 2020 were available, we chose 2019 to avoid bias caused by the COVID-19 pandemic restrictions in 2020. We split three components of the otherwise country-wide ESM—forest biomass availability, power and heat, and industry production and energy services consumption—into 14 relatively small sub-systems (≈3000-11,000 km^2) defined by EUROSTAT's NUTS3 regions. We use individual data on facilities participating in the EU ETS scheme, annual reports on electricity and heat grids (ERU, 2019a, 2019b), regional energy balances (Ministry of Industry and Trade.,

2021), and sample surveys on energy consumption in households (CZSO, 2017) to divide data on power, heat, and industry production and energy services consumption into 14 NUTS3 regions. Figure 2.1 represents regionalized Czechia. Only transport and non-energy-intensive industry production remain aggregated at the level of Czechia as a single region due to a lack of regionalized data in this area.

Figure 2.1: Czech NUTS 3 regions

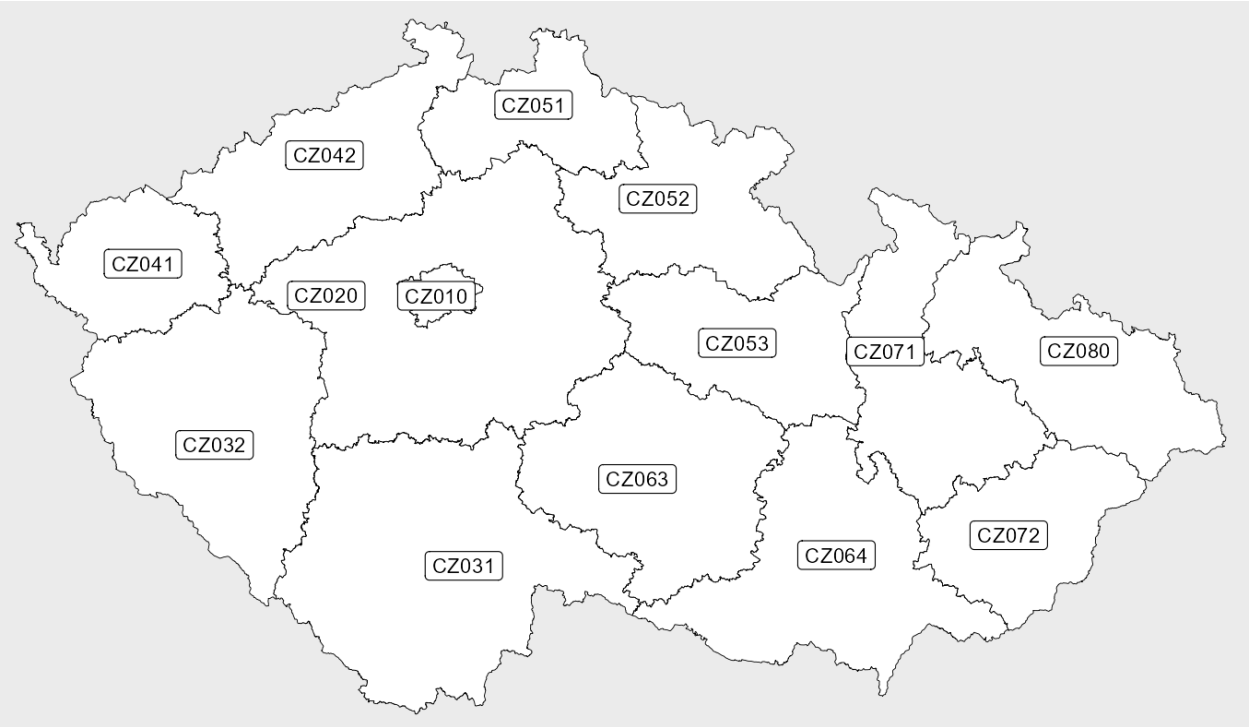

Notes: Czech NUTS 3 regions are the building blocks of our regionalized TIMES-CZ model.

We categorize forest biomass based on both the harvesting method and its form of energy utilization. Additionally, we incorporate the forest biomass development scenarios projected by Cienciala and Melichar (2023) to estimate biomass availability for energy purposes. Further elaboration on this biomass extension is provided in subsequent sections.

Spruce bark beetles have become a major problem for Czech forests since 2012 (Lorenc, 2022). These beetles destroy massive areas of forests, as spruce is one of the most widespread species of trees (Janová, Hampel, Kadlec, & Vrška, 2022). With climate warming, bark beetles multiply even faster (Hlásny, Zimová, et al., 2021), and the pace of felling trees and removing them from the forests has failed to keep pace. The infestation threatens the availability of biomass for various purposes, including energy. Our paper focuses exclusively on forest biomass and does not consider biomass from agricultural and marginal lands, unlike Knápek et al. (2020). Therefore, when we mention biomass in the text, we imply solely forest biomass.

IFER analyzed possible pathways for managing and adapting Czech forests to respond to the challenge (Cienciala & Melichar, 2023). They designed four possible scenarios envisioning forest development and the amount of timber harvested, taking into account probable changes in forest management and the impact of spruce bark beetle infestation. Considering these

scenarios, we calculated the percentage of biomass available for energy purposes, factoring in the past patterns of all potential uses of forest biomass (e.g., energy, timber, production of furniture, pulp, and paper). These scenarios include all types of biomass, both softwoods and hardwoods, which are referred to as conifers and broadleaf, respectively. Biomass is classified into three narrower categories based on its most likely use: firewood, forest chips, and white chips. This classification indicates the quality of the wood itself, but not necessarily its final state. For example, white chips are raw materials and can be transformed into wood pellets, but they may be used for other purposes, retaining their original state.

In the following, we define all four scenarios. The RED scenario, which we use as the baseline, anticipates that the spruce beetle infestation will subside. The GREEN scenario predicts that the infestation will end sooner than in RED and enable a 6% greater timber harvest than in the other scenarios. The BLACK scenario conjectures that the infestation will spread into more western regions given the riskiness level involved, and finally, the BLACK-REP scenario envisions that the infestation will repeat every decade. Figure 2.2 depicts the maximum possible amount of biomass harvest for energy purposes by categories under these four scenarios.

Figure 2.2 shows four biomass products. For firewood, the authors consider the distinctions between broadleaf and conifer relevant, while such a distinction is not crucial for forest chips and white chips. In the model, firewood and white chips are primarily used in the residential sector, because most white chips are transformed into wood pellets. In contrast, forest chips are favoured for power, heat production and industrial sectors. Figure 2.2 depicts the maximum possible supply of each type. To avoid the unnecessary conversion of biomass into more expensive products, such as wood pellets, the model directs unprocessed white chips to power, heat, and industry. From Figure 2.2, it is clear that the largest differences between forest biomass development scenarios occur in 2025-2035. Nevertheless, the magnitude may not be large enough to create significant differences in the final allocation of resources. The figure also demonstrates the lasting nature of the infestation, especially up to the year 2035. This infestation significantly diminishes biomass availability by more than 14% in both the RED and BLACK scenarios. The biomass flows in the TIMES-CZ model are shown in Figure 2.3. To produce biomass products, we assume a stepwise cost function with decreasing returns to scale in Table 2.1.

Our regionalized TIMES-CZ model considers distance-specific and time-variant transportation costs. Our assumptions on moisture, gross calorific value, weight, and truck volume capacity to calculate average transportation costs for different biomass products are described in Table 2.2.

Wood pellets and briquettes made from white chips are available from online shops for fixed transportation costs of around €55. Given our assumptions listed in Table 2.2, the transportation of wood pellets costs about 0.8 €/GJ regardless of the distance.

Calculating the transportation cost of firewood is more complex. Firewood is typically sold in one-cubic-meter pallets, where, depending on whether the wood is stacked or not, weight and embodied energy will differ (TZB-info, 2022). Coniferous firewood is lighter and has less embodied energy than broadleaf firewood per cubic meter. Furthermore, the maximum transportation volume by service providers is limited. We rely on average figures and assume

Figure 2.2: Biomass availability for energy purposes 2019-2050

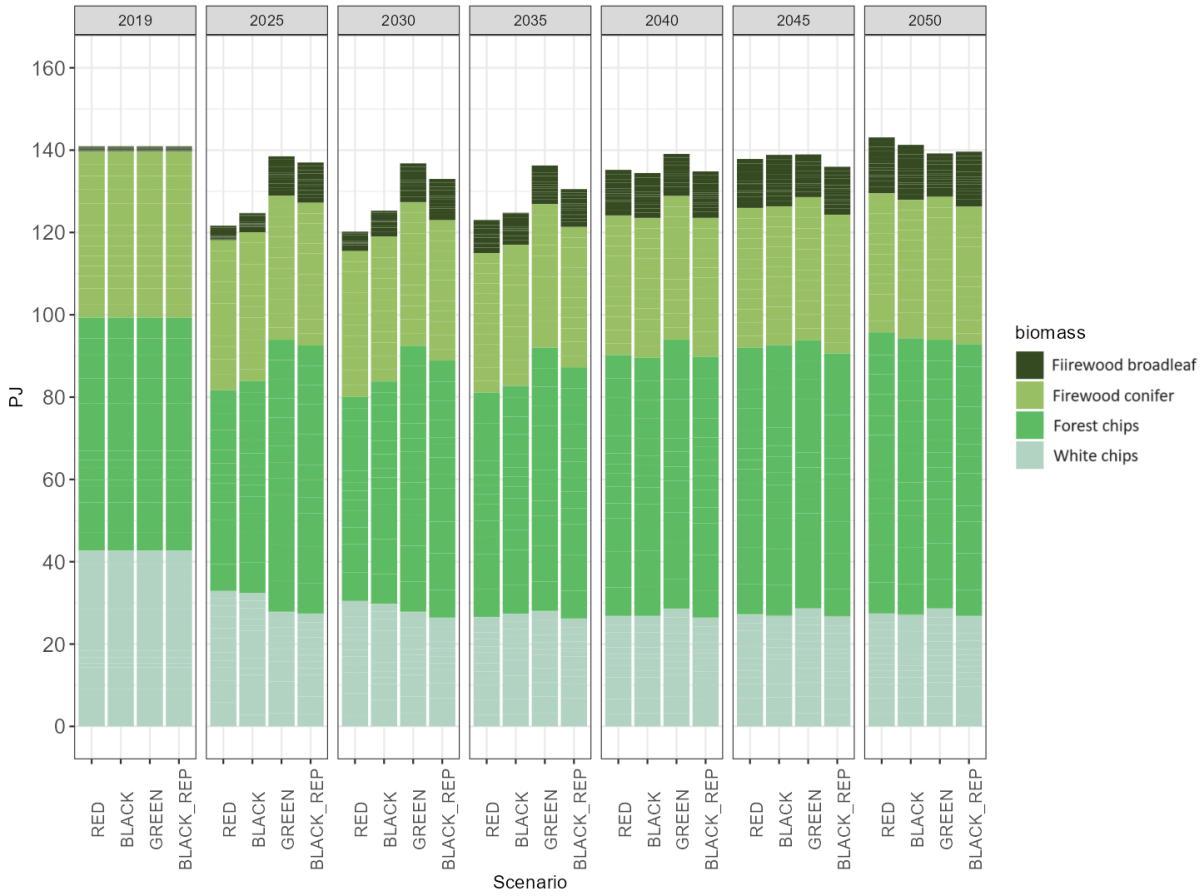

Source: Authors' computations based on Cienciala and Melichar (2023). Notes: Biomass is broken down into four products based on their most likely use.

Figure 2.3: Biomass flows in the TIMES-CZ model

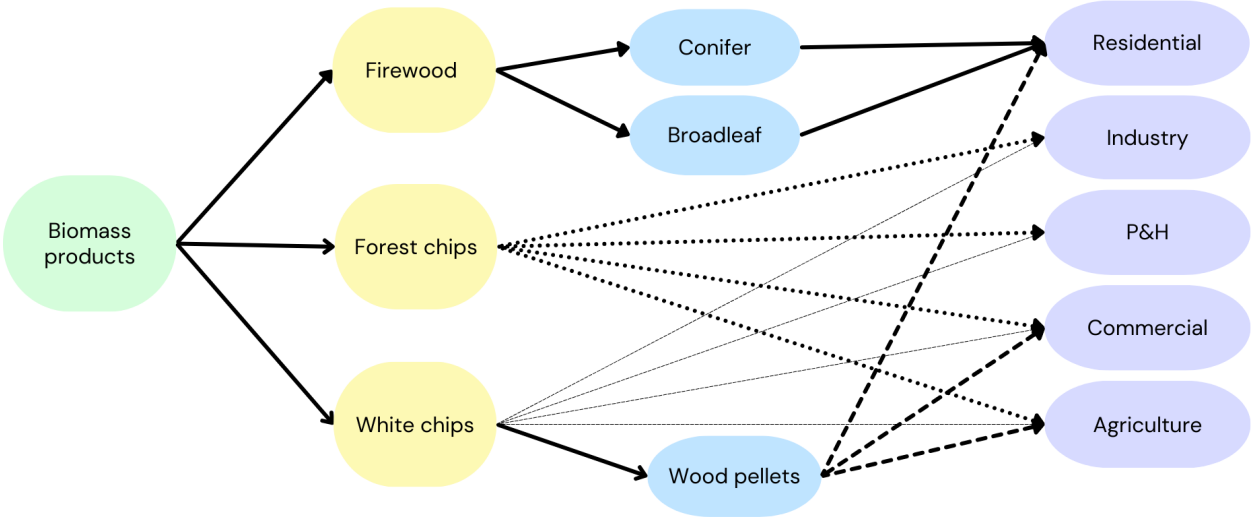

Table 2.1: Costs of biomass production, stepwise cost function, in €/GJ (2015 prices).

Biomass Product	Cost Steps
Firewood conifer	0.10, 9.50, 11.1, 12.7, 14.3
Firewood broadleaf	10.8, 15.0
Wood Pellets	12.0, 12.5, 13.0, 13.5, 14.1, 14.6, 15.1, 15.6
White chips	6.30
Forest chips	4.70, 5.10, 5.50, 5.90, 6.30

Note: We assume a stepwise production cost function of biomass products with decreasing returns to scale. The number of equal steps in the production cost function within each biomass product increases with the total availability of the biomass product. The biomass available for energy purposes, estimated on the basis of IFER data (Cienciala & Melichar, 2023), is 27 PJ less than the biomass consumption in the energy balance in 2019 (Ministry of Industry and Trade, 2021). This gap is assumed to represent the households' own firewood production, which we have assumed to have close to zero cost. Source: Czech Statistical Office (CZSO, 2019).

Table 2.2: Assumptions used to calculate transportation costs of biomass per trip.

Biomass Product	Volume (m^3)	Weight (kg/m^3)	GCV (MJ/kg)	Moisture (%)
Firewood conifer	9	340	15.6	15
Firewood broadleaf	9	475	14.6	15
Wood pellets	4-5 *	-	18.0	10
Forest chips	85	170	16.4	10

Notes: * Tons, rather than cubic metres, are used to measure the size of wood pellets per trip. Typical homeowners use about 4-5 tonnes of wood pellets per year. Forest chips are primarily used in the power, heat, and industrial sectors, where transporting larger quantities in one trip is more likely; we assume the maximum capacity of a truck at 85 m^3. Source: Lyčka (2010); Avydon (2023); TZB-info (2022); Vytečka (2016); Wang and Rakha (2017); Natural Resources Canada (2014).

nine cubic meters of capacity (if stacked) to calculate the total embodied energy transported per trip. According to TZB-info (2022), one cubic meter of wood pallet contains roughly 475 kg of broadleaf wood with a gross calorific value of 14.6 MJ/kg and 340 kg of coniferous wood with a gross calorific value of 15.6 MJ/kg with a moisture content of 15%. The embodied energy E_b carried per trip is then a product of volume, weight and gross calorific value (and 1000 to obtain GJ).

To calculate the total biomass transportation cost per trip, we first derive a 14 × 14 distance matrix between the centres of Czech regions to allow for trade between them. Because transportation companies typically charge for both the outbound and inbound transportation of biomass, we double the distance between regions i and j (D_{ij}). Based on a review of the offers by transportation companies, we obtain the average transportation cost per kilometre (C_0) that is increasing over time t due to pricing fuel within the EU ETS2 (column 3, Table 2.3) and $k = 1.08$ kg CO_2/km (we assume large transport trucks consume roughly 0.4 L of diesel per kilometre (Wang & Rakha, 2017) and each litre of diesel produces 2.7 kg of CO_2 (Natural

Table 2.3: EUA carbon price trajectory.

Year	EUA1	EUA2
2030	75	47
2035	113	131
2040	235	216
2045	339	301
2050	386	386

Notes: The EUA ETS prices are expressed in €2015 / tCO_2. The EUA's projections are based on the recommendation of the European Commission on Harmonised Common Trajectories for the With Additional Measures (WAM) Scenario, HCT 2023 WAM (European Comission Directorate-General Climate Action, 2023). EUA2 represents the revized ETS price trajectory linked to the ETS2 package, commencing at €47 and linearly converging to match EUA1 prices by 2050.

Resources Canada, 2014), giving $k = 1.08$ [kg CO_2/km]). Dividing the total transportation cost between two regions i and j by the embodied energy E_b of transported biomass product b, we obtain transportation costs TC_{btij}, which are expressed in €/GJ between regions i and j by biomass products b:

$$TC_{btij} = \frac{2 \times D_{ij} \times (C_0 + EUA2_t \times k)}{E_b}, \qquad i, j \in [0, 14] \tag{2.1}$$

In the model, we also assume the transport of biomass from the regions to the aggregate region of Czechia. We calculate the distance from each region to the Czechia region as an average of all distances, excluding Prague and Brno, where the availability of biomass is not significant. For the rest of the calculations, Equation (2.1) applies.

2.3 Scenarios

This paper primarily examines how different trajectories of forest biomass development will influence the overall energy composition of the Czech economy and Czechia's efforts to attain climate neutrality. We do not present a business-as-usual scenario, as seen in Rečka et al. (2023). Our scenarios share common assumptions about prices, the potential of photovoltaic (PV) and wind energy, and the potential of electricity and hydrogen imports, along with energy service demand projections. The variable availability of biomass depicted in Figure 2.2 is the only difference among our first four scenarios (RED, BLACK, GREEN, BLACK-REP).

We also evaluate three policies using the RED scenario as a baseline. RED-0 requires an exogenous reduction in GHG emissions, resulting in a maximum of 2.2 megaton emissions balance in 2050. The purpose of the policy evaluation is to see whether increased pressure to reduce emissions would encourage renewable production. The RED-HH assumes that starting from 2035, biomass available from forests can only be used by households, meaning that forest chips are no longer available for power, heat, and industrial sectors. This scenario aligns with ecological requirements, maximising the biomass that remains in the forest. The

Table 2.4: Description of scenarios.

Scenario Name	Carbon Pricing	GHG Cap	Biomass Consumption	Subsidies
RED	HCT WAM	NO	ALL sectors	NO
Green	HCT WAM	NO	ALL sectors	NO
Black	HCT WAM	NO	ALL sectors	NO
Black-REP	HCT WAM	NO	ALL sectors	NO
RED-P50	HCT WAM	NO	Residential (since 2025)	50% prod. cost
RED-0	HCT WAM	3 Mt in 2050	ALL sectors	NO
RED-HH	HCT WAM	NO	Residential (since 2035)	NO

goal of this scenario is to see how the ecological requirements, i.e., limiting the availability of biomass, would affect the overall energy mix and annualized system costs. Finally, RED-P50 considers a 50% production cost subsidy on wood pellets for households from 2025 onwards. Here, the objective is to investigate whether these subsidies facilitate the full utilization of biomass resources. All the scenarios are briefly described in Table 2.4.

The prices of fossil fuels and emission allowances (EUAs) follow the trajectory of the WAM scenario according to the recent HCT trajectory (European Comission Directorate-General Climate Action, 2023). The price of EUA2 for buildings and transport starts at €47 in 2030 and then converges linearly to the current EUA1 price of 2050 (see Table 2.3). We assume energy-saving potentials in buildings according to the progressive scenario of the Czech Strategy of Building Renovation (Ministry of Industry and Trade., 2020). The development of new nuclear power plants is not constrained; however, our assumption is that 1450 MW of new capacity will be installed around 2035. This assumption aligns with the expectations of the Czech Ministry of Industry and the Ministry of Environment. The optimization problem within the model determines any potential installations beyond this 1450 MW threshold. The profile of possible electricity imports is described according to the Czech Transmission System Operator (ČEPS) and assumes no bottlenecks. The maximum installed capacity of wind farms and solar PV is limited to 7 GW and 30.1 GW in 2050, respectively. Hydrogen imports are assumed to rise to 36.7 TWh in 2050. Carbon capture, use, and storage (CCUS) is limited to 18 Mt of captured CO_2 emissions.

2.4 Results

2.4.1 Greenhouse Gas Emissions

Figure 2.4 illustrates greenhouse gas (GHG) emissions across all scenarios, which are categorized by their primary sources of emissions. Meanwhile, the total GHG emissions decline in

all scenarios, reaching 10-20 Mt of CO_2e in 2050. The exception is RED-0, which reaches the pre-defined (exogenous) cap of 2.2 Mt of CO_2e in 2050. We note that the near-zero-carbon level in RED-0 is achieved without any further increase in bioenergy with carbon capture and storage (BECCS).

Figure 2.4: Total greenhouse gas emissions, Czechia, 2025-2050.

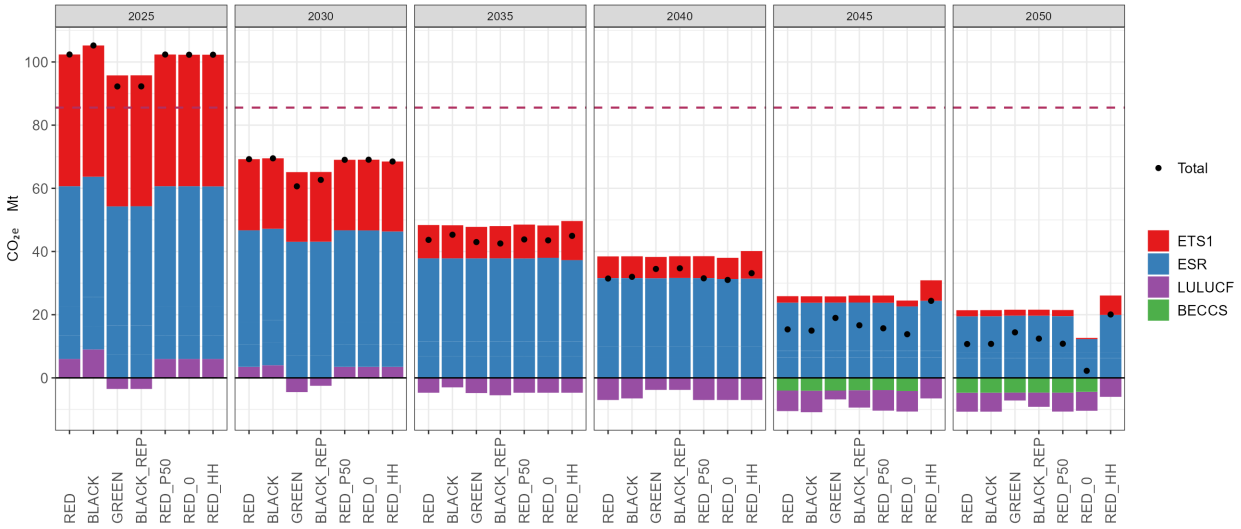

Notes: ETS1 represents the current scope of EU ETS. LULUCF accounts for emissions or carbon savings associated with Land Use, Land Use Change, and Forestry. ESR covers the remaining sectors and small industrial installations. BECCS refers to biomass combustion installations equipped with carbon capture and storage (CCS), resulting in a negative emissions balance. The red dashed line indicates the EU target to reduce greenhouse gas emissions by 55% in 2030 compared to 1990 levels.

It is evident that even with a European Union Allowance (EUA) price of €386 (expressed in 2015 euros), climate neutrality by 2050 remains unattainable. The red dashed line signifies the EU's binding target of a 55% reduction in greenhouse gas emissions for member countries by 2030 compared to 1990 levels, which is a goal that Czechia is realistically poised to achieve across all scenarios.

In the RED-0 scenario, GHG emissions align with the 2.2 Mt CO_2e cap in 2050, with this cap being the sole driver of emissions reduction compared to other RED scenarios. Notably, the RED-HH scenario exhibits relatively higher GHG emissions. In this scenario, only the residential sector utilizes biomass as an energy source starting from 2035, prompting other sectors to replace biomass with alternative energy sources, primarily natural gas. In this particular situation, BECCS, which could have reduced GHG emissions by 4-4.5 megatons in 2045 and 2050, as seen in other scenarios, is unavailable.

The emissions associated with facilities included in the current EU Emission Trading System (ETS1) substantially contribute to reducing GHG emissions. Additionally, sectors covered by the extended system Effort Sharing Regulation (ESR), which includes areas like agriculture, small industrial facilities, transportation, and buildings, also demonstrate noteworthy reductions in GHG emissions (European Comission, 2021). Meanwhile, emissions linked to Land Use, Land Use Change, and Forestry (LULUCF) are the primary factors driving variability in GHG emissions across forest biomass development scenarios RED, BLACK, GREEN, and

BLACK-REP. This underscores the crucial role of forests in sequestering carbon emissions, which appears to be more influential than fluctuations in forest biomass availability for energy use. Therefore, based on Figure 2.4, it can be concluded that the spruce bark beetle infestation does not impact decarbonization pathways in the long term. In the BLACK-REP and GREEN scenarios, LULUCF GHG emissions are negative in 2025 and 2030, while other scenarios incur GHG emissions from forests. Lastly, it appears that using subsidies to promote wood pellet use by households in the RED-P50 scenario does not contribute to achieving GHG emission reduction goals compared to the RED scenario.

2.4.2 Primary Energy Sources

Figure 2.5: Primary energy sources, Czechia, 2019-2050.

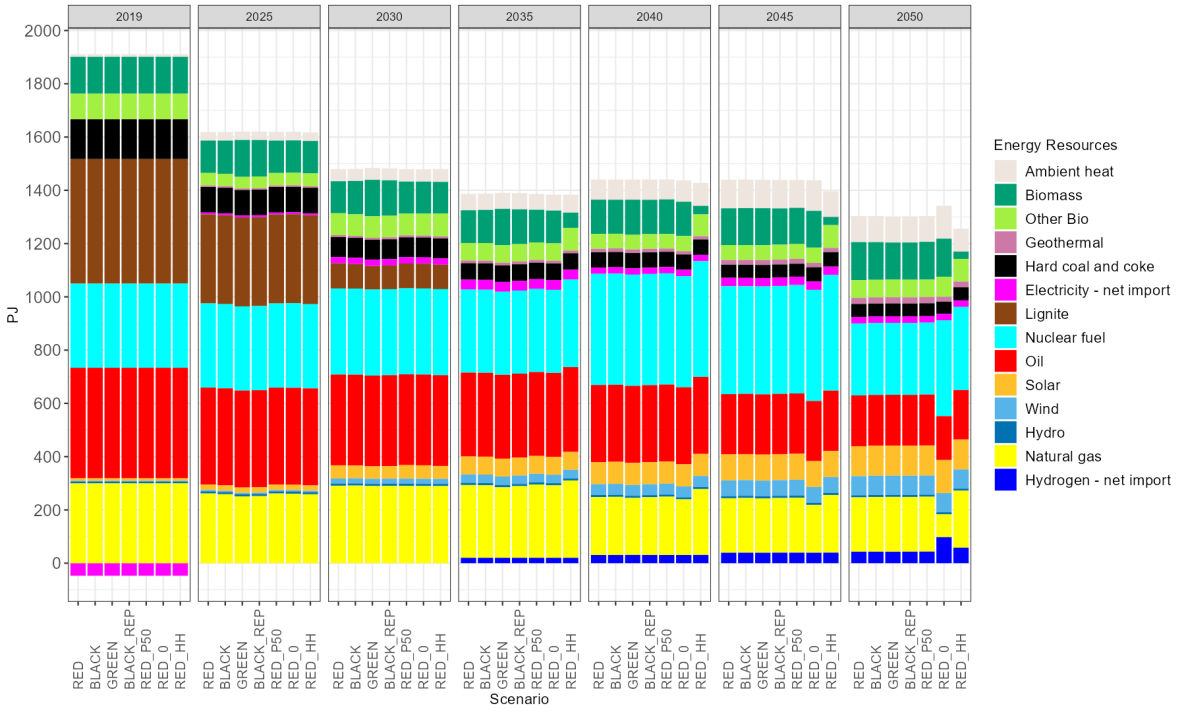

Figure 2.5 shows primary energy sources (PES) consumption spanning 2019 to 2050. An estimation of all modelled scenarios delivers approximately a 30% decrease in the consumption of PES. From 2040, there is a significant decrease in gas consumption, which is primarily replaced by hydrogen, whereas brown coal will be almost phased out by 2035. Limiting biomass to household consumption RED-HH and pursuing ecological constraints primarily involves substitution by natural gas and nuclear energy, with a GHG cap of a net 2.2 Mt in 2050. Conversely, in the RED-0 scenario, the primary replacements for natural gas and oil include hydrogen, nuclear, and ambient heat technologies. Solar and wind energy are maximally utilized in all scenarios. The degree of availability of biomass significantly influences its usage in all scenarios, with only a temporary deviation occurring in 2040, where biomass demand lags behind its increased availability.

2.4.3 Final Energy Consumption

Figure 2.6: Final energy consumption, Czechia, 2019-2050.

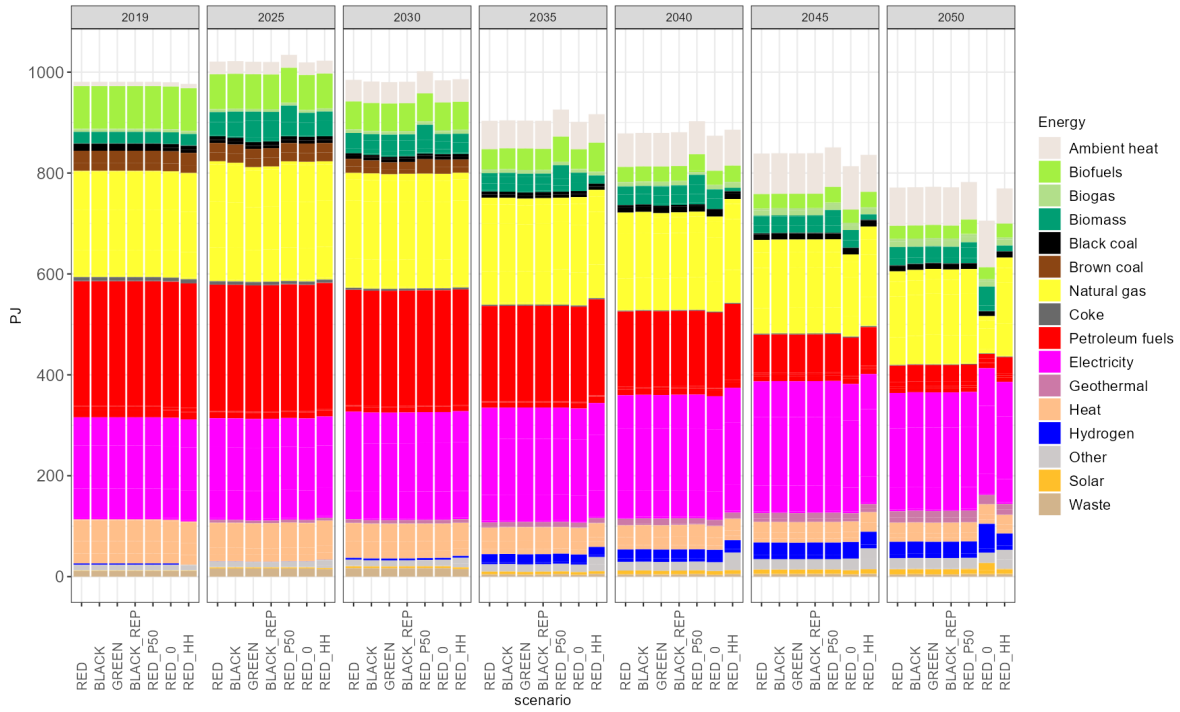

Final energy consumption according to the model results is illustrated in Figure 2.6. As a result of improvements in energy efficiency, there is a substantial reduction in total final energy consumption across the entire timeframe, and this trend is consistent across almost all scenarios. The sole exception is the RED-0 scenario, which notably exhibits lower final energy consumption than the other scenarios, starting from 2040. In this scenario, there is a decreased reliance on natural gas and an increased utilization of hydrogen. The overarching trend across all scenarios involves a shift away from more environmentally hazardous technologies, such as petroleum-based fuels and coal, in favor of cleaner alternatives. Figure 2.7 also highlights an overall increase in renewable energy shares across all scenarios. In the RED-HH scenario, where biomass is allocated solely to residential use, there is a reduction in biomass consumption in the final energy sector compared to the other scenarios. In general, it seems that the spruce bark beetle infestation has no discernible impact on the overall energy mix when we examine the forest biomass development scenarios, including RED, BLACK, GREEN, and BLACK-REP.

2.4.4 Share of Renewable Energy Sources

As depicted in Figure 2.7, the proportion of renewables within the overall energy mix exhibits a consistent upward trajectory. By 2050, the model's average projection anticipates a 55% share of renewables. The RED-0 renewables reach almost 65% in 2050. However, achieving

Figure 2.7: Share of renewable energy sources in gross final energy consumption, Czechia, 2019-2050.

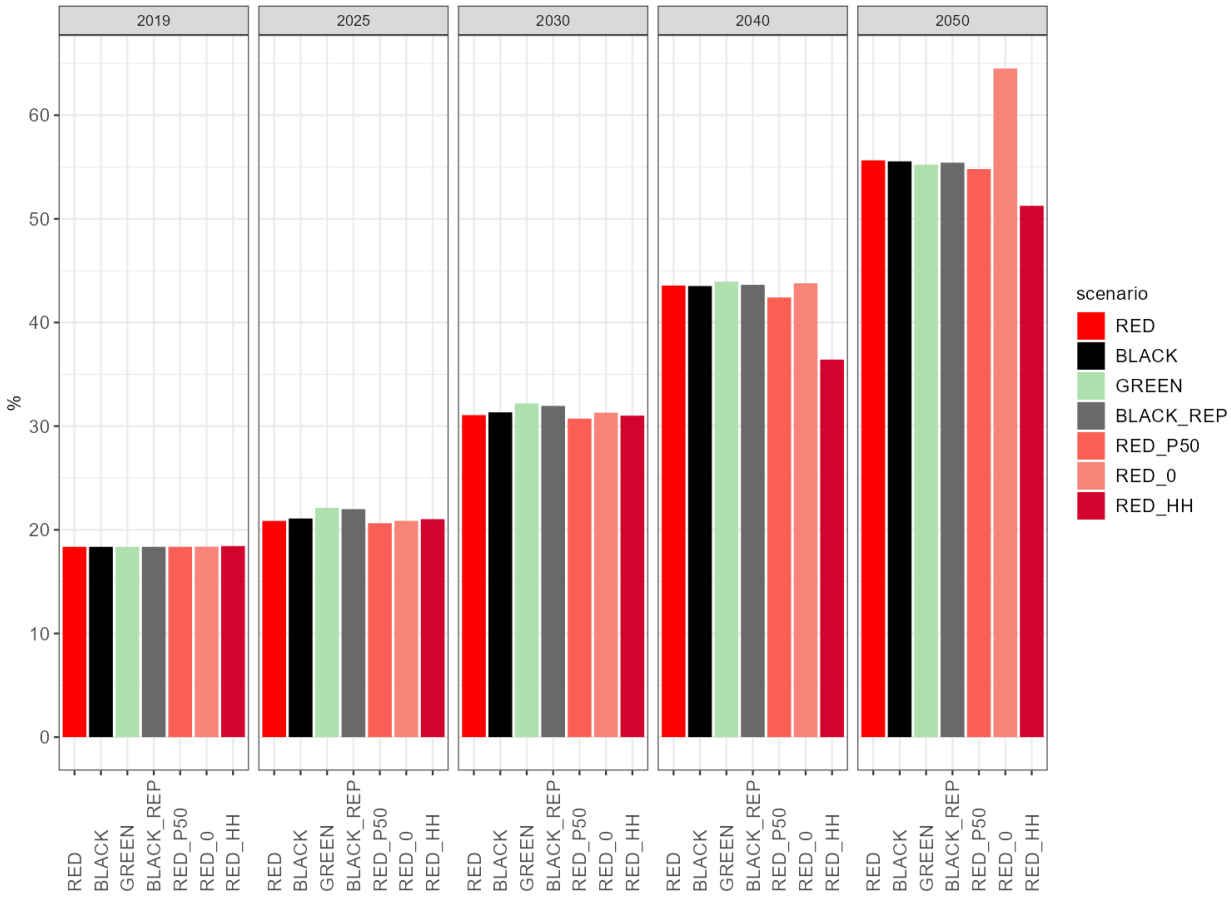

the EU's recommended target of 45% renewables by 2030 appears unlikely across all scenarios. In Figure 2.7, it is noteworthy that subsidies aimed to encourage household use of wood pellets (RED-HH) do not contribute significantly to achieving renewable energy objectives. This intriguing observation prompts further investigation, and we will seek to clarify this in the next subsection.

While the proportion of renewable energy sources is strictly increasing throughout the period, the proportion of forest biomass within the overall renewable energy mix follows a contrasting pattern. To illustrate, in 2019, the average share of biomass in total renewable energy is approximately 12%, but it diminishes to an average of 7% by 2050. Within the range of forest development scenarios, the more optimistic GREEN and BLACK-REP scenarios stand out, with the share of renewable energy in gross final energy consumption increasing by about one percentage point between 2025 and 2030 compared to the other scenarios. Clearly, the spruce bark beetle infestation will exert only a transient, relatively limited influence on renewable energy goals.

2.4.5 Biomass

Focusing on forest biomass, first, we repeat the claim that the regionalized TIMES-CZ model increases the spatial resolution of the Czech energy system. In Figure 2.8, forest biomass supply for energy purposes is more abundant in southwest Czechia. Due to the increasing transportation costs with distance, regionalized TIMES-CZ allows more realistic choices for locating new biomass-burning or co-burning plants. As the southwestern regions of Czechia have the highest availability of forest biomass, it would be advantageous to locate new biomass CHP plants in these regions.

Figure 2.8: Forest biomass supply in RED scenario, by region, 2025-2050.

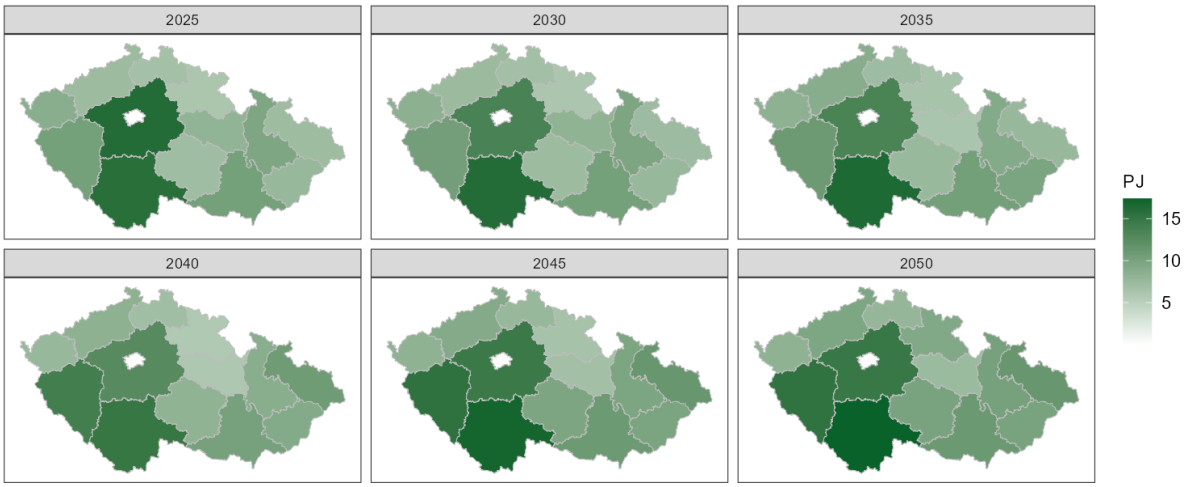

Figure 2.9 shows the final consumption of forest biomass by sectors, contrasting it with the availability of biomass according to Figure 2.2. The utilization of biomass as an energy source does not fully align with the available biomass resources by 2040. This discrepancy arises because timber harvesting experiences a slowdown between 2025 and 2035. With the reduced availability of biomass, the model adapts by incorporating new technologies that are less reliant on biomass. Even though timber harvesting experiences a significant resurgence in 2040, the replacement of previously installed technologies is not instantaneous. Consequently, biomass consumption does not catch up as quickly as timber harvesting recovers in 2040.

Another explanation for this mismatch is that some steps on the cost curve of the broadleaf firewood and white chips are more expensive than natural gas. Subsidies of biomass production may be one avenue that would help to unlock the full potential of biomass, as illustrated in the RED-P50 scenario in 2040. Nonetheless, in other years, biomass resources are already fully utilized, necessitating a thorough cost-benefit analysis before subsidies are implemented. In fact, in the years 2045 and 2050, the subsidy policy seems counterproductive: the full potential of biomass is no longer being exploited compared to the RED scenario. This occurrence can be attributed to the rise in household wood pellet consumption, displacing other sectors and compelling them to consider alternative technologies utilizing different fuels.

Figure 2.9 also reveals other crucial trends. In all scenarios, the residential consumption of biomass steadily declines over the period under review. The opposite is true for the power and

Figure 2.9: Forest biomass consumption by sectors and its availability, 2019-2050.

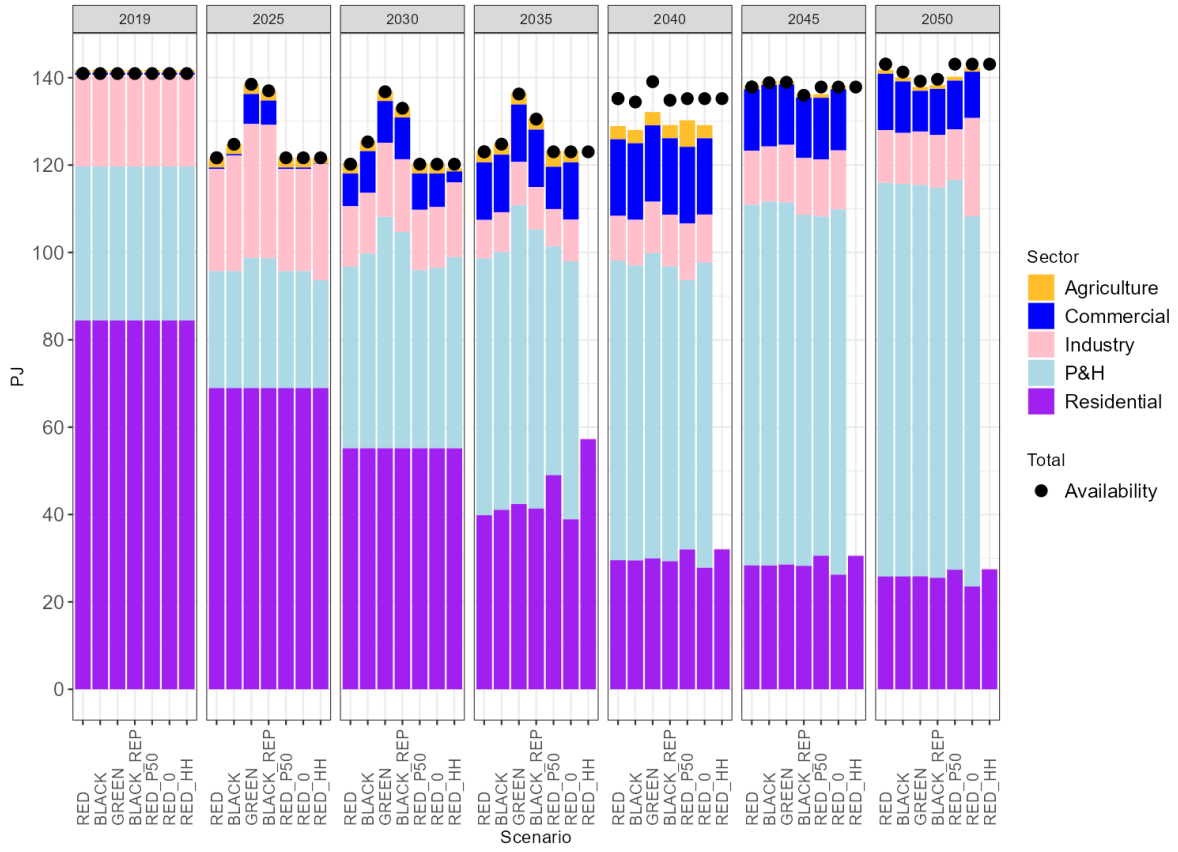

Note: P&H stands for power and heat sector.

heat sector. Hence, large sources can absorb available biomass even at the expense of households; nevertheless, from a system-wide perspective, this may appear to be more efficient. A more detailed overview of the residential sector follows in Figures 2.10 and 2.11.

2.4.6 Residential Sector

The residential sector consumed more than 62% of all biomass energy in Czechia in 2019. As this is substantial, we present detailed results of energy consumption in the residential sector.

In all scenarios, residential sector energy consumption generally shows a downward trend over time. Starting from 2035, district heating and biomass are predominantly replaced by ambient heat and electricity used by heat pumps.

Interestingly, in scenario RED-0, which involves an exogenous reduction of GHG emissions to a net of 2.2 Mt in 2050, biomass does not appear to be the preferred choice in the residential sector. Instead, ambient heat and solar energy gain prominence. This shift is influenced by the fact that the power and heat sector and industry absorb most of the available biomass.

Figure 2.10: Final energy consumption in the residential sector, by energy sources, Czechia, 2019-2050.

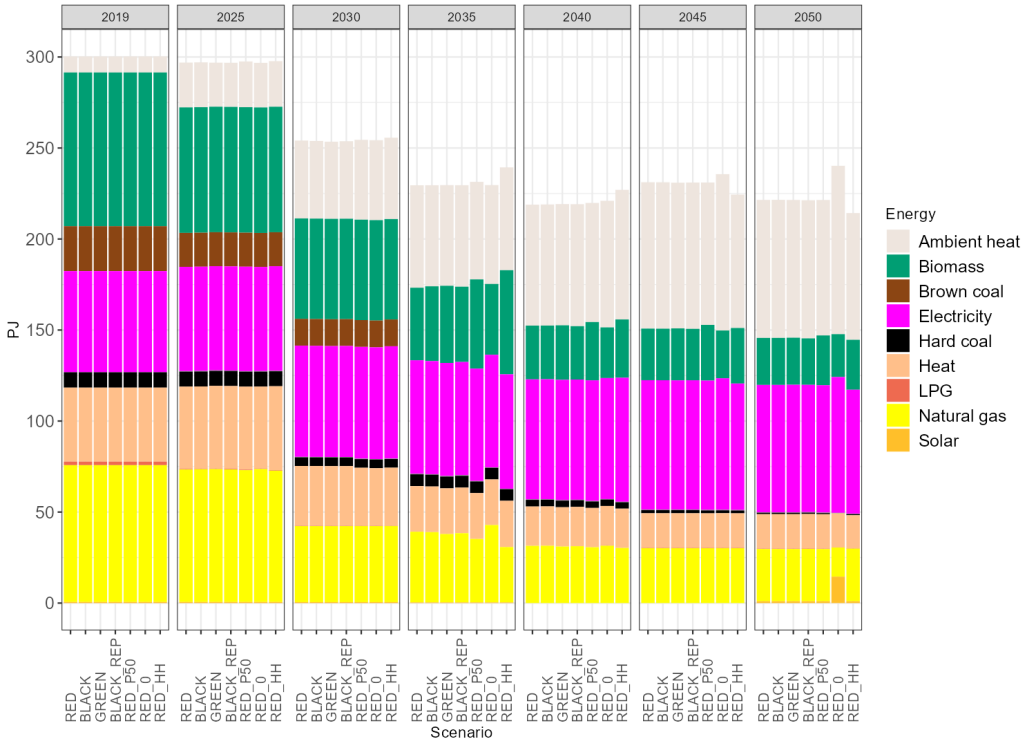

Figure 2.11: Final energy consumption in the residential sector by purpose in Czechia 2019-2050.

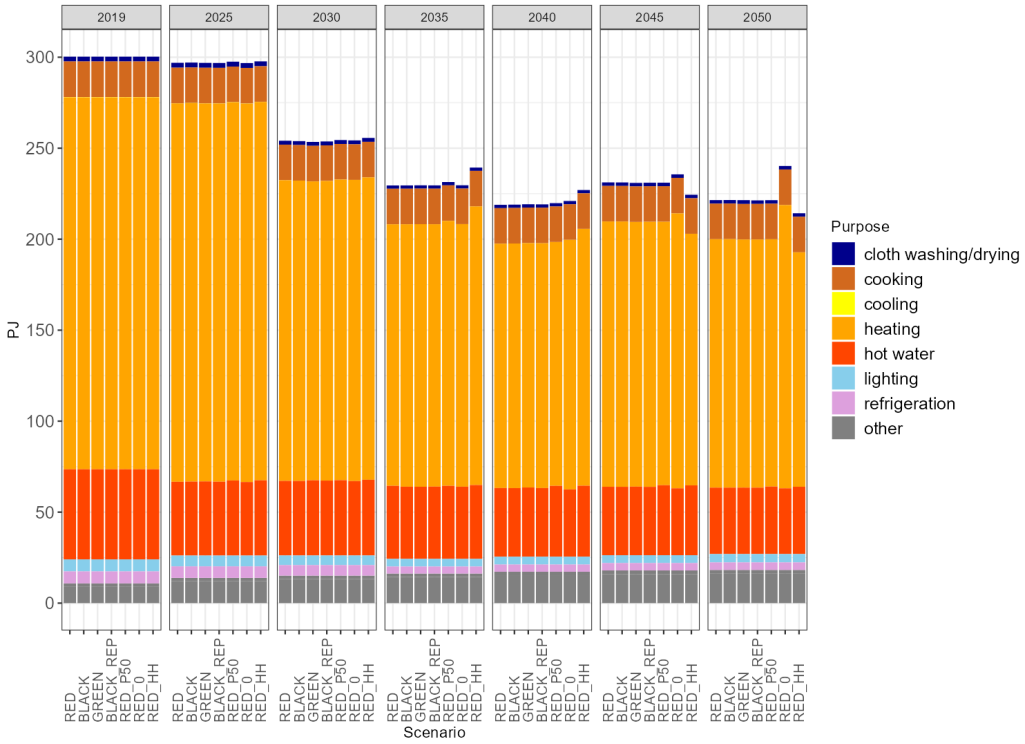

This observation is further supported by the RED-HH scenario, where the residential sector does not face competition for biomass consumption from other sectors. As a result, its biomass consumption exceeds that of the other scenarios. However, in this scenario, the residential sector is not able to fully utilize the available potential of biomass energy.

Figure 2.11 offers a detailed breakdown of energy use within the residential sector, which is categorized by its intended purposes. The "other" category includes small electric appliances like televisions. Notably, the most substantial portion of household energy consumption is attributed to heating. The decline in energy demand by households is a result of advancements in appliance efficiency and enhanced building insulation.

2.4.7 Annualized Costs

Figure 2.12: Difference in total annualized energy system-wide costs compared to the RED scenario.

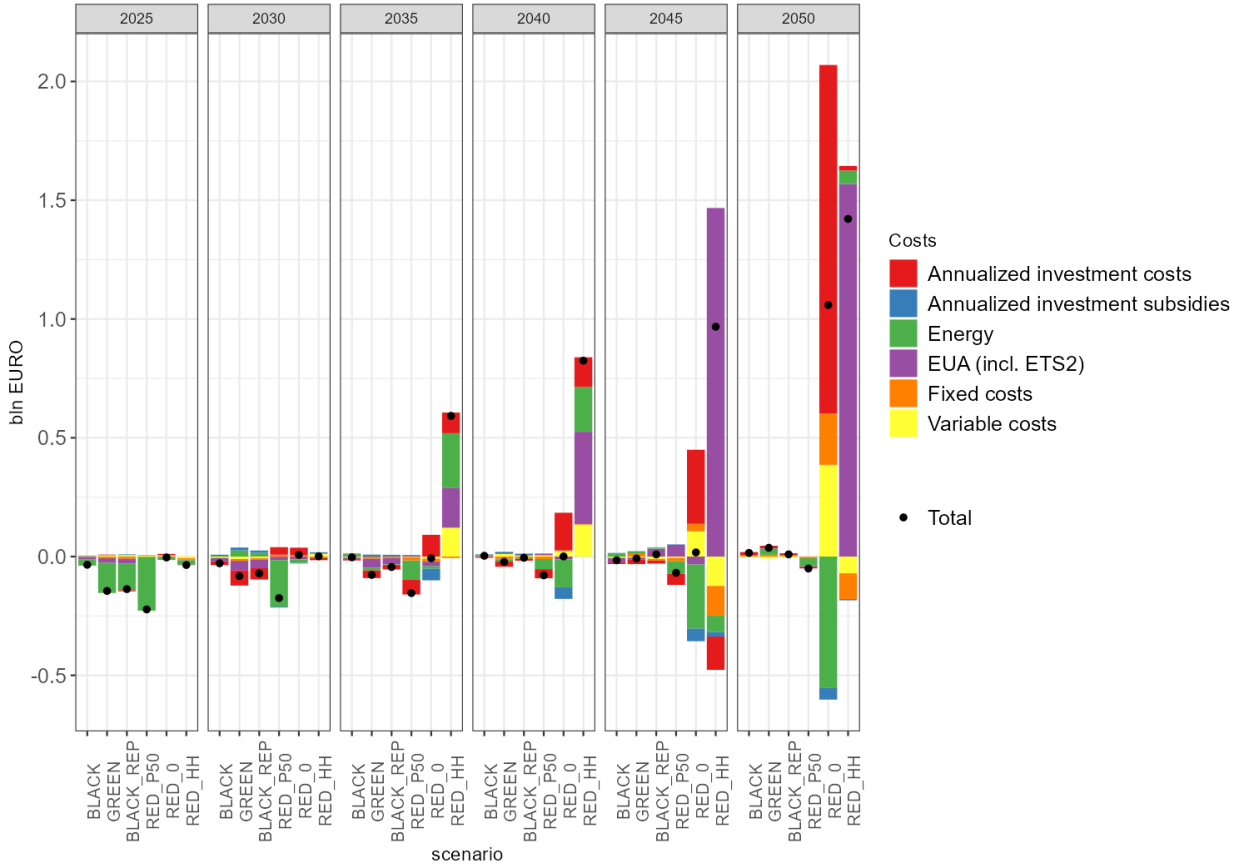

Note: Negative bars signify that the particular cost component is lower than its counterpart in the RED scenario.

Figure 2.12 shows the difference in total annualized system-wide costs compared to a reference scenario, which is RED. The annualized total system-wide costs include the sum of investments, expenditures for energy and EUAs, and fixed and variable costs of technologies, and are

shown from an energy system perspective, i.e., after deducting subsidies for clean technologies or wood pellet production. The subsidy for wood pellet production is included in the price of wood pellets, i.e., in the energy category. The bars show the costs per category, and the black dots show the totals. When the bars or black dots appear below (above) the zero line, the costs are lower (higher) than in the RED scenario. For example, the total annualized costs in RED-P50 are around €175 million lower each year in 2028-2032 than in RED; cumulatively, these costs are €875 million lower over the same five years.

It is noteworthy that none of the four forest development scenarios differs significantly from the others, indicating that the impact of the spruce bark beetle infestation on energy system costs is very limited.

However, regarding the three policy scenarios, we observe notable spikes in annualized total costs, particularly in the case of the RED-HH and RED-0 scenarios. The RED-HH scenario is the only one in which annual costs significantly exceed the costs of all four forest scenarios, starting from 2035. This occurs because adhering to ecological constraints forces the system to rely on costlier and more carbon-intensive fuels, substantially increasing the system costs. Because the availability of forest biomass is constrained in the RED-HH scenario, higher carbon emissions result in higher payments on EUAs. The scenario is the most expensive, costing €16 billion more than RED.

For the RED-0 scenario, total annualized costs significantly surpass the costs in RED baseline only in 2050, because the scenario requires reducing greenhouse gas emissions to a net 2.2 million tons by 2050. This requirement triggers investments in costly abatement technologies like nuclear power and energy-saving measures, resulting in €3.3 billion higher overall annual costs up to 2050.

RED-P50 seems to be the least costly scenario, which is mainly due to the expenditures on energy use, which are €3.1 billion (cumulatively, until 2050) smaller than in all four scenarios on forest development. Lower energy bills are partly due to subsidies for wood pellets, which cost €4.54 billion cumulatively until 2050. Annually, these subsidies amount to €227 million during 2023-2027. Then, as a result of increased energy efficiency in residential buildings and resulting lower energy consumption, wood pellet subsidies fall to €143 million around 2040 and €80 million around 2050. This subsidy is implicitly reflected in reduced energy bills. This scenario is, however, not the least costly from a social planner's perspective when all subsidies are factored into the annualized total costs. Including subsidies in the annualized costs, the total costs are €0.9 billion higher than the costs in the baseline scenario, whereas GREEN and then BLACK-REP are the cheapest ones, with €1.4, and €1.0 billion lower annualized total costs than in the baseline.

2.5 Conclusions

Forest biomass is the main source of renewable energy in Czechia. This precious resource is currently facing challenges from spruce bark beetles. In this paper, we explore the impact of possible forest biomass development pathways on the Czech energy system, taking the current spruce bark beetle infestation into account. In particular, we evaluate the impact on

greenhouse gas reduction efforts, renewable objectives and the final allocation of resources. We use a spatially enriched energy system optimization model, TIMES-CZ, enhancing its spatial resolution by regionalizing biomass availability, power and heat generation, and energy service demands, following Eurostat's NUTS3 levels. Our regionalized model accounts for the fact that forests are unevenly distributed across the country and that transporting biomass over long distances is not economical. Our updated model informs more realistic choices for locating new biomass-burning or co-burning plants. More broadly, regionalization incorporates various constraints, specific details, and heterogeneities across regions, improving the accuracy of our results. This type of incorporation of spatial granularity in optimization ESM is notably lacking in the literature, particularly when considering the relatively small and compact nature of the TIMES-CZ regions. This contribution to the existing literature is quite evident.

This paper underscores several key findings. Firstly, it highlights that even at an EUA price of €386, Czechia is unlikely to achieve climate neutrality by 2050 across all scenarios. Furthermore, attaining climate neutrality by 2050 necessitates investments in costlier technologies. Regarding pathways for reducing greenhouse gas emissions, neither the impact of the spruce bark beetle infestation nor special subsidies aimed at promoting wood pellet consumption by households seems to influence the outcomes significantly. Instead, the primary drivers concerning biomass are the adoption of BECCS technologies, which could lead to a reduction of 4-4.5 megatons in emissions during the period of 2045-2050, along with sustainable activities related to land use, land use change, and forestry.

Regarding ecological constraints, it becomes evident that at times, there is a need to prioritize specific objectives over others. Limiting the use of biomass to households and conserving the remaining biomass in forests does not align with the goal of reducing greenhouse gas emissions. This misalignment has a significant impact particularly by constraining the potential of BECCS.

The disparities among biomass development scenarios are substantial until 2035. However, these distinctions do not seem to have a long-lasting impact on the overall energy mix. Nonetheless, the more optimistic scenarios permit an additional 1 percentage point increase in the share of renewable energy sources (RESs) in total final energy consumption compared to other forest biomass development scenarios in 2025-2030. Consequently, the spruce bark beetle infestation does exert a negative influence on medium-term renewable energy objectives.

Irrespective of the spruce bark beetle infestation, our results suggest that the energy system will make full use of biomass potential, with the exception of a temporary deviation in 2040 when biomass demand will likely lag behind increasing availability. In this context, one could suggest the implementation of subsidies to encourage household adoption of biomass. However, this policy does not appear to yield positive changes in key variables of interest, including greenhouse gas emission reduction, the achievement of renewable energy targets, or cost savings. In addition, such subsidies seem to distort the allocation of this precious resource by crowding it out of sectors that could use it more efficiently.

Chapter 3

A Practical Model-based Approach to Oil Price Projections with an Application to Monetary Policy Facing Oil Price Shocks Under Different Credibility Regimes

---

This chapter was coauthored with Jared Laxton (Advanced Macro Policy Modelling LLC.)

3.1 Introduction

The likelihood of transitioning from an age of resource abundance to one of resource exhaustion is becoming increasingly plausible. Key drivers of this shift include a declining labour forces, de-globalization trends, and the peak of cheap energy resources (Goodhart & Pradhan, 2020; White, 2023). While the effects of these developments vary across countries, the overarching trends are likely to carry stagflationary implications for the global economy. Oil prices, in particular, can trigger stagflationary outcomes, especially for oil-importing countries. Although climate initiatives and greenhouse gas reduction plans may reduce the significance of oil in the long term, rising oil prices remain plausible in the near future. This is due to peaks in cheap oil, supply constraints, and the slow and complex transition to renewable energy (Bachner, Steininger, Williges, & Tuerk, 2019; Tran & Smith, 2017). In the medium term, oil prices will continue to play a critical role in shaping the global economy. Given this context, monetary policy frameworks of inflation-targeting central banks have performed effectively in resource-abundant environments. However, their performance remains uncertain as resources become scarcer and stagflationary shocks become more prominent (Blanchard & Simon, 2001).

We evaluate these outlined challenges using a framework that integrates oil price dynamics

into monetary policy analysis. Specifically, we develop a global economic model for oil prices (OILMOD), that is similar in nature to the existing semi-structural workhorse macroeconomic models as utilized by many successful smaller central banks, i.e., in Armenia, Georgia, Ukraine, and Botswana, among others. The model is meant to be accessible enough so that central banks are encouraged to conduct more in-house oil market analyses rather than relying more heavily on third-party baseline forecast scenarios. This approach allows central banks to generate multiple oil price scenarios and to test various narratives, including stagflationary outcomes. We then analyze a high oil price scenario under the lens of the endogenous policy credibility model (ENDOCRED), to evaluate possible monetary policy responses in a world in which perfect central bank credibility should not be assumed. Our findings highlight the importance of proactive and immediate responses to possible stagflationary shocks and demonstrate how a lack of credibility can amplify the long-term economic costs of a crisis.

A stagflationary environment, with declining output and rising inflation, challenges the effectiveness of traditional monetary policy frameworks. The post-COVID-19 period, marked by stagflationary pressures and inflation exceeding targets from 2021 to 2024, offers a relevant case study. Despite stable inflation expectations in bond markets, evidence from wages and sticky prices suggests anchored inflation should not be assumed. The Atlanta Fed's sticky and flexible price paradigm, inspired by the concepts in Dornbusch's overshooting model (1976), shows how infrequently adjusted prices may naturally convey relevant information about inflation expectations among price setters. Lord Mervyn King (2024) and Augustin Carstens (Fleming & Arnold, 2024) warn that it is dangerous for central banks to assume that inflation is always anchored. In reality, inflation can become unanchored, and when it does, it amplifies stagflationary shocks and necessitates stronger policy responses (Alichi et al., 2009).

The pandemic has also prompted central banks to rethink how they address macroeconomic uncertainty. As noted in Ben Bernanke's 2024 review of the Bank of England, there is a growing need for the "expanded use of alternative scenarios to facilitate comparisons of possible policy choices, (to) more accurately quantify the risks to the forecast, and (to) help learn from past forecast errors" (Bernanke, 2024).

Adopting scenario-based approaches to monetary policy highlights how oil prices could play a more prominent role within their analytical frameworks. Many central banks such as the Czech National Bank, the Central Bank of Armenia and the National Bank of Georgia rely on oil price projections from third-party institutions such as the EIA (CNB, 2024), which often assume mean-reverting prices (see fig. 3.4) and fail to capture inherent market risks. While more advanced models exist, central banks have yet to explicitly incorporate them into their regular analyses, which is understandable due to their perceived costs and complexity.

To analyze the interaction between oil prices and monetary policy, we propose a two-step modelling approach. In the first step, we build on the semi-structural model of oil price dynamics developed by Benes et al. (2015), adapting it for our purposes. This adapted model can be readily integrated into existing monetary policy frameworks of central banks. We analyze scenarios involving OPEC production cuts and their potential impact on spare oil capacity, a critical variable in oil price volatility. Using a geology versus technology framework, we examine how geological constraints may push oil prices higher, thus exacer-

bating stagflationary risks. In the second step, we simulate a high oil price scenario within the ENDOCRED model under varying levels of central bank credibility: perfect credibility, imperfect credibility, and delayed policy responses.

Our findings suggest that standard monetary policy practices under a high oil price scenario, when the credibility of the central bank is questioned, are costly. Attempting a soft landing through a delayed interest rate response, as seen during the COVID-19 crisis, risks exacerbating economic pain and prolonging the path to steady-state recovery. We argue that a more immediate reaction to stagflationary shocks is more effective, as it helps to mitigate the long-term costs associated with delayed action. Further, addressing credibility issues before a shock occurs is essential to ensure more effective policy responses.

In summary, the value of our analysis and proposed model provides institutions such as central banks a guide to strengthen oil price analysis within a familiar modelling environment. The exercise should illustrate that it can be relatively simple for central banks to take firmer control over their oil price outlook and to avoid outsourcing such a critical area of monetary policy analysis. We also provide consistent macroeconomic projections for oil prices that can be used for external assumptions in a standard macro model to prepare case scenarios. Finally, we present what we believe are some relevant oil price scenarios that have important implications for strategic monetary policymaking in an environment where credibility should not be assumed to be perfect.

The paper is structured as follows. Section 3.2 defines the key considerations in constructing an oil price model, and section 3.3 introduces OILMOD, a global oil price model for scenario analysis. Section 3.4 discusses these scenarios, particularly stressing the plausibility of a high-oil price scenario. Section 3.5 introduces ENDOCRED, a policy credibility model incorporating oil price dynamics for macroeconomic scenarios. This section also simulates an oil supply shock and evaluates policy responses under different central bank credibility assumptions. The conclusion highlights the need for proactive strategies to anchor inflation and to strengthen credibility, and it advocates for stabilization policies with built-in buffers against economic uncertainty.

3.2 Building Blocks of the Oil Market Analytical Framework

Oil prices have the capacity to drive stagflationary outcomes by simultaneously raising production costs and slowing economic growth. However, many central banks have not been thoroughly tested by a stagflationary environment, in which supply-side shocks dominate. To address this gap, we first introduce OILMOD, a semi-structural oil price model that examines the macroeconomic implications of oil price dynamics. There are many sophisticated oil price models, some fully structural and others strictly empirical. The model presented in this paper is meant to strike the aforementioned balance between structural and empirical, to be used as a way to synthesize different perspectives in the oil market, as the motivation behind different oil price projections. The ability to express alternative views within the framework as presented in this paper will hopefully lend itself to a better understanding of

uncertainty in the oil market that can be applied to constructing monetary policy strategies that are equipped to manage stagflation. We next analyze a high oil price scenario using the ENDOCRED model to evaluate monetary policy responses under varying levels of central bank credibility.

In the development of our analytical framework for the oil market, we mirror the structure of the Forecasting and Policy Analysis System (FPAS) frameworks utilized by the leading central banks for monetary policy. These frameworks attempt to answer three essential questions within a semi-structural model: What is the current state of the economy? What are its current primary underlying forces? What do we need to do with our instruments to achieve our objectives? In the monetary policy framework, the instrument is an endogenous interest rate path. In the oil market version, we are searching for an endogenous oil price path that would balance demand and supply.

Central banks often rely on oil price forecasts from financial markets or external institutions, as illustrated by the Czech National Bank's monthly Global Economic Outlook (2024). Yet a persistent and contentious debate between major players such as the International Energy Agency (IEA) and OPEC over future oil demand and supply underscores the uncertainty surrounding these forecasts, with potentially far-reaching consequences for oil prices (IEA, 2023; OPEC, 2023a) (IEA, 2023; OPEC, 2023a) (see fig. 3.1). Considering that oil prices can significantly impact the uncertainty landscape and risk management in almost every economy, policymaking institutions should ideally be able to do their own in-house analysis on this topic rather than subscribing solely to outside views. This underscores the necessity of establishing a structured framework for analyzing oil markets, and it should not be difficult for central bankers to add relevant expertise to their existing frameworks in this area.

A notable portion of the literature concerning oil price forecasting underscores the significance of demand-side shocks on oil prices. Such forecasts often employ econometric models that use macroeconomic variables to project the demand for oil and predict future oil prices (Alquist, Kilian, & Vigfusson, 2013). These macroeconomic variables are highly correlated with fluctuations in aggregate demand; therefore, oil price changes are mainly captured by variations in aggregate demand. Because aggregate demand tends to revert to a trend, these macroeconomic variables are unlikely to be fully successful in predicting a persistent oil price increase. Furthermore, it is evident when examining professional forecasters such as the EIA, IEA, and OPEC, that they routinely focus on demand-centric scenarios that reflect the "world business cycle" view of analyzing oil prices (Arezki et al., 2017).

Kilian (2009) highlights three main drivers affecting US oil prices: aggregate demand for goods, precautionary oil demand, and oil supply. The author observes that historical data indicate demand shocks notably influence oil prices, while supply shocks have minimal impact, but this overlooks persistent supply shocks arising from geological constraints. Conversely, Hamilton (2009) emphasizes the significant role of temporary disruptions in physical oil supplies on historical oil price dynamics. Additionally, he attributes the surge in oil prices from 2003 to 2008 partly to stagnation in global oil production. While he acknowledges short-term supply effects due to limited substitutions for oil, he contends that high prices over time encourage technological advancements and the development of oil substitutes, ultimately having a decisive impact on production levels.

Figure 3.1: World petroleum demand.

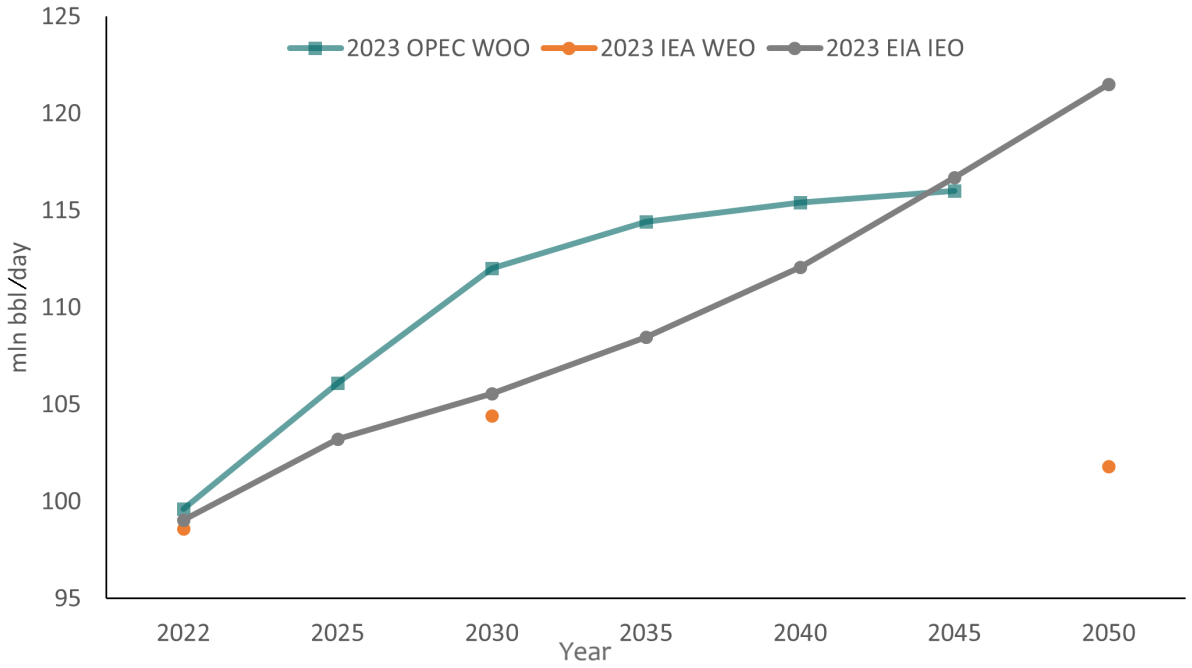

Sources: EIA (2023a), IEA (2023), and OPEC (2023a). The figure demonstrates divergent forecasts regarding oil demand from prominent institutions. The projected outlook for oil prices based on these would vary dramatically.

Meanwhile, advocates of the geological view argue that oil reserves are finite. They suggest that easily accessible oil is depleted first, and that production costs increase as cumulative oil production rises (Campbell & Laherrère, 1998; Höök, 2014). They also recognize that when conventional oil production remains stagnant despite increasing oil prices, it indicates the beginning of physical scarcity that will eventually outweigh the stimulative effects of higher prices. They contend that no suitable substitutes for oil exist at the required scale and that oil recovery technologies will eventually encounter limits determined by the laws of thermodynamics. This perspective traces its roots back to Hubbert's (1956) prediction that US oil output would peak in 1970, with extensive support found in studies like Hirsch (2005) and Sorrell, Speirs, Bentley, Brandt, and Miller (2010), which warns of a substantial risk of conventional oil production reaching a peak before 2020, with an inevitable decline thereafter.

Figure 3.2 illustrates the plausibility of this risk as global oil production ex-US shale has not exceeded the levels of 2018, with tight US oil production accounting entirely for the growth story in global oil production since US shale became available for use. Although COVID-19 induced a demand collapse that disrupted this trend, notably in places like Saudi Arabia, the recent cuts by OPEC (OPEC, 2023b) could be part of a larger story connected to peak oil that is reemerging among both conventional and unconventional oilfields. Although new oil extraction projects in the non-OPEC world, such as those in Canada, Argentina, and Brazil, are expected to start producing new oil, their contributions will be modest and likely insufficient to offset the potential impact of a stall in US shale production growth. While OPEC has around 4 million barrels per day of spare capacity, it would only provide

Figure 3.2: Illustrating the shale revolution: (a) US oil production (b) Global oil production

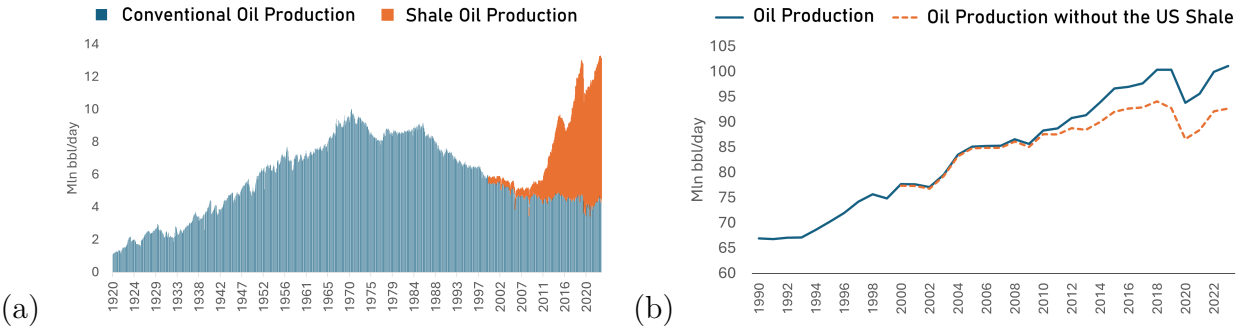

Source. EIA (2024c) and EIA (2024b). (a) depicts the growth in US oil production as a result of unconventional sources. Panel (b) shows what global oil production would look like without US shale production as the key source of global supply growth.

temporary relief if US shale no longer supplies the 0.6–1 million barrels per day of new oil that global markets have relied on over the past decade.

Aside from the pure geological perspective, there are numerous sources of oil supply uncertainty, including regulation. Perhaps the peak oil geological perspective is exaggerated, and oil supply is much more of a political choice than a geological constraint at times. The judgment on this will impact the potential elasticity of supply to respond to higher prices. Nevertheless, we can already see the medium-run oil supply potential as summarized by global upstream capital investment in figure 3.3.

The past ten years show an unambiguous decline in global investment, which should prompt analysts to worry about whether future oil production will be sufficient to meet even modest oil demand scenarios. Rystad Energy (2023) has downplayed this development with rising efficiency gains over recent years, suggesting that the stock of capital investment required to service oil demand is lower. However, if oil demand were to continue to rise, then large efficiency gains would need to be maintained over the coming years to keep oil prices from rising, which is possible but would be a strong assumption.

Future oil prices have been notoriously difficult to predict. As Alquist et al. (2013) conclude, forecasts based on monthly futures prices, monthly surveys of forecasts, simple econometric models, and other commonly employed forecasting techniques cannot consistently beat a random walk forecast out-of-sample. There should be no pretence that a single-point forecast is fully reliable; instead, the types of macroeconomic models that can help an analyst build and test different types of narratives for oil prices based on different underlying assumptions and analyses need to be developed and applied. The aim of the model we present is not to forecast oil prices but to provide a simple and intuitive structure for constructing consistent oil price scenarios. Crucially, these models should incorporate mechanisms in which demand and supply curves for oil interact, potentially leading to changes in oil inventories and oil prices. Surveys of demand and supply forecasts by entities like the EIA and OPEC often assume that changes in inventories are zero, implying that supply always matches demand and the market clears (EIA, 2023a). This assumption can result in misleading analyses, as observed between 2003 and 2008, when oil demand continued to rise. Yet, the EIA maintained a mean-reverting oil price forecast (see fig. 3.4), effectively treating oil resources

Figure 3.3: Upstream oil and gas capital expenditures

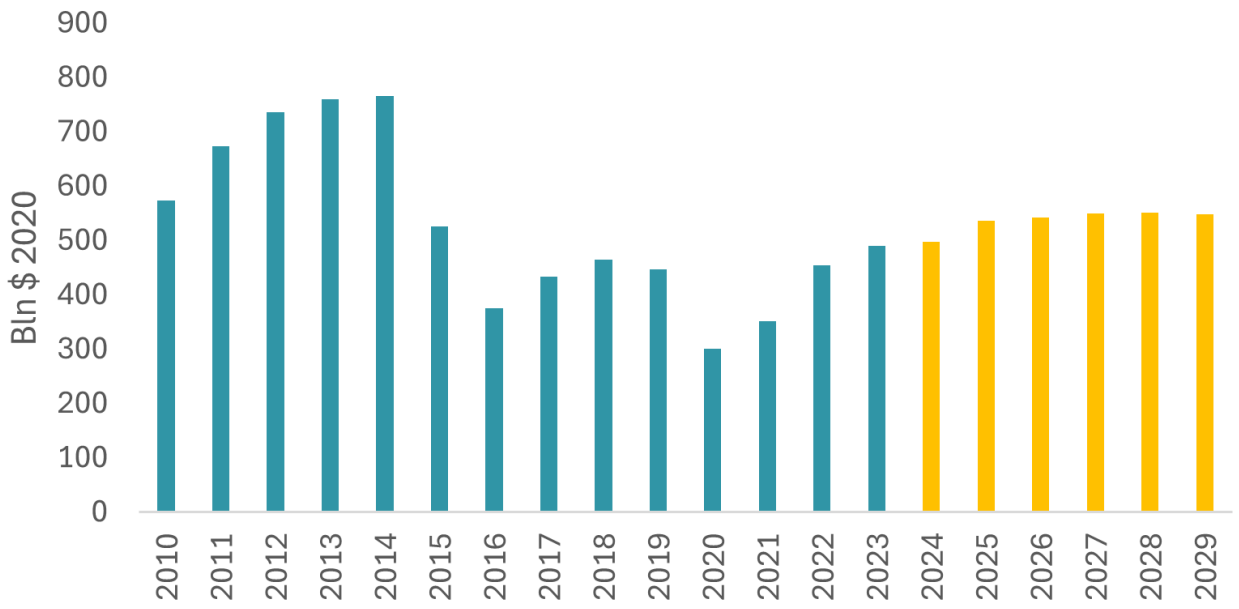

Sources: compiled by the authors based on a report from the International Energy Forum and S&P Global Commodity Insights (2024). The CapEx is expressed in real 2020 dollars based on the US CPI indices (IMF, 2024). Notes: The figure shows that oil and gas production investments are expected to remain subdued in real terms over the coming decade.

as unconstrained and expecting that whenever prices increase, supply will respond through technological innovations or spare capacity.

Work has already begun to bring oil prices within a semi-structural macroeconomic modelling environment in Benes et al. (2015). This is where we emphasize the practical part of our contribution. The models we choose should recognize the environment in which they are deployed. The target audience for this model is central banks and, therefore, it should be accessible to central bank economists, policymakers, and perhaps financial markets. Usually, the path to deploying production models within a policymaking institution begins with more modest models that capture a core idea or concept, where there is a low barrier of entry for economists to operate and communicate to policymakers.

We consider Benes et al. (2015) a useful model to analyze the geological view of oil, in which they explicitly model how oil becomes increasingly difficult to produce as cumulative production increases (peak oil). However, from the perspective of an analyst who employs the oil model within a central bank's analytical framework, this restrictive assumption may tilt their outlook in a certain direction and limit their ability to represent uncertainty objectively. Therefore, we advocate for a less constrained model that requires minimal assumptions. While insights from more restrictive models can be useful for developing alternative scenarios, they should not serve as a starting point.

This method contrasts with EIA oil models, which rely almost exclusively on econometric regression methods. We believe that these fail to capture the dynamism in analyzing the oil market in both the short- and long-run, and for constructing meaningful oil price scenarios.

Figure 3.4: Historical oil prices forecasts by the EIA

Sources: compiled by the authors based on data from the EIA Short-Term Energy Outlooks (1983-2023).
Notes: The figure plots the historical EIA Short-Term Energy Outlooks oil price forecasts from the first quarter of each year. Between 1983 and 2007, there was a tendency for the forecasts to mean-revert.

In our view, good economic analyses and forecasting never include the vernacular "the model says X or the model says Y" but that forecasts should be generated by a combination of careful analysis by an expert, where models are used to provide structure and nothing more. The EIA seems to share this approach in principle: "Ultimately, EIA analysts formulate a Brent price forecast by expert judgment, using expert judgment, using the output of the pooled and linear regression models as guides" (EIA, 2024a). We agree that the best practice for macroeconomic analysis includes a combination of models and expert judgment. The oil model we present in this paper positions itself as a production model that broadly reflects current literature on oil prices, which helps the analyst provide a more realistic picture of uncertainty by applying plausible alternative scenarios.

We develop a simple macroeconomic model that follows the calibration of Benes et al. (2015) when relevant and combines a conventional linear demand specification with a linear supply equation; however, we add a variable in the OPEC supply equation based on OPEC's spare capacity that acts as a proxy for oil market tightness. We find that this variable can help explain historical price shocks related to tighter conventional oil supply conditions and can be used to construct future scenarios assuming a tight oil market.

We provide scenarios that consider different levels of oil market tightness in light of the decision by OPEC in the summer of 2023 to cut production (OPEC, 2023b), which can move oil prices in a much more profound way than the current market anticipates. This is what we refer to as the beginning of another oil price rollercoaster, where the conceptual dynamics unfold as follows: there is a period of low oil prices along with a period of rapid

depletion rates in both US shale and conventional oilfields. This, in turn, leads to a period of insufficient investment to develop new sources of oil to meet future demand. OPEC can provide relief, but this would not be a long-term solution. Ultimately, oil prices would need to reach new highs to make previously economically unviable oil viable.

3.3 The Global Oil Model (OILMOD)

The model aims to capture several crucial concepts regarding the dynamics of demand and supply in the oil market. First, we acknowledge that, in the short run, both demand and supply are highly inelastic, implying that minor shifts in demand and supply result in significant fluctuations in oil prices. This inherent characteristic makes oil prices notoriously difficult to predict. Instead, this analytical exercise and our development of a simple macroeconomic model are meant to better illustrate how an economist can explore uncertainty surrounding the future longer-term outlook of oil prices through the use of plausible scenario analysis. This approach diverges from that of the EIA, where oil price scenarios are treated purely as an exogenous exercise (EIA, 2023a). Of course, demand and supply become more elastic in the longer run, as time allows consumers to shift away from oil and producers to fund new projects. These different responses by consumers and producers to oil prices are illustrated in the model's impulse response functions (check figure in the Appendix 3.A) and describe the dynamics of shocks on oil demand and supply.

Oil demand burst. Global growth unexpectedly raises oil demand. Oil prices rise as a consequence; suppliers are then incentivized to take advantage of higher prices and sell off existing sources of oil, i.e., to reduce spare capacity, and to temporarily increase oil supply to meet demand. However, if higher demand persists, it becomes more difficult for suppliers to respond, as spare capacity has been exhausted, creating more acute supply shortages, and oil prices can skyrocket in the short run. Over time, oil demand should fall in response to higher prices, but there are limits given the unique importance of oil in the global output of goods and services. Therefore, we would expect oil prices to remain elevated. Suppliers respond to a more permanent increase in oil prices by deploying new technologies to extract non-economic oil at previous price levels. A greater supply eventually helps to moderate oil prices (see fig. 3.5). This type of scenario largely played out between 2002 and 2015, barring the intermittent negative demand shock from the Global Financial Crisis (GFC).

Oil supply burst. It is difficult to predict the size of a supply burst when it comes, but the general idea is that when it comes, oil production increases and oil prices decline. The decline in prices depends on the size of the shock. Nevertheless, it makes sense conceptually that the producer of the new oil on the market becomes the marginal producer and oil prices would gravitate towards the break-even price of the marginal oil producer. This is the type of scenario that played out from 2015 to 2023, barring the effects generated by the COVID-19 pandemic. US shale producers responded to a persistent increase in oil prices by deploying new technologies (fracking). They managed to add a tremendous amount of oil onto the market quickly (see fig. 3.2), whereby oil prices equilibrated around the break-even price of US shale.

These two shocks, demand and supply, capture the rollercoaster nature of oil prices, which

Figure 3.5: Illustrates demand-side shock on oil and the market response in the a Short run b Long run

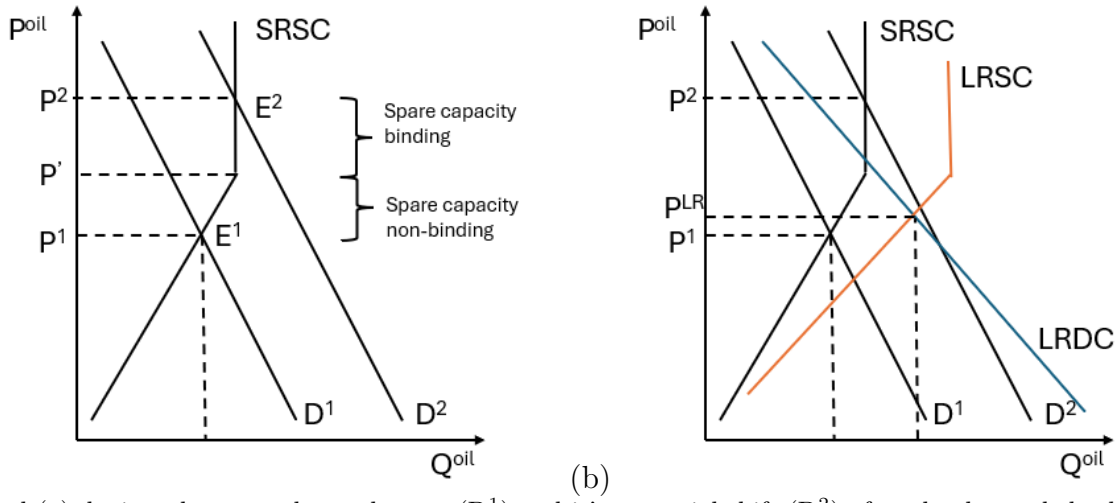

Panel (a) depicts short-run demand curve (D^1) and it's potential shift (D^2) after the demand shock and resulting prices. SRSC is a short-run supply curve. Panel (b) shows the changes of the long-run demand (LRDC) and supply curves (LRSC) due to increased elasticities as well as possible technological innovations on the supply side.

help explain some major episodes that oil prices have experienced in their history. These are key features we wanted reflected in the model and are illustrated by the model's historical forecasts (see fig. 3.7). The current question is how oil prices will develop as we move beyond the COVID-19 pandemic: in which directions will demand and supply conditions normalize? Is the world awaiting a new oil price rollercoaster? We will present such a scenario and its rationale in the following section.

3.3.1 Oil Supply

The oil supply equation is comprised of a standard supply curve's economic/technological view, where production responds positively to current and past oil prices. In the short run, the impact of oil prices on production arises from the ability and willingness of producers to accelerate production from existing fields and to utilize available spare capacity. Over the medium term, further adjustments can occur as high prices incentivize new exploration and technological advancements. These projects tend to have lead times of between four to six years. However, oil producers must first interpret an increase in oil prices as relatively permanent and therefore, oil prices must grow persistently before such projects are approved.

According to table 3.1, there is significant uncertainty regarding the development timelines of oilfields. Nevertheless, the development of US shale can serve as a useful comparison, given its execution within a favourable infrastructure and regulatory framework. Starting from the emergence of a tight oil market in 2003, the first shale oil entered the market a decade later. However, it was not until 2015, after around 13 years, that production actually surged and brought about significant drops in oil prices. Consequently, in our model, the

long-run elasticity of supply is based on a 13-year moving average to account for a period of persistently high prices, the approval process for new projects, and the length of time it takes to place oil on the market.

Table 3.1: Estimated time required to develop new oil production capacity

The article	Years	Note
Wachtmeister and Höök (2020)	5.5	First investment - first production
Wachtmeister and Höök (2020)	12-17	Maximum investment to maximum production
Darko (2014)	9-25	Explore 1-5, appraisal 4-10 and development 4-10 yrs
Tullow Oil plc (2024)	5-20	Explore and appraisal 2-10, and development 3-10 yrs

The supply equation is:

$$ln(\frac{q_t^s}{q_{t-1}^s}) = \alpha_1 q^{tr} - \alpha_2 ln\tau_t + \alpha_3 ln(\frac{p_t}{p_{t-1}}) + \alpha_4 \frac{1}{12} ln\frac{p_{t-1}}{p_{t-13}} + \epsilon_t^s \tag{3.1}$$

Oil supply q_t^s grows with the supply trend growth rate q^{tr} (calibrated using the EIA's long-run average of production growth), rises in real oil prices p_t and the 13-year moving average of real oil prices. The parameters $\alpha_3 > 0$ and $\alpha_4 > 0$ capture the short-run and long-run price elasticities of the oil supply. The magnitude of price elasticities should be treated cautiously because our knowledge about the oil supply response to price increases is limited, as most economic model estimations focus only on demand elasticities. The variable τ representing oil market tightness adheres to a straightforward logic: when the market is tight (with low spare capacity), oil production growth is negatively impacted, potentially leading to acute shortages in supply that are insufficient to meet demand. The parameter is calibrated to generate a large and persistent increase in oil prices when spare capacity approaches one million barrels per day, largely reflecting the experience between 2003-2008.

Oil market tightness

The significance of incorporating OPEC spare capacity into analyses has been acknowledged by institutions, including the EIA (2023c). However, little has been done to formally model OPEC spare capacity and oil prices except for some recent examples from Pierru, Smith, and Almutairi (2020) and Almutairi, Pierru, and Smith (2021), which extended the modelling work of Pierru et al. Pierru, Smith, and Zamrik (2018). These papers model OPEC's spare capacity within a structural modelling environment and illustrate how OPEC's spare capacity has been used to calm the overall volatility of oil prices. This insight can be helpful for describing the potential impact of OPEC spare capacity on future oil price scenarios. Still, the magnitude would need to be compared to the underlying forces in the oil market at any given time. The novelty of this paper lies in our ability to test different macroeconomic and oil market narratives using the implications of OPEC spare capacity on oil market tightness and, thus, on oil prices.

The EIA provides data concerning global crude oil spare capacity (EIA, 2022), defined as "the production volume that can be brought online within 30 days and sustained for at least

90 days" (EIA, 2023b). This definition excludes oil production capacity that is offline due to unplanned outages or sanctions. Figure 3.6 provides data on OPEC spare capacity.

Figure 3.6: OPEC spare capacity and oil market tightness.

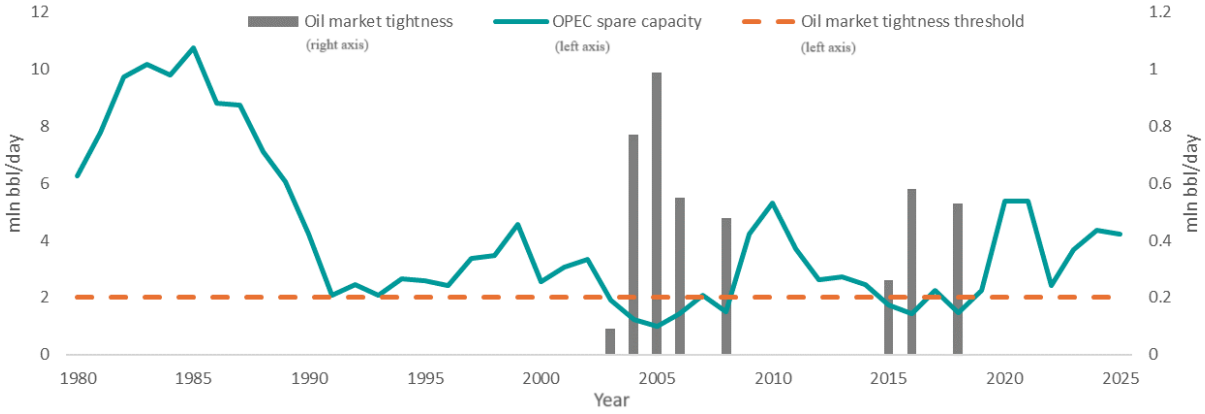

Source: EIA (2022). Notes: The orange line on the graph indicates the threshold below which the oil market becomes tight according to our historical interpretation of the oil market. The OPEC spare capacity in 2024 and 2025 is based on EIA's expectations that the 2023 OPEC production cuts will not be permanent.

The challenge of maintaining a sufficiently high surplus capacity primarily stems from geological factors. Oil extraction is often compared to a cake-eating problem in literature, drawing on Hotelling (1931), which posits that production can be adjusted in response to price signals beginning when an oil reservoir is tapped. However, when a well is drilled, the reservoir pressure, which propels oil to the surface, begins to decline with oil flow, diminishing the overall cheaply recoverable crude oil. More recent literature instead compares this phenomenon to a keg-tapping problem (Anderson, Kellogg, & Salant, 2018). Shutting down an oil well during periods of low prices is thus economically unjustifiable. Anderson et al. (2018) observe that production from drilled wells consistently declines and does not react to price fluctuations. What responds to price signals is the decision to drill new wells, a costly endeavour.

OPEC spare capacity is recognized for its role in stabilizing crude oil prices (Almutairi et al., 2021). During periods of high oil prices, this spare capacity can be injected into the market, shifting the global supply curve rightward and lowering prices. However, a pertinent question arises when spare capacity is already being used to stabilize prices and a new demand or supply shock hits the economy.

By understanding how OPEC's spare capacity is estimated, we believe that its methodology has a clear weakness in accommodating fundamental factors such as depletion rates connected to peak oil production. Such factors could significantly influence the interpretation of available spare capacity. For instance, once Saudi Arabia sees that its production capacity is slowing down, it may want to announce that the 1 million barrels of oil it removed from the market in 2023 (OPEC, 2023b) will never return, in an effort to prolong its oil reserves and oil revenue. Saudis have the added benefit of controlling enough of the market, so that this type of policy can be implemented unilaterally, and can have a net-zero effect on their revenues in the short run. A 1 million-barrel-per-day reduction represents about 10% of Saudi production and

1% of global production. A 1% reduction in global production is typically associated with a 10% increase in oil prices after elasticities of demand and supply are factored in. In such a scenario, it would be inaccurate to interpret these underlying conditions as additional spare capacity, as anticipated by EIA (2023a) in 2024 in fig. 3.6. Armed with this perspective, we can explore alternative hypotheses using OPEC's spare capacity, such as whether production cuts by OPEC and Saudi Arabia are temporary or permanent. As time progresses, we become better positioned to revise our beliefs on this issue, which regularly appears in risks and assumptions in oil price analysis.

This paper introduces the use of OPEC's spare capacity as a proxy for oil market tightness, τ. We use 2 mln barrels of oil per day as the level of spare capacity that does not apply supply-side pressure on oil prices[1] (Benes et al., 2015; EIA, 2023c). We then subtract the actual spare capacity from this 2 mln threshold to obtain our oil market tightness variable (grey columns on fig. 3.6), and we are only interested in its positive values, which signal that the market is tight or cannot respond well to positive demand conditions. Because supply and demand curves are both highly inelastic in the short run, a small shift in demand will have large implications for oil prices. The chosen value of τ should be seen as an approximate benchmark rather than a precise empirical cutoff, reflecting a level of spare capacity that has been observed in history to exert upward pressure on oil prices.

The effect is linear, but we can imagine that this process can easily be non-linear, and the analyst should be attuned to such an outcome when producing scenarios in which spare capacity falls further from this threshold. The model, and specifically the oil market tightness variable here, is constructed to help explain the rise in oil prices in the lead-up to the GFC and potential future scenarios in which similar conditions can materialize.

Figure 3.6 thus shows the empirically constructed tightness variable, which measures how far actual spare capacity falls below the threshold. Equation 3.2 does not redefine this variable but shows how the variable is treated in the model that captures the persistence of tight market conditions once they occur:

$$\tau = \alpha_5 \tau_{t-1} + \epsilon^{\tau} \tag{3.2}$$

Oil tightness, τ, is a persistent autoregressive process whereby, when the oil market becomes tight, it is difficult to add new supply capacity quickly. Therefore, a scenario that considers limited spare capacity from fundamental supply constraints would be slow-moving and produce persistently elevated oil prices. Of course, the spare capacity could rise quickly over the short or long run due to negative demand shocks, such as the GFC and more aggressive climate change initiatives.

[1]We have experimented with various levels of OPEC spare capacity, including making the ratio of spare capacity to global consumption constant, thereby implying the spare capacity threshold should rise over time. However, these alternative specifications produced very similar dynamics and did not materially change the model's results, so we kept the simpler fixed threshold for clarity.

3.3.2 Oil Demand

The traditional perspective suggests that global oil demand is influenced by a mix of economic activity Y_t (the log of GDP) and real oil prices p_t. Increased economic activity leads to higher oil demand as oil is a crucial input in production processes. In contrast, higher oil prices tend to lower oil demand due to increased incentives for substituting away from oil. In the short term, the price elasticity of demand γ_2 is expected to be modest, but in the long term, γ_3, it may rise as substitution occurs. Therefore, our explanatory variables incorporate current oil prices and a 10-year moving average (Benes et al., 2015) of oil prices. The demand equation mirrors the construction of the supply equation, utilizing log differences. Thus, we have:

$$ln(\frac{q_t}{q_{t-1}}) = \gamma_1(Y_t - Y_{t-1}) - \gamma_2 ln(\frac{p_t}{p_{t-1}}) - \gamma_3 \frac{1}{9} ln \frac{p_{t-1}}{p_{t-10}} + \epsilon_t^d \tag{3.3}$$

The γ_1 parameter has historically been used to reflect the strong correlation between GDP and oil demand, as evidenced by numerous prior studies (Helbling et al., 2011). However, this correlation is likely to weaken in future due to ongoing climate change policies and China's evolution into a more mature economy. Developed nations already exhibit a notably lower income elasticity, averaging around 0.5 (Helbling et al., 2011), indicating a production structure that is less reliant on oil and more focused on services. In contrast, several key emerging markets show higher income elasticities. The calibrated price elasticities of demand align with estimates from the Helbling et al. (2011), indicating a very low short-term elasticity of 0.02 and a long-term elasticity (after ten years) of 0.06[2].

The combination of low-price elasticities of supply and demand suggests that any decrease in available supply or insufficient supply growth compared to historical trends will likely result in substantially higher oil prices, an economic downturn, or a combination of both.

3.3.3 World GDP

We capture the feedback from oil prices to economic activity and vice versa with a series of simple world GDP equations. These equations allow us to distinguish shocks to the output gap y_t - transitory shocks to the output, shocks to log of potential output $\bar{Y}$ - permanent shocks to the level of output, and shocks to potential output growth ϵ_t^g - permanent shocks to the growth rate of output. This detailed specification enables us to model the interactions between oil price fluctuations and GDP, wherein both the trend and the gap in GDP decline with rising oil prices. However, deriving precise estimates of these distinct effects remains challenging due to limited variation in historical data. The GDP equation is as follows:

$$Y_t = \bar{Y} + y_t \tag{3.4}$$

in which permanent shocks to the level of log output can be represented as:

[2]Certainly, these elasticities could be made time-variant, but we are looking for a simple solution to maintain basic macroeconomic consistency.

$$\bar{Y}_t - \bar{Y}_{t-1} = g_t + \epsilon_t^{\bar{Y}} \tag{3.5}$$

In equation 3.5, g_t is the growth rate of potential output. This indicates that the potential level varies around its trend trajectory. The global potential GDP growth rate oscillates around an exogenous long-run trend, with oil price fluctuations intensifying these variations. Oil prices can exert persistent but not permanent effects on the GDP growth rate. We have:

$$g_t = \lambda_1 g_{t-1} + (1-\lambda_1)g^{ss} - \lambda_2(log\frac{p_t}{p_{t-1}} - \rho) - \lambda_3(log\frac{p_{t-1}}{p_{t-2}} - \rho) + \epsilon_t^g \tag{3.6}$$

In equation 3.6, g^{ss} represents the average or steady-state growth rate of global GDP, ρ is the average growth rate of real oil prices, and ϵ_t^g denotes a shock to the growth rate of potential output. The estimated steady-state annual growth rate of potential global GDP is 2.8% (EIA, 2023a). The average annual growth rate of real oil prices, at which the model assumes zero impact of oil prices on output growth, is 5%. The findings indicate that a higher-than-average oil price growth rate has a modest yet significant negative impact on the potential growth rate. Both exogenous shocks ϵ_t^g and oil price fluctuations cause the growth rate to persistently deviate from its long-run value, as evidenced by the estimated coefficient on the lagged growth rate, which equals 0.9.

In addition to accounting for the impact of higher oil prices on the growth rate of potential output, the model also considers the potential for higher oil prices to induce fluctuations in the economy's excess demand. Following standard practice for equations of this nature, we model fluctuations in the output gap as persistent. We define the process as follows:

$$y_t = \phi_1 y_{t-1} - \phi_2(log\frac{p_t}{p_{t-1}} - \rho) - \phi_3(log\frac{p_{t-1}}{p_{t-2}} - \rho) + \epsilon_t^y \tag{3.7}$$

where ϵ_t^y denotes a shock to the level of aggregate demand. Similar to the equation for potential, the coefficient estimates indicate that higher oil prices have a modest yet notable negative impact on excess demand, and this effect is highly persistent. The impulse response functions produced using our model can be found in Appendix 3.A.

This model can be improved in several ways, but these additions need individual care and attention:

- Offer greater detail on the impact of the desired stock of oil inventory on oil prices. The oil market tightness variable captures this type of dynamic when low oil inventories become acute, but it is more binary and conceptual. Greater detail on inventories can offer a more accurate and continuous view of oil market tightness.
- Improve the modelling of oil supply, following Benes et al. (2015), where geological constraints are explicitly incorporated. However, such incorporation is perhaps better suited for a satellite model that focuses on a specific research question on oil geology, rather than for a production oil model that requires simplification for institutional adoption.

- Model the feedback loop between oil prices and economic growth in greater detail, especially in the context of separating world GDP by importing and exporting countries, in which oil prices have very different effects on their economies.
- Separate the demand side of the model by the economic status of countries, because more advanced economies have a lower income elasticity of demand for oil than their emerging market counterparts.
- Separate the supply equation into OPEC and non-OPEC production. Based on supply forecasts by the EIA, there is a realistic view that OPEC production is slowing down and that non-OPEC production will increase to fill the growing demand for oil in the forecast. Modelling these separately would offer useful granularity to describe alternative supply scenarios more realistically.
- Model oil market tightness as a Markov-switching process rather than as a purely judgmental approach that allows for non-linearity at different levels of oil market tightness.

3.3.4 Evaluating the Model Through a Historical Narrative

Describing the historical narrative of oil prices and comparing them with the out-of-sample rolling forecasts by OILMOD offers crucial context for understanding the structure and application of our model, which highlights key periods of oil market dynamics that the model seeks to capture. For example, the era from 1990 to 2003, characterized by abundant "easy oil", saw relatively stable prices and mean-reverting forecasts. This stability gave way to the tight oil market from 2003 to 2013, when OPEC spare capacity dwindled, causing prices to soar. Such conditions underscore the importance of accurately interpreting oil market tightness and its macroeconomic implications, as demonstrated in OILMOD. The out-of-sample forecasts of the model in figure 3.7 show in what ways the model performs well and poorly relative to the EIA benchmark, and ultimately, we can evaluate its capacity to generate plausible and useful scenarios under reasonable assumptions.

1990-2003: Loose Oil Supply and Belief in Markets

Before and throughout the 1990s, the oil market was considered an era of geological abundance, so-called "easy oil". Even though the predictions made by Hubbert (1956) in the 1950s about peak oil in the US materialized in the 1970s, and a similar fate was anticipated for other major conventional oil producers such as Saudi Arabia, the oil market still operated under the assumption that regardless of short-run shifts in demand and supply, adjustments would follow to moderate oil prices. This belief is exemplified by the historical forecasts from the EIA, which tended to revert to the mean during this period (refer to fig. 3.4).

Indeed, this paradigm for thinking about oil prices performed very well during this period; however, the market, as well as the EIA, were slow to react to changes in the market, which can be attributed to a combination of rising oil demand and the oil supply situation becoming acutely tighter beginning in 2003. This is our central critique of the EIA: their econometrically driven analysis largely behaves as a mean-reverting machine, which, when the supply of oil is

Figure 3.7: Historical out-of-sample forecasts of our model

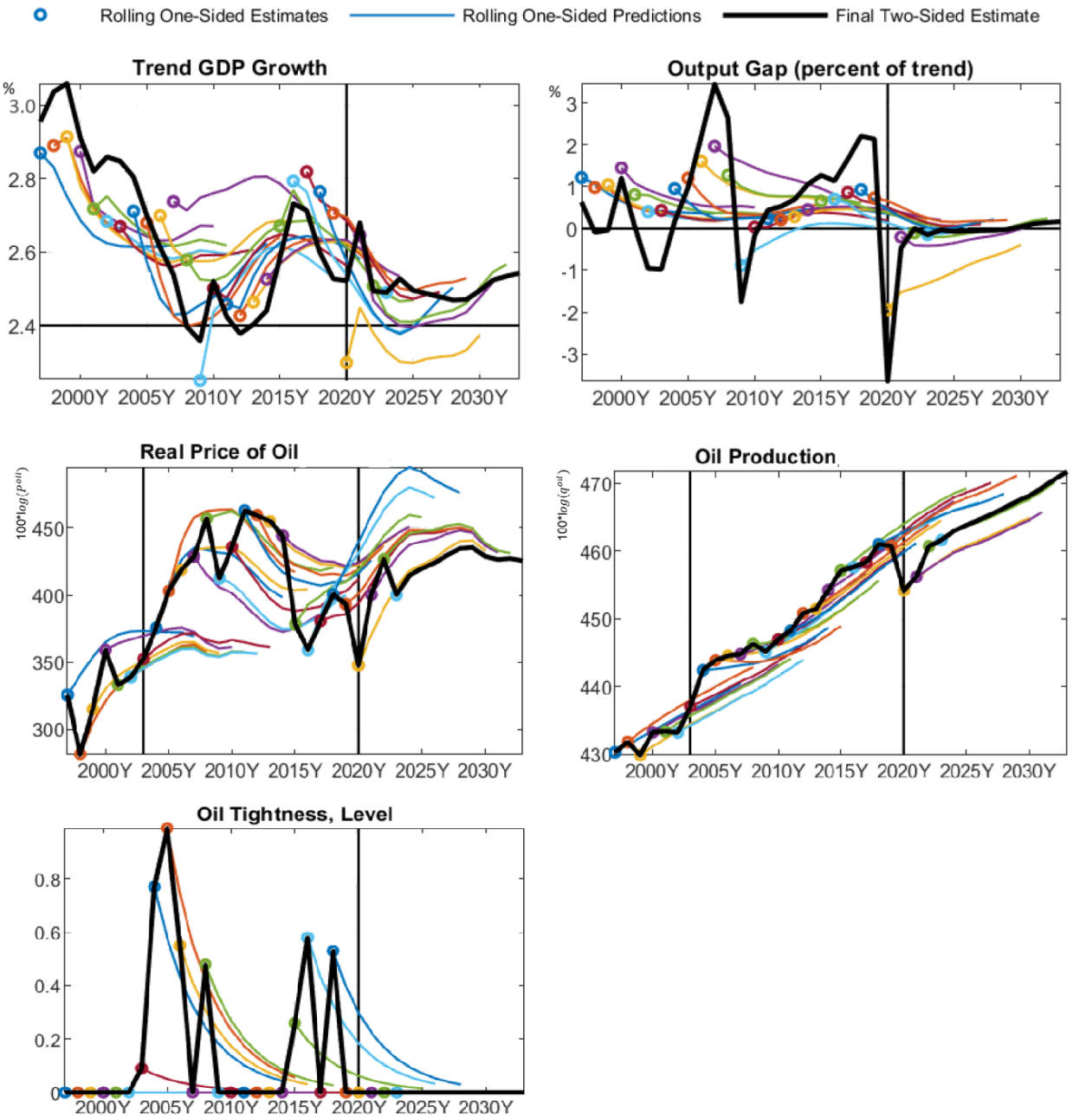

Source: Authors' own computations. Notes: The figure shows historical out-of-sample forecasts for key variables, where the solid black line is the final reference scenario, assuming no oil supply or demand shocks. These results illustrate OILMOD's ability to reflect major historical oil market developments. Notably, the model reproduces the mean-reverting price patterns of the loose oil period before 2003 and effectively captures rising price expectations before the financial crisis, thanks to the inclusion of the oil tightness variable. However, it fails to anticipate the shale oil revolution and, therefore, forecasts that oil prices will rise due to perceived market tightness from OPEC's perspective.

plentiful, is a good model to follow. However, depletion of oil in conventional oilfields, by as much as 6 million barrels per day each year (Al-Murshed, 2024) or Saudi Arabia's contribution to global oil supplies every two years, suggests that the probability of experiencing a period of plentiful oil diminishes over time unless there is a more serious reduction in reliance on oil.

2003-2013: Tight Oil Supply and the Global Financial Crisis and Recovery

The period between 2003 and 2014 was exemplified by OPEC spare capacity reaching historic lows, suggesting an extremely tight oil market and contributing to the rapid rise in oil prices during this period. However, figure 3.8 clearly illustrates that a seasoned analyst could have generated plausible scenarios ex-ante that the oil market was in a state of extreme tightness and, therefore, could have anticipated that prices would continue their meteoric rise. This dynamic is captured nicely by our model in the out-of-sample forecasts during this period, which is perhaps the most important period to get right in terms of considering implications for monetary policy. During this period, most oil market researchers, both in academia and in policy institutions, attributed the pre-GFC rise in oil prices to a demand boom, largely overlooking supply-side constraints. However, if demand alone had been the driving force, we would not have seen oil prices quickly return to historical highs after the GFC. In fact, the return of high oil prices following the GFC and their persistence were likely a key driver for developing shale oil technology and unlocking new sources of oil. This suggests the need to consider potential fundamental changes on both the supply and demand sides of the oil market. Even if such information cannot be directly incorporated into the oil model, it should at least guide the modeller in shaping narratives and constructing plausible scenarios.

Figure 3.8: OPEC spare capacity and historical oil prices.

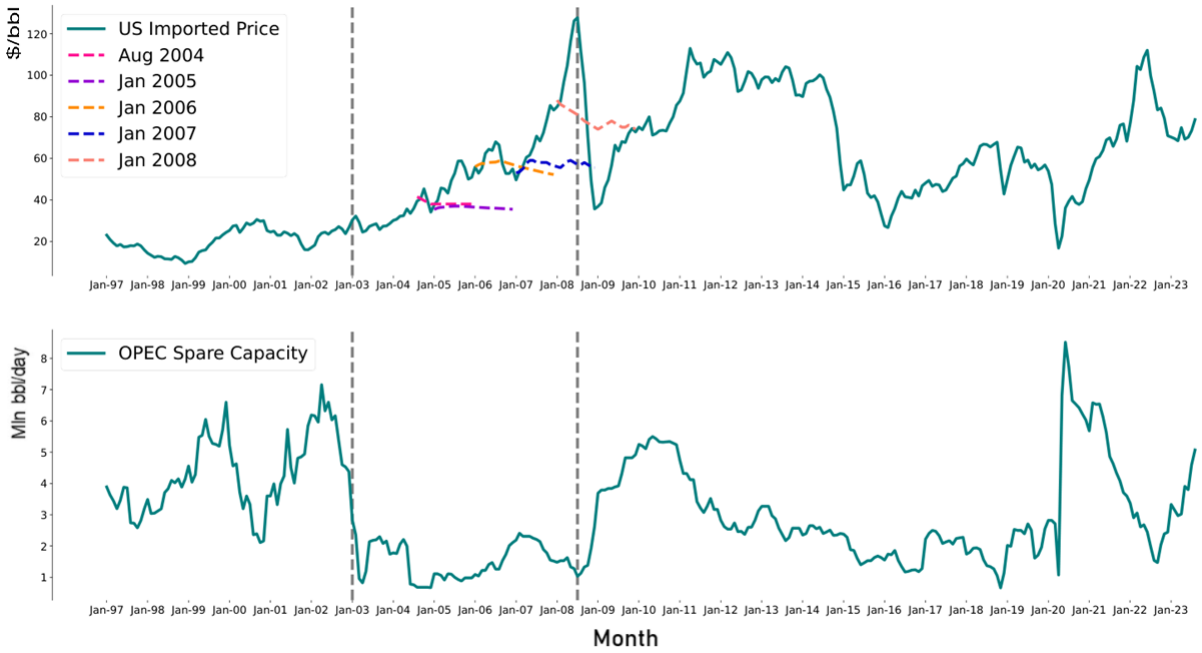

Sources: EIA (1983-2023) and EIA (2022). Notes: The figure highlights the specific historical period 2003-2008, in which OPEC spare capacity fell below 2mln bbl/day, and prices skyrocketed, yet the EIA maintained its mean-reverting forecasts.

2014-2019: The Shale Revolution

The final period under consideration in this paper is 2014-2019. Our model predictably does a poor job of forecasting prices using OPEC's spare capacity, given that OPEC continued to operate at historic lows amid a massive positive supply shock from new oil supplies from US shale (see fig. 3.2a). However, it should be fairly easy to imagine that an analyst would not blindly follow the implications of the model based on OPEC's spare capacity for oil market tightness during this time. Instead, one could see the build-up in the capacity of the US shale industry under a regime of high oil prices before that shock materialized in terms of a sharp decline in oil prices. Under these conditions, the US shale industry becomes a marginal producer of oil, and therefore, oil prices would naturally fall to the cost of production for US shale. This is a prime example of the long-run elasticity of oil supply in action, but it is difficult to capture accurately in a model. One would need a broader analytical framework that could help to triage which issues are most relevant for a given period.

Analyzing these historical periods helps us to develop a conceptual range of plausible supply-side scenarios in a forecasting exercise in which, on one end, scenarios predicated on a persistently negative oil supply shock would rise to levels experienced in the lead-up to the GFC and, on the other end, scenarios for lower oil prices would fall to wherever the cost of production is for a marginal producer. These two historical examples help shape the magnitude of uncertainty and thinking about what would be necessary to generate such scenarios from a supply perspective. However, considering such a scenario today would likely require another round of substantial investment into unconventional oil, where there are currently no obvious candidates, thus placing the globe on the upward path towards another rollercoaster, where oil prices must rise first to a level that will justify the investment to build new capacity.

3.4 Scenario Analysis

Building on the historical insights provided by the rolling forecasts, we now shift our focus to forward-looking scenario analysis. While the historical narrative highlights the factors that drove past oil price dynamics, the scenario analysis demonstrates how OILMOD can be used to construct narrative-driven conditional forecasts for oil prices that are consistent with macroeconomic fundamentals. We produce forecasts based on variables including OPEC spare capacity. We also illustrate how our oil model can be used to generate an oil price scenario that would bring oil prices near the level of the EIA's High Oil Price Scenario, where the oil price is an exogenous assumption. The exercise allows us to better understand what oil production and global output conditions would be necessary to generate an extreme scenario, and to estimate its timing. Then, we can ask ourselves whether it is in fact an extreme event, and we can draw conclusions as to whether central banks would be well-advised to be prepared for this possibility in the future, which we simulate in the following section.

We also include a series of scenarios from the EIA (2023a) to compare with our scenarios. These EIA scenarios come from their October 2023 International Energy Outlook, and we highlight their Reference scenario, a High Oil Price scenario, and a Low Oil Price scenario (EIA, 2023a). The Low and High oil price scenarios demonstrate how the EIA treats oil

prices as an exogenous variable, under the assumption that oil prices are permanently higher or lower at the start of the forecast period, which indicates a lack of an analytical framework that integrates supply and demand and also maintains some basic macroeconomic consistency in their scenario process. However, given the historical volatility of oil prices, the magnitudes of their high and low-price scenarios are reasonable. While these are possible scenarios for oil prices to reach, these extreme shifts to either end would likely have a profound impact on the oil market, an aspect we aim to capture in our scenarios.

Figure 3.9: Oil production scenarios

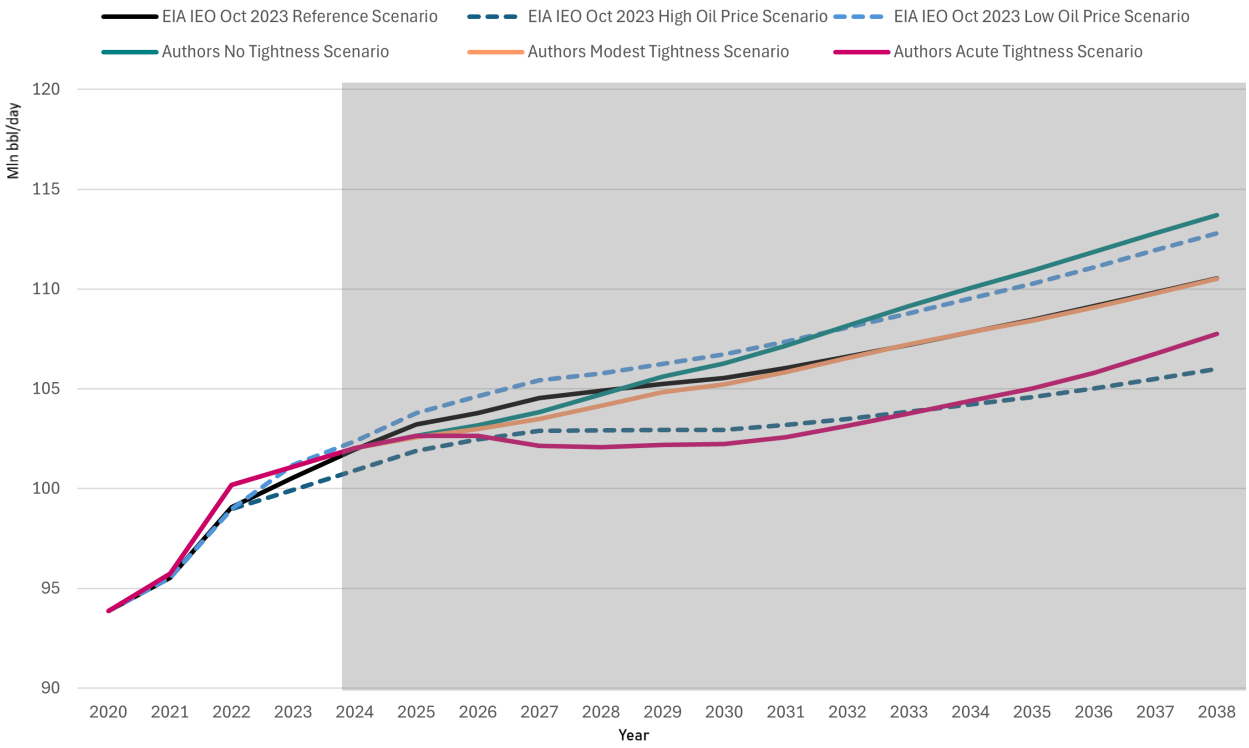

Source: EIA (2023a) and Authors' own computations.

The initial scenario we introduce is one in which our oil tightness variable is zero for the forecast, offering a model-driven reference projection that does not incorporate any shocks. The projection outlines a trajectory with slightly lower oil prices and higher production compared to the EIA Reference scenario (see figures 3.9 and 3.10). The scenario can be categorized as a flexible oil market in which OPEC's spare capacity can respond to modest changes in demand, and therefore, oil prices can remain near the cost of producing a barrel of US shale oil. However, this is still a very imprecise top-down forecast of production and consumption, in which there is potential to apply a more detailed bottom-up approach that looks at current projects under development and their estimated completion times. Regardless, achieving a sustainably low oil price in the future will likely require either a large decoupling of global real growth and oil demand or an overly optimistic outlook for global growth under major climate change initiatives.

In the second scenario, we tune the last value of the projection horizon for oil production to the values in the EIA's Reference scenario to test how the model would replicate such a

Figure 3.10: Oil price scenarios

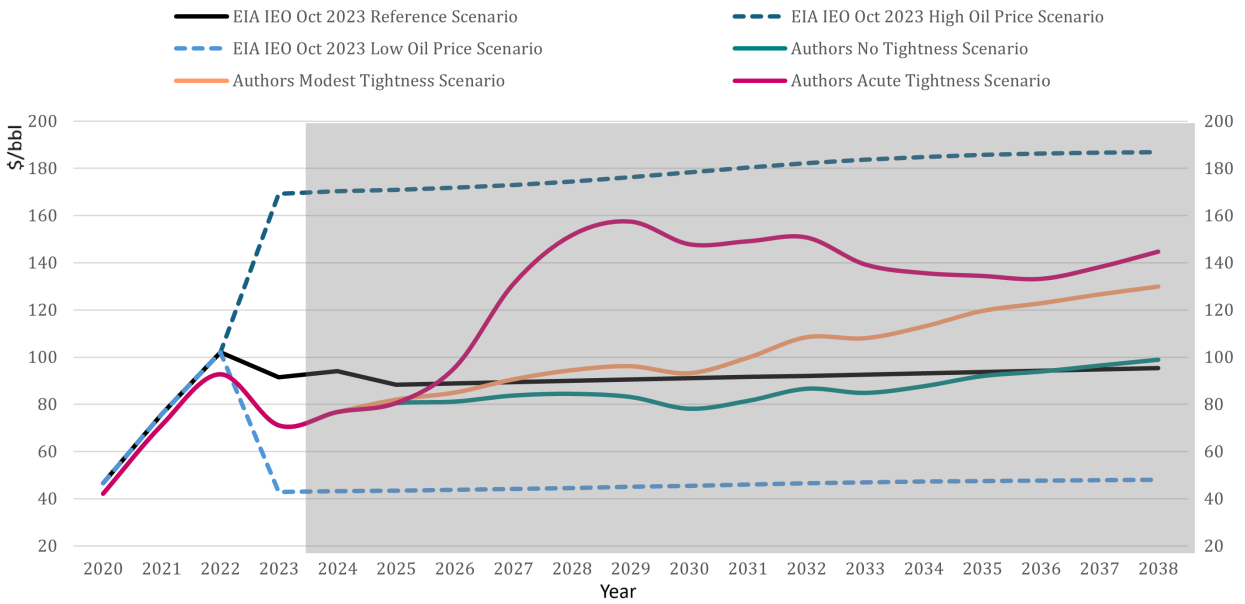

Source: EIA (2023a) and Authors' own computations. Notes: EIA (2023a) quotes Brent Prices in 2022 USD; we use Imported Acquisition Cost by US Refiners in 2022 USD. In EIA (2023a), projections start in 2022, which explains the large price discrepancy between EIA (2023a) and our reference scenarios in 2023. In the high oil price scenario, OPEC spare capacity begins to bind by the beginning of 2026.

production outlook. The results are intuitive, and the shortfall in production is attributed to a modest increase in oil market tightness, in which OPEC spare capacity would fall to support the market in the short run and keep oil prices near production costs. However, as the oil market becomes tighter, producers become less responsive to positive changes in demand, and investors would need to be compensated for this risk; therefore, steady upward pressure is applied on oil prices in the long run, which is not depicted in the EIA's Reference scenario.

Our final scenario leverages the oil market tightness variable to construct a high oil price outlook based on key supply and demand assumptions. As of 2025, the oil market is oversupplied, evidenced by OPEC's elevated spare capacity. However, this balance could quickly shift if US shale production peaks and non-OPEC production forecasts fall short, and would result in a shortfall of about 1 million barrels per day. With OPEC's spare capacity at approximately 4 million barrels per day, the market could absorb two years of lower-than-expected production before entering a state of significant tightness, historically a precursor to rising oil prices. In the scenario, oil prices would remain range-bound between 70-75 USD per barrel in 2025, nominally, but as OPEC spare capacity declines and the oil market tightens, oil prices rise swiftly.

We calibrate the oil market tightness variable in the scenario to reflect conditions similar to those in the pre-GFC period. This acute supply shortage would trigger a sharp increase in oil prices, akin to a rollercoaster trajectory. The scenario underscores the risk of deeper geological constraints to oil supply and OPEC's inability to compensate over the medium term. Over time, oil prices are projected to rise due to the initial supply shock before stabilizing at a

level high enough to incentivize significant new investments, such as the $12 trillion OPEC estimates are needed to meet future demand (Cooban, 2023).

Based on these considerations, we tend to believe that unless there are major reductions in oil demand from climate change initiatives, underlying supply-side factors can potentially dominate the future of oil prices and have implications for monetary policy.

3.5 The Endogenous Policy Credibility Model (ENDOCRED)

Having established the plausibility of a high-oil price scenario, it is essential to understand why such a scenario should be incorporated into central bank risk assessments and policy discussions. Central banks must assign reasonable probabilities to the occurrence of a high-oil price scenario and evaluate potential implications within their broader monetary policy strategy. This is crucial because oil prices have the ability in some countries to cause significant stagflationary pressures, and many traditional policy frameworks, which primarily focus on demand-driven inflation, may not perform optimally in such an environment. This is because a rise in oil prices will put upward pressure on the overall rate of inflation, but conversely, can also put downward pressure not only on the actual level of output, but also on potential output, depending on the economy. This dual effect on actual and potential output makes it a particularly difficult type of shock to analyze in *real time*. Integrating a high-oil price scenario into a central bank's models and regular analyses enables them to develop more adaptive policy strategies and to mitigate the risks of inflationary spirals and excessive output contractions.

In this section, we analyze a near-term outlook for oil prices within the Endogenous Policy Credibility (ENDOCRED) model framework to generate policy-relevant simulations for the US economy. We select ENDOCRED for its insightful property that does not presume perfect monetary policy credibility and allows inflation expectations to deviate from the target as a result of central bank actions. This feature is particularly relevant, given the monetary policy environment of the past few years, starting with the onset of the COVID-19 pandemic. This period acted as a stagflationary shock due to supply-side constraints and led to higher prices while the global economy was in recession. This situation contributed to a delayed response from most central banks globally, many of which kept interest rates too low for too long under the assumption that inflation was transitory. Additionally, central banks hesitated to implement immediate policy actions for fear of harming an already struggling economy.

The development of credibility-focused models has been transformative for central banks, fundamentally reshaping inflation-targeting frameworks. This evolution began with the pioneering work of Laxton, Ricketts, and Rose (1994) at the Bank of Canada and was further advanced by subsequent research, including Laxton, Isard, Faruqee, Prasad, and Turtelboom (1998), Laxton and N'Diaye (2002), Argov, Epstein, Karam, Laxton, and Rose (2007), and Alichi et al. (2009). These studies emphasize the critical role of credibility for monetary policy to function properly, whereby long-term interest rates, the exchange rate and asset prices all act as shock absorbers, which help to steer the economy back to a stable

equilibrium in response to macroeconomic fluctuations. For monetary policy to succeed in this manner, medium- and long-term inflation expectations among those in the bond market, as well as wage and price setters, must be well anchored. As noted previously, while inflation expectations in the bond market have been remarkably stable throughout the pandemic era in the US, there remains a question of whether inflation expectations among wage and price setters are consistent with inflation targets. Therefore, credibility probably should not be assumed to be perfect, because if monetary policy credibility is damaged, rebuilding it can entail significant costs. In contrast, well-anchored expectations reduce the economic slack required to stabilize inflation, highlighting the importance of monetary policy strategies that enhance confidence in the credibility of the policy regime.

The ENDOCRED model includes equations for the output gap, a non-linear Phillips curve, and a monetary policy loss function that responds to deviations in inflation from its target, the price level gap, the output gap, and interest rate variability. The model's parameters and initial conditions are calibrated using quarterly data for the US. We generate projections for the path macroeconomic variables take to re-equilibrate after an initial shock, with policy credibility playing a central role in shaping the dynamics. Because the simulations of monetary policy responses to oil price shocks are intended to illustrate our argument for the value of an in-house oil market framework for central bankers, we do not provide an in-depth analysis of the ENDOCRED model. Instead, appendix 3.B complements our main analysis by providing technical details of the ENDOCRED model for those interested in its methodological foundations. Readers can also refer to the cited sources for further inquiries or replications.

To explore the effects of high oil price shocks, we simulate policy outcomes under different credibility regimes, in which central bank credibility varies in its ability to anchor inflation expectations. We examine both delayed and immediate interest rate responses. These results are presented in figure 3.11. To demonstrate the model's capabilities, we introduce a 40% increase in oil prices in the second quarter of 2025, a magnitude chosen to reflect a plausible scenario in a period in which the US administration threatened to apply "maximum pressure" on Iran, that would have seen their oil production fall by 2 mln barrels per day. This scenario simulates the effects of a significant oil supply shock on inflation, output, and interest rates. The following section discusses the results, emphasizing the importance of timely and credible policy actions for mitigating the long-term economic costs of stagflationary shocks.

3.5.1 Policy Simulations Under Different Credibility Regimes

The results of the ENDOCRED simulations, as illustrated in figure 3.11, reveal significant differences in policy responses depending on the credibility regime. In a scenario in which monetary policy credibility is strong, inflation expectations remain well-anchored, allowing the central bank to implement a more gradual tightening of interest rates while still achieving price stability. In contrast, in regimes with lower credibility, inflation expectations become unanchored, necessitating more aggressive policy interventions to restore confidence. The credibility of monetary policy plays a crucial role in determining the trade-offs between stabilizing inflation and mitigating output losses.

Figure 3.11: Macroeconomic responses under different credibility regimes

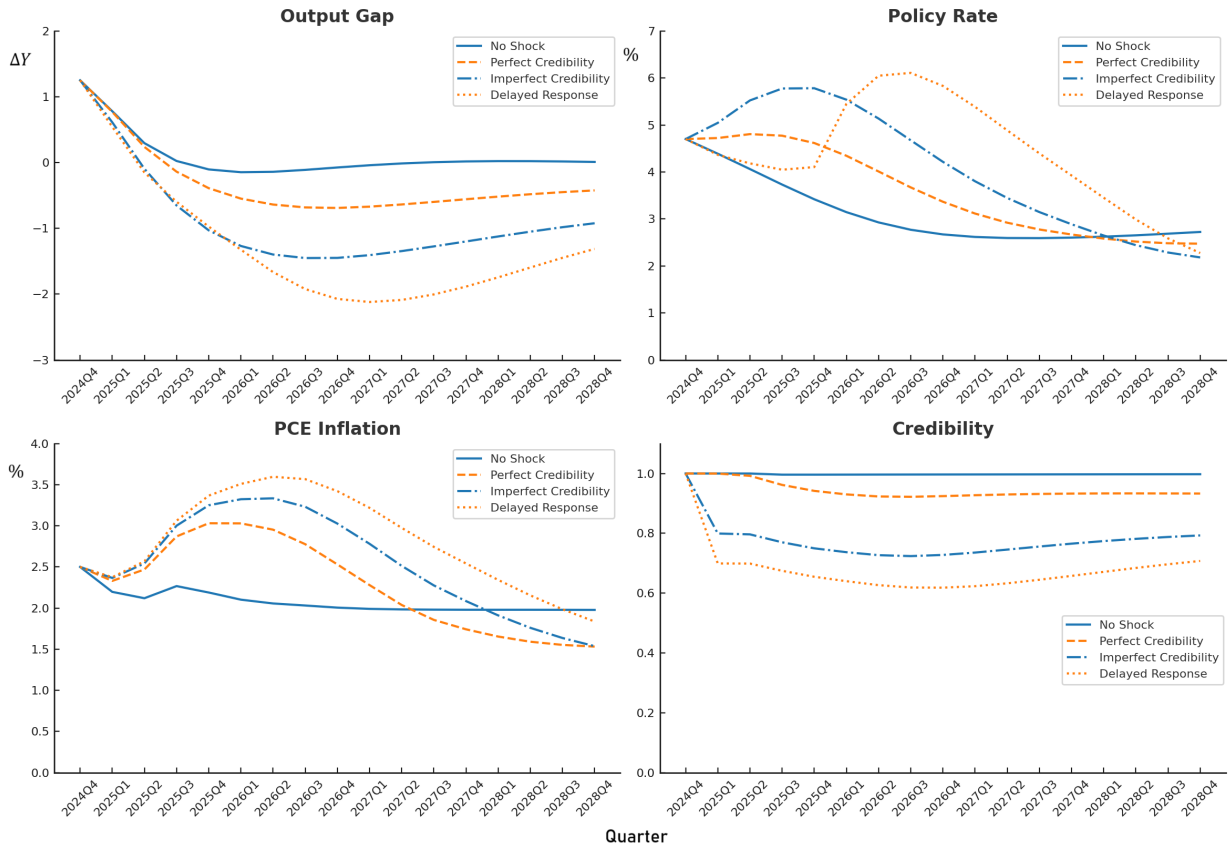

Source: Authors' own computations. Notes: The "No Shock" scenario represents the current macroeconomic status quo in the US, where no oil price shock occurs. The four panels depict the re-equilibration process for the output gap, policy rate, PCE inflation, and credibility. While "Perfect Credibility" allows for a smoother adjustment, "Imperfect Credibility" and "Delayed Response" lead to prolonged inflationary pressures, higher interest rates, and deeper output contractions, underscoring the importance of timely and credible policy actions. The fourth figure on the panel shows that loss of credibility is a persistent, long-term process, continuing even when inflation falls back to the target rate, until credibility is fully restored.

Credibility-dependent policy responses are evident in the dynamics of the output gap, policy rate, and inflation. In a delayed response scenario, in which credibility is lower, inflation remains elevated for a prolonged period, and requires sharper interest rate increases that ultimately result in more pronounced output contractions. This pattern reflects recent policy behaviour during the COVID-19 pandemic, when central banks delayed interest rate adjustments under the assumption that inflation was transitory. However, as inflation persisted, central banks were forced to raise rates more aggressively, resulting in prolonged economic slack and higher nominal interest rates for an extended period. A short-term reluctance to act evolved into a long-term tightening cycle, reinforcing the importance of credibility in monetary policy.

Moreover, the delay in raising the interest rate initially supports demand but comes at the cost of sustained inflationary pressures, which require higher future interest rates and cause a deeper economic downturn. This scenario illustrates how delayed responses to supply shocks,

such as oil price increases, can expose the economy to more severe stagflationary effects. The prolonged policy lag exacerbates economic vulnerabilities, leaving the economy less resilient to future supply-side shocks. This underscores the importance of preemptively addressing credibility issues before an inflationary shock occurs, rather than reacting after expectations have already become unanchored.

The key takeaway from these results is that central banks must proactively manage expectations by reinforcing their commitment to inflation control. Delayed or hesitant policy actions in response to supply-side shocks, as observed in the lower-credibility scenario, can lead to higher economic costs in the long run. The experience of recent years demonstrates that when central banks hesitate to acknowledge credibility concerns, policy adjustments become more costly and prolonged. Even when appropriate actions are taken to bring inflation back to its target, once credibility is lost, it takes a long time to be fully restored. By maintaining credibility through consistent and transparent policy frameworks, central banks can enhance their ability to stabilize inflation while minimizing adverse effects on economic growth. The findings suggest that a well-communicated and preemptive policy stance is essential in mitigating the risks associated with supply-driven inflationary pressures.

3.6 Conclusion and Policy Implications

Among the taxonomy of shocks that monetary and fiscal authorities face, stagflationary shocks, such as an increase in oil prices, are among the most difficult to manage, as demonstrated during the COVID-19 pandemic. The crisis exposed weaknesses even among leading central banks in effectively communicating policy in a stagflationary environment. As a result, there is a growing emphasis on scenario-based forward guidance (Archer, Galstyan, & Laxton, 2022; Goodhart, 2023; Bernanke, 2024), a prudent risk management approach to monetary policy originally championed by Alan Greenspan (2004).

The best-case scenario for a central bank facing a supply shock, such as an oil price spike, is to have inflation expectations well anchored to its target. However, the experience of recent years suggests that prolonged inflation above the target can weaken credibility, making economies more vulnerable to future supply shocks. While many central banks are attempting to engineer a "soft landing", i.e., gradually returning inflation to target without significantly harming the real economy, there is a risk that premature normalization of policy can leave inflation expectations unanchored, as seen in the 1970s.

Given the role of oil prices in shaping macroeconomic conditions, there is an increasing need to condition macroeconomic projections on alternative oil price scenarios. This necessity is even more pressing in a potential peak oil environment, in which supply constraints could make stagflationary shocks more frequent. Developing a robust analytical framework for oil price projections and uncertainty, rather than relying solely on scenarios provided by institutions such as the EIA, is essential for forward-looking monetary policy planning.

This paper presents a practical approach to integrating oil price modelling into central bank macroeconomic frameworks, addressing a gap in existing policy analysis. By embedding oil price dynamics within a semi-structural model, we enhance the depth of analysis compared

to purely econometric or structural DSGE approaches. Our framework allows economists to make more structured assessments of longer-term oil price trajectories and to capture fundamental market dynamics rather than relying on exogenous assumptions. Additionally, the approach sheds light on the ongoing debate among leading oil market forecasters regarding the future trajectory of prices.

Ultimately, our findings reinforce the importance of proactive and credible policy responses to future stagflationary shocks. Our simulations demonstrate that a delayed response exacerbates inflation persistence, necessitates a more aggressive policy tightening later, and leads to deeper output contractions. This strengthens the argument that timely intervention is crucial to minimizing the economic costs of supply-driven stagflationary shocks. A delayed or hesitant response increases the long-term economic costs, as seen in the COVID-19 period, where inflation persistence and policy lags complicated disinflation efforts. By strengthening policy credibility and integrating scenario-based risk assessments, central banks can improve their ability to navigate supply shocks while maintaining macroeconomic stability.

Abbreviations

The following abbreviations are used in this chapter:

EIA Energy Information Administration
FPAS Forecasting and Policy Analysis Systems
GFC Global Financial Crisis
IEA International Energy Agency
OPEC Organization of the Petroleum Exporting Countries

3.A. Impulse Response Functions from OILMOD

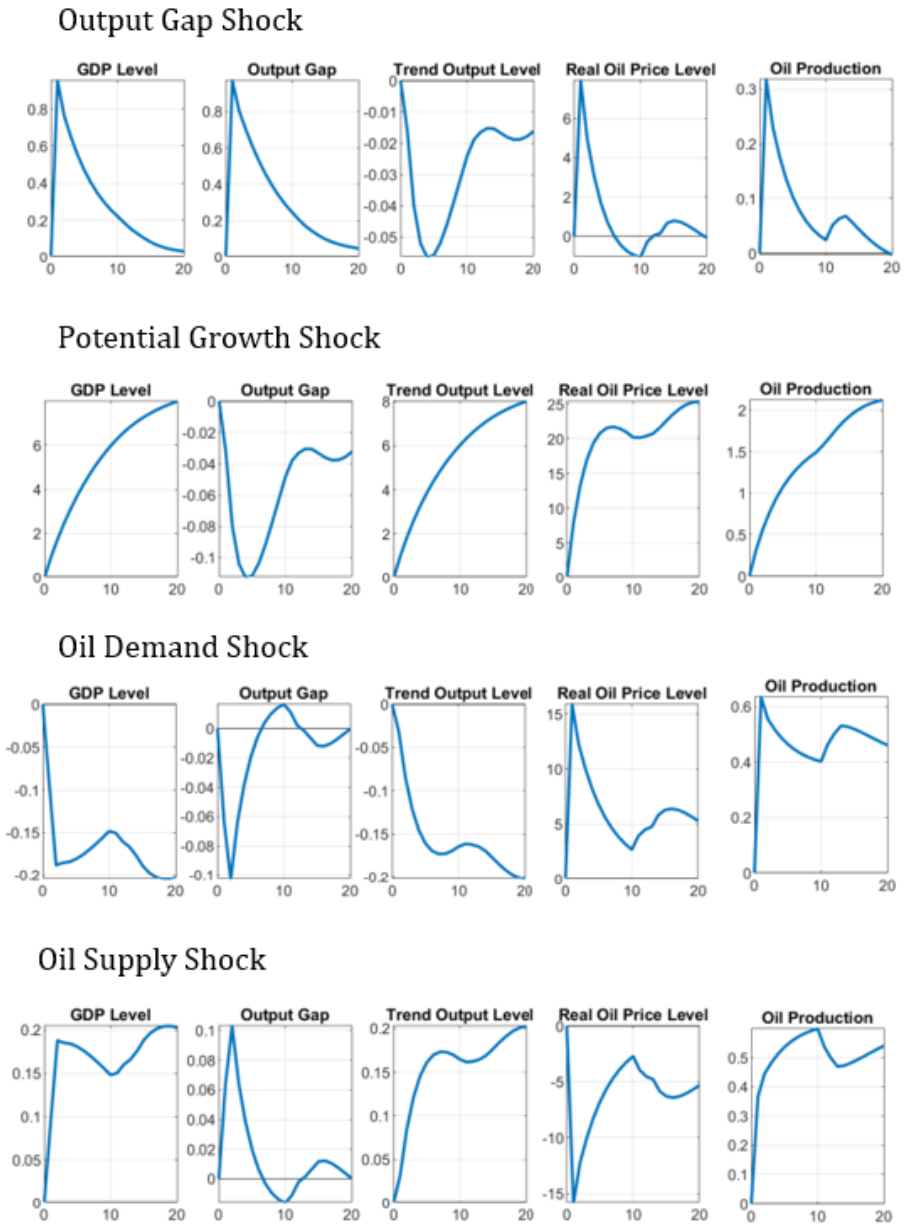

Source: Authors' Own computations.

3.B. Endogenous Credibility Model ENDOCRED

This appendix provides the detailed structural equations used in the ENDOCRED model for readers who are interested in the technical specifications. These equations form the backbone of the model and illustrate how key economic variables interact in response to shocks, with a focus on central bank credibility and policy transmission.

List of notations used for the ENDOCRED model:

Notation	**Description**
π_t	Inflation rate
π^*	Central bank's inflation target
π_t^e	Expected inflation rate
$\pi 4_t$	Year-on-year inflation rate
$\pi 4_t^e$	Expected year-on-year inflation rate
p_t	Price level
p^*	Price level target
$\hat{y}_t$	Output gap: deviation of actual output from potential output; negative gaps are explicitly weighted in the central bank's loss function.
$\hat{y}_{\max}$	Maximum possible output gap, representing capacity constraints
$\hat{r}_{t-1}$	Real interest rate gap: deviation of the real interest rate from its equilibrium level
$\hat{\phi}_t^{10YR}$	Term premium gap: deviation of the 10-year term premium from its equilibrium, representing long-term interest rate effects
i_t	Policy interest rate
ε_t	Shock terms (used for output gap, inflation, credibility, etc.)
λ_1	Parameter for forward-looking and backward-looking inflation in the Phillips curve
λ_2	Parameter for the output gap in the Phillips curve
λ_3, λ_4	Parameters for current and lagged real oil prices in the Phillips curve
π_t^{RPOIL}	Real oil price
$\omega_1, \omega_2, \omega_3, \omega_4$	Weights in the monetary policy loss function for inflation deviation, output gap, interest rate changes, and price level target deviation, respectively
$Loss_t$	Central bank loss function, penalizing deviations in inflation, output, and policy changes
ζ	Intertemporal discount factor used in summing expected future losses.
ρ_1	Persistence parameter for credibility (weight on past credibility)

Notation	Description
ρ_2	Adjustment factor for credibility evolution (weight on central bank performance)
η_t	Flow variable capturing central bank performance, influencing credibility evolution over time.
γ_t	Central bank credibility at time t, determining how inflation expectations are anchored in the Phillips curve

We present the main structural equations of the model that drive its dynamics in response to shocks. The model does not include an uncovered interest rate parity (UIP) equation: this omission is based on the specific focus of our policy simulations rather than an assumption that the US economy operates in a closed system. Given our emphasis on domestic monetary policy transmission and credibility dynamics, we abstract from exchange rate movements and external capital flows, which would otherwise play a role in an open economy framework.

3.B.1. Output Gap Equation

The output gap ($\hat{y}_t$) measures the percentage deviation of actual output from its potential level. It is modelled as a function of past and future output gaps, the real interest rate gap, and the term premium gap, incorporating the term structure of interest rates into its dynamics. Central banks often emphasize the short-term policy rate as the primary measure of monetary policy stance, despite the significant role of longer-term rates in economic decision-making. These rates, shaped by expectations of future policy actions and risk premia, directly influence household and business decisions regarding consumption, investment, and credit creation. Forward guidance plays a crucial role in this process by shaping expectations of future policy rates, thereby affecting borrowing costs and the overall transmission of monetary policy.

$$\hat{y}_t = \beta_1 * \hat{y}_{t-1} + \beta_2 * \hat{y}_{t+1} - \beta_3 * \hat{r}_{t-1} + \beta_4 * \hat{\phi}_t^{10YR} + \varepsilon_t^{\hat{y}} \tag{3.8}$$

3.B.2. Monetary Policy Loss Function

Central banks' aversion to sharp movements in the policy rate, evident in their gradual adjustments in response to economic changes, is technically motivated. While the policy rate is a short-term interest rate, market rates that influence consumer spending, investment, and output are medium- to long-term. Effective transmission of policy actions depends on market rates reacting predictably to the expected path of the policy rate. Gradual adjustments allow financial markets to project sustained changes, strengthening the response of medium- and long-term rates. In contrast, high variability in the policy rate diminishes its effect on relevant market rates and weakens the policy transmission mechanism.

The loss function assigns a high cost to deviations of inflation from the target. In the short run, monetary actions also impact output, and policymakers seek to minimize deviations from potential output and to avoid significant policy rate variability. Stabilizing output near its current potential is a key macroeconomic objective. Given the Federal Reserve's historical

focus on minimizing recessions and employment shortfalls, we emphasize negative output gaps in the loss function. To incorporate an element of history dependence, we include a price level gap component with a small weight. While the Federal Reserve follows an Average Inflation Targeting (AIT) framework, which allows inflation to temporarily exceed 2% without committing to a strict price level path, introducing a price level gap ensures some degree of accountability for past inflation deviations. This approach provides flexibility in the regime while reinforcing long-term inflation expectations.

With these considerations in mind, the loss function in the model cumulates a weighted sum of:

- Squared deviations of inflation ($\pi 4_t$) from the target (π^*) (year-to-year)
- Squared negative output gaps ($\hat{y}$),
- squared one-quarter changes in the policy rate (i_t),
- Squared deviations from the price level target.

The loss function is expressed as:

$$Loss_t = \sum_{j=0}^{\infty} \zeta^j \Big[\omega_1 (\pi 4_{t+j} - \pi^*)^2 + \omega_2 \hat{y}_{t+j}^2 + \omega_3 (i_{t+j} - i_{t+j-1})^2 + \omega_4 (p_{t+j} - p^*)^2 \Big] \tag{3.9}$$

3.B.3. Non-Linear Phillips Curve

We employ an inflation expectations-augmented Phillips curve, where inflation (π_t) is determined by both forward- and backward-looking components, the output gap, and maximum possible excess demand pressures ($\hat{y}_{\max}$). We also explicitly include oil prices into the inflation equation π_t^{RPOIL}. The higher the rate of increase in the real price of oil, the higher the overall rate of inflation. Additionally, cost-push supply shocks (ε_t^{π}) directly impact inflation, creating a short-run tradeoff between inflation and the output gap. To account for energy price effects, we include current and lagged real oil prices.

$$\pi_t = \lambda_1 \pi 4_t^e + (1 - \lambda_1)\pi 4_{t-1} + \lambda_2 \left(\frac{\hat{y}_{t-1}}{\hat{y}_{max} - \hat{y}_{t-1}} \hat{y}_{max} \right) + \lambda_3 \pi_t^{\text{RPOIL}} + \lambda_4 \pi_{t-1}^{\text{RPOIL}} + \varepsilon_t^{\pi} \tag{3.10}$$

3.B.4. Central Bank Credibility

The credibility equation in the ENDOCRED model captures the evolution of central bank credibility (γ_t) and its role in shaping inflation expectations. Following the framework established by Laxton et al. (1994) and extended by Laxton et al. (1998); Laxton and N'Diaye (2002), the model assumes that inflation expectations are a weighted average of forward- and backward-looking components, where credibility determines the extent to which expectations align with the central bank's inflation target rather than past inflation outcomes.

To ensure that higher credibility directly translates into expectations aligning with the target, we modify the credibility-adjusted inflation expectation equation to explicitly incorporate the inflation target (π^*) as follows:

$$\pi 4_t^e = \gamma_t \pi^* + (1 - \gamma_t)\pi 4_{t-1} + \varepsilon_t^{\pi^e} \tag{3.11}$$

This formulation ensures that when credibility is high ($\gamma_t \to 1$), inflation expectations ($\pi 4_t^e$) are firmly anchored around the central bank's target (π^*), reducing the influence of past inflation persistence. Conversely, when credibility is low ($\gamma_t \to 0$), expectations rely more on past inflation, leading to greater inertia.

To capture credibility shifts, we define two regimes: a low-inflation regime where expectations gradually converge toward a 2% target, and a high-inflation regime where credibility deteriorates, increasing inflation inertia Argov et al. (2007); Alichi et al. (2009). The credibility transition follows an autoregressive process:

$$\gamma_t = \rho_1 \gamma_{t-1} + \rho_2 \eta_{t-1} + \varepsilon_t^{\gamma} \tag{3.12}$$

where η_{t-1} is a flow variable tracking central bank performance in meeting its inflation target, further detailed in Kostanyan et al. (2022).

This specification allows credibility to evolve dynamically in response to past policy performance, reinforcing the role of expectations in monetary policy transmission.

References

Alichi, A., Chen, H., Clinton, K., Freedman, C., Johnson, M., Kamenik, O., ... Laxton, D. (2009). *Inflation targeting under imperfect policy credibility.* Working paper, International Monetary Fund.

Al-Murshed, S. A. (2024). *Saudi aramco: 6 million bpd of global oil production is being lost every year.* Interview published by Bloomberg Middle East on X (formerly Twitter). Retrieved from https://x.com/middleeast/status/1759590783034745060?mx=2 (Accessed: April 2024)

Almutairi, H., Pierru, A., & Smith, J. L. (2021). The value of opec's spare capacity to the oil market and global economy. *OPEC Energy Review*, *45*(1), 29–43.

Alquist, R., Kilian, L., & Vigfusson, R. J. (2013). Forecasting the price of oil. In *Handbook of economic forecasting* (Vol. 2, pp. 427–507). Elsevier.

American Wind Energy Association. (2013-2017). *Wind industry annual market reports.* (Retrieved April, 2019, from https://www.awea.org/resources/publications-and-reports/market-reports)

Anderson, S. T., Kellogg, R., & Salant, S. W. (2018). Hotelling under pressure. *Journal of Political Economy*, *126*(3), 984–1026.

Archer, D., Galstyan, M., & Laxton, D. (2022). FPAS Mark II: Avoiding Dark Corners and Eliminating the Folly in Baselines and Local Approximations. Retrieved May, 2024, from https://www.cba.am/EN/panalyticalmaterialsresearches/Archer-Galstyan-Laxton-FPAS-Mark-II.pdf

Arezki, R., Jakab, Z., Laxton, D., Matsumoto, A., Nurbekyan, A., Wang, H., & Yao, J. (2017). *Oil prices and the global economy.* International Monetary Fund.

Argov, E., Epstein, N. P., Karam, P. D., Laxton, D., & Rose, D. (2007). *Endogenous monetary policy credibility in a small macro model of israel* (Tech. Rep. No. 07/207). International Monetary Fund. Retrieved May, 2024, from https://www.imf.org/en/Publications/WP/Issues/2016/12/31/Endogenous-Monetary-Policy-Credibility-in-a-Small-Macro-Model-of-Israel-21231

Arrow, K. J. (1962). The economic implications of learning by doing. *The review of economic studies*, *29*(3), 155–173.

Avydon. (2023). *Topení peletami: Jaká je cena a spotřeba pelet na topnou sezónu?* (Retrieved August, 2023, from https://www.avydon.cz/topeni-pelety-spotreba)

Bachner, G., Steininger, K. W., Williges, K., & Tuerk, A. (2019). The economy-wide effects of large-scale renewable electricity expansion in europe: The role of integration costs. *Renewable energy*, *134*, 1369–1380.

Benes, J., Chauvet, M., Kamenik, O., Kumhof, M., Laxton, D., Mursula, S., & Selody,

J. (2015). The future of oil: Geology versus technology. *International Journal of Forecasting*, *31*(1), 207–221.

Bernanke, B. S. (2024). Forecasting for monetary policy making and communication at the bank of england: a review. Retrieved May, 2024, from https://www.bankofengland.co.uk/-/media/boe/files/independent-evaluation-office/2024/forecasting-for-monetary-policy-making-and-communication-at-the-bank-of-england-a-review.pdf

Blanchard, O., & Simon, J. (2001). The long and large decline in us output volatility. *Brookings papers on economic activity*, *2001*(1), 135–174.

Bolinger, M. (2014). *An Analysis of the Costs, Benefits, and Implications of Different Approaches to Capturing the Value of Renewable Energy Tax Incentives* (Tech. Rep.). Lawrence Berkeley National Laboratory. LBNL-6610E.

Bolinger, M., & Wiser, R. (2012). Understanding wind turbine price trends in the US over the past decade. *Energy Policy*, *42*, 628–641.

Bureau of Labor Statistics. (2017). *Producer price index - industry data, 1998-2014 [time series].* (Retrieved February, 2017, from http://data.bls.gov)

Campbell, C. J., & Laherrère, J. H. (1998). The end of cheap oil. *Scientific American*, *278*(3), 78–83.

Capros, P., Paroussos, L., Fragkos, P., Tsani, S., Boitier, B., Wagner, F., ... Bollen, J. (2014). Description of models and scenarios used to assess european decarbonisation pathways. *Energy Strategy Reviews*, *2*(3-4), 220–230.

Carpio, L. G. (2021). Efficient spatial allocation of solar photovoltaic electric energy generation in different regions of brazil: a portfolio approach. *Energy Sources, Part B: Economics, Planning, and Policy*, *16*(6), 542–557.

Castillo, C. P., e Silva, F. B., & Lavalle, C. (2016). An assessment of the regional potential for solar power generation in eu-28. *Energy policy*, *88*, 86–99.

Chabot, B., & Saulnier, B. (2001). Fair and efficient rates for large scale development of wind power: the new French solution. *Small Hydro Power*, *4*.

Cienciala, E., & Melichar, J. (2023). *Forest carbon stock budget development following extreme drought-induced dieback of coniferous stands in central europe – a cbm-cfs3 model application.* Carbon Balance and Management, preprint.

CNB. (2024). Global economic outlook. Retrieved May, 2024, from https://www.cnb.cz/export/sites/cnb/en/monetary-policy/.galleries/geo/geo_2024/gev_2024_04_en.pdf (Czech National Bank)

Cooban, A. (2023). *Head of opec warns of a 'dangerous' lack of investment in oil.* Retrieved April, 2024, from https://edition.cnn.com/2023/10/02/energy/opec-dangerous-lack-oil-investment-oil-prices/index.html

CZSO. (2017). *Spotřeba paliv a energií v domácnostech.* (Czech Satitistical Office - ENERGO 2015 data. Retrieved June, 2020, from https://www.czso.cz/csu/czso/spotreba-paliv-a-energii-v-domacnostech)

CZSO. (2019). *Indexy cen v lesnictví.* (Czech Satitistical Office Retrieved August, 2023, from https://www.czso.cz/csu/czso/indexy-cen-v-lesnictvi-surove-drivi-4-ctvrtleti-2019)

Darko, E. (2014, October). *Short guide summarising the oil and gas industry lifecycle for a non-technical audience* (Research Paper). Overseas Development Institute.

Retrieved January, 2025, from https://assets.publishing.service.gov.uk/media/57a089efed915d3cfd0004d4/Short_guide_summarising_the_oil_and_gas_industry_lifecycle-43.pdf

Dornbusch, R. (1976). Exchange rate expectations and monetary policy. *Journal of International Economics*, *6*(3), 231–244.

DSIRE. (2019a). *Modified accelerated cost-recovery system.* U.S. Department of Energy. Retrieved February, 2019, from http://programs.dsireusa.org/system/program/detail/676

DSIRE. (2019b). *Renewable portfolio standards.* U.S. Department of Energy. Retrieved May, 2019, from http://www.dsireusa.org/resources/detailed-summary-maps/

Dykes, K. (2015). *New Cost and Scaling Model.* National Renewable Energy Laboratory. GitHub. (Retrieved February, 2019, from https://github.com/WISDEM/Turbine_CostsSE)

EIA. (1983-2023). *Short-term energy outlooks.* Retrieved February, 2023, from https://www.eia.gov/outlooks/steo/outlook.php (EIA-STEO, U.S. Department of Energy)

EIA. (2022). *Global surplus crude oil production capacity 1970–2021.* Retrieved March, 2024, from https://www.eia.gov/international/analysis/special-topics/Global_Surplus_Crude_Oil_Production_Capacity (U.S. Department of Energy)

EIA. (2023a). *International energy outlook.* Retrieved March, 2023, from https://www.eia.gov/outlooks/ieo/ (U.S. Department of Energy)

EIA. (2023b). *Oil and petroleum products explained oil prices and outlook.* Retrieved March, 2024, from https://www.eia.gov/energyexplained/oil-and-petroleum-products/prices-and-outlook.php#:~:text=The%20U.S.%20Energy%20Information%20Administration,its%20maximum%20oil%20production%20capacity (U.S. Department of Energy)

EIA. (2023c). *What drives crude oil prices?* Retrieved March, 2023, from https://www.eia.gov/finance/markets/crudeoil/supply-opec.php (U.S. Department of Energy)

EIA. (2024a). *Short-term energy outlook: Crude oil price forecast.* Retrieved February, 2024, from https://www.eia.gov/analysis/handbook/pdf/STEO_Crude_Oil_Price.pdf (U.S. Department of Energy)

EIA. (2024b). *Total world crude oil production.* Retrieved August, 2024, from https://www.eia.gov/outlooks/steo/data/browser/#/?v=30&f=A&s=&start=1997&end=2025&id=&maptype=0&ctype=linechart&linechart=COPR_WORLD (U.S. Department of Energy)

EIA. (2024c). *U.S. crude oil production.* Retrieved August, 2024, from https://www.eia.gov/dnav/pet/pet_crd_crpdn_adc_mbbl_m.htm (U.S. Department of Energy)

ERU. (2019a). *Roční zpráva o provozu elektrizační soustavy ČR.* (Retrieved May, 2022, from https://www.eru.cz/rocni-zprava-o-provozu-elektrizacni-soustavy-cr-pro-rok-2019)

ERU. (2019b). *Roční zpráva o provozu teplárenských soustav ČR.* (Retrieved May, 2022, from https://www.eru.cz/rocni-zprava-o-provozu-teplarenskych-soustav-cr-za-rok-2019)

European Comission. (2021). *Questions and answers - the effort sharing regulation and*

land, forestry and agriculture regulation. (Retrieved August, 2023, from https://ec.europa.eu/commission/presscorner/detail/en/qanda_21_3543)

European Comission Directorate-General Climate Action. (2023). *Recommended parameters for reporting on ghg projections in 2023.* ([Report])

EWEA. (2012). *Wind energy-the facts: a guide to the technology, economics and future of wind power*. Routledge.

Federal Energy Regulatory Commission. (2015). *Energy primer: A handbook of energy market basics.* Federal Energy Regulatory Commission: Washington, DC, USA.

Federal Energy Regulatory Commission. (2019). *Electric power markets: National overview.* (Retrieved May, 2019, from https://www.ferc.gov/market-oversight/mkt-electric/overview.asp)

Fingersh, L. J., Hand, M. M., & Laxson, A. S. (2006). *Wind turbine design cost and scaling model.* National Renewable Energy Laboratory. Report No. NREL/TP-500-40566.

Fleming, S., & Arnold, M. (2024). *Central banks should set a 'high bar' for interest rate cuts, BIS warns.* Financial Times. Retrieved August, 2024, from https://www.ft.com/content/cef32cf8-d10c-4f09-8e1b-eeec9ca12733

Fodstad, M., del Granado, P. C., Hellemo, L., Knudsen, B. R., Pisciella, P., Silvast, A., ... Straus, J. (2022). Next frontiers in energy system modelling: A review on challenges and the state of the art. *Renewable and Sustainable Energy Reviews*, *160*, 112246.

Global Wind Energy Council. (2019). *Global Wind Report 2018.* (Retrieved May, 2019, from https://gwec.net/wp-content/uploads/2019/04/GWEC-Global-Wind-Report-2018.pdf)

Goodhart, C. (2023). Should central banks abandon single point forecasts? Retrieved May, 2024, from https://cepr.org/voxeu/columns/should-central-banks-abandon-single-point-forecasts

Goodhart, C., & Pradhan, M. (2020). The great demographic reversal and its effect on future growth. *The Great Demographic Reversal: Ageing Societies, Waning Inequality, and an Inflation Revival*, 41–51.

Grafström, J., & Lindman, Å. (2017). Invention, innovation and diffusion in the European wind power sector. *Technological Forecasting and Social Change*, *114*, 179-191.

Greenspan, A. (2004). Risk and uncertainty in monetary policy. Retrieved May, 2024, from https://www.federalreserve.gov/boarddocs/speeches/2004/20040103/default.htm (Meetings of the American Economic Association, San Diego, California)

Hamilton, J. D. (2009). Understanding crude oil prices. *The energy journal*, *30*(2).

Hayward, J. A., & Graham, P. W. (2013). A global and local endogenous experience curve model for projecting future uptake and cost of electricity generation technologies. *Energy Economics*, *40*, 537-548.

Helbling, T., Kang, J., Kumhof, M., Muir, D., Pescatori, A., & Roache, S. (2011). Oil scarcity, growth, and global imbalances. *World economic outlook*, *1*, 89–124.

Hemami, A. (2012). *Wind Turbine Technology.* Cengage Learning.

Hirsch, B. R. W. R., R. (2005). *Peaking of world oil production: Impacts, mitigation, and risk management* (Technical Report). U.S. Department of Energy, National Energy Technology Laboratory.

Hlásny, T., König, L., Krokene, P., Lindner, M., Montagné-Huck, C., Müller, J., ... others (2021). Bark beetle outbreaks in europe: state of knowledge and ways forward for management. *Current Forestry Reports*, *7*, 138–165.

Hlásny, T., Zimová, S., Merganičová, K., Štěpánek, P., Modlinger, R., & Turčáni, M. (2021). Devastating outbreak of bark beetles in the czech republic: Drivers, impacts, and management implications. *Forest Ecology and Management*, *490*, 119075.

Holttinen, H., Meibom, P., Orths, A., Lange, B., O'Malley, M., Tande, J. O., ... others (2011). Impacts of large amounts of wind power on design and operation of power systems, results of iea collaboration. *Wind Energy*, *14*(2), 179–192.

Hörsch, J., & Brown, T. (2017). The role of spatial scale in joint optimisations of generation and transmission for european highly renewable scenarios. In *2017 14th international conference on the european energy market (eem)* (pp. 1–7).

Hotelling, H. (1931). *The economics of exhaustible resources. journal of political economy.* vol.

Hubbert, M. K. (1956). Darcy's law and the field equations of the flow of underground fluids. *Transactions of the AIME*, *207*(01), 222–239.

Huenteler, J., Schmidt, T. S., Ossenbrink, J., & Hoffmann, V. H. (2016). Technology life-cycles in the energy sector—technological characteristics and the role of deployment for innovation. *Technological Forecasting and Social Change*, *104*, 102-121.

Höök, M. (2014). Depletion rate analysis of fields and regions: A methodological foundation. *Fuel*, *121*, 95–108. Retrieved from https://doi.org/10.1016/j.fuel.2013.12.024 doi: 10.1016/j.fuel.2013.12.024

Ibenholt, K. (2002). Explaining learning curves for wind power. *Energy Policy*, *30*(13), 1181–1189.

IEA. (2023). World energy outlook 2023. Retrieved March, 2024, from https://www.iea.org/reports/world-energy-outlook-2023

IMF. (2024). World economic outlook database. Retrieved August, 2024, from https://www.imf.org/en/Publications/WEO/weo-database/2024/April

International Energy Agency. (1991-2018). IEA Wind Technology Collaboration Programme Annual Reports. Paris, France.

International Energy Forum and S&P Global Commodity Insights. (2024). Upstream oil and gas investment outlook. Retrieved August, 2024, from https://www.ief.org/focus/ief-reports/upstream-oil-and-gas-investment-outlook-2024

Janová, J., Hampel, D., Kadlec, J., & Vrška, T. (2022). Motivations behind the forest managers' decision making about mixed forests in the Czech Republic. *Forest Policy and Economics*, *144*, 102841.

Junginger, M., Faaij, A., & Turkenburg, W. C. (2005). Global experience curves for wind farms. *Energy policy*, *33*(2), 133–150.

Kilian, L. (2009). Not all oil price shocks are alike: Disentangling demand and supply shocks in the crude oil market. *American Economic Review*, *99*(3), 1053–1069.

King, M. A. (2024). *Inflation targets: Practice ahead of theory* (Working Paper No. 32594). National Bureau of Economic Research. Retrieved from https://www.nber.org/papers/w32594

Knápek, J., Králík, T., Vávrová, K., & Weger, J. (2020). Dynamic biomass potential from agricultural land. *Renewable and Sustainable Energy Reviews*, *134*, 110319.

Kobos, P. H., Erickson, J. D., & Drennen, T. E. (2006). Technological learning and renewable energy costs: implications for US renewable energy policy. *Energy policy*, *34*(13), 1645–1658.

Kostanyan, A., Matinyan, A., Papikyan, A., Avagyan, V., Avetisyan, H., Galstyan, M., ... others (2022). *Getting fit with imperfect policy credibility. dynare/julia workshops with an application for the us economy* (Tech. Rep.). CBA Working Paper 2022/04.

Laxton, D., Isard, P., Faruqee, H., Prasad, E., & Turtelboom, B. (1998, May). *Multimod mark iii: The core dynamic and steady-state models* (IMF Occasional Paper No. 164). International Monetary Fund. Retrieved from https://www.imf.org/external/pubs/ft/op/op164/index.htm

Laxton, D., & N'Diaye, P. (2002, December). *Monetary policy credibility and the unemployment-inflation tradeoff: Some evidence from 17 industrial countries* (IMF Working Paper No. 02/220). International Monetary Fund. Retrieved from https://www.imf.org/en/Publications/WP/Issues/2016/12/30/Monetary-Policy-Credibility-and-the-Unemployment-Inflation-Tradeoff-Some-Evidence-From-17-16093 doi: 10.5089/9781451875218.001

Laxton, D., Ricketts, N., & Rose, D. (1994). Uncertainty, learning and policy credibility. *Economic Behaviour and Policy Choice Under Price Stability*, 173–226.

Lorenc, F. (2022). Škodliví činitelé v lesích Česka 2021/2022. *Výzkumný ústav lesního hospodářství a myslivosti, v. v. i. Lesní ochranná služba, Ministerstvo zemědělství*.

Loulou, R., Goldstein, G., & Noble, K. (2004). *Documentation for the markal family of models* (Technical Report). Energy Technology Systems Analysis Program (ETSAP).

Lozano-García, D. F., Santibañez-Aguilar, J. E., Lozano, F. J., & Flores-Tlacuahuac, A. (2020). Gis-based modeling of residual biomass availability for energy and production in mexico. *Renewable and Sustainable Energy Reviews*, *120*, 109610.

Lyčka, Z. (2010). *Náklady na vytápění dřevními peletami.* (Retrieved June, 2022, from https://oze.tzb-info.cz/biomasa/6263-naklady-na-vytapeni-drevnimi-peletami)

Maimó-Far, A., Homar, V., Tantet, A., & Drobinski, P. (2022). The effect of spatial granularity on optimal renewable energy portfolios in an integrated climate-energy assessment model. *Sustainable Energy Technologies and Assessments*, *54*, 102827.

Malcolm, D. J., & Hansen, A. C. (2002). *Windpact turbine rotor design study.* Golden, CO, 5: National Renewable Energy Laboratory.

Martínez-Gordón, R., Morales-España, G., Sijm, J., & Faaij, A. (2021). A review of the role of spatial resolution in energy systems modelling: Lessons learned and applicability to the north sea region. *Renewable and Sustainable Energy Reviews*, *141*, 110857.

McKenna, R., Hollnaicher, S., & Fichtner, W. (2014). Cost-potential curves for onshore wind energy: A high-resolution analysis for Germany. *Applied Energy*, *115*, 103–115.

Milligan, M., & Kirby, B. (2009). *Calculating wind integration costs: Separating wind energy value from integration cost impacts* (Tech. Rep.). National Renewable Energy Lab.(NREL), Golden, CO (United States).

Ministry of Industry and Trade. (2020). *Dlouhodobá strategie renovací na podporu renovace vnitrostátního fondu obytných a jiných než obytných budov, veřejných i soukromých.* (Retrieved September, 2023, from https://www.mpo.cz/cz/energetika/energeticka-ucinnost/strategicke-dokumenty/

dlouhodoba-strategie-renovaci-budov--255200/)
Ministry of Industry and Trade. (2021). *Energy balance of the czech republic 2019.* (Retrieved June, 2023, from https://www.mpo.cz/cz/energetika/statistika/energeticke-bilance/souhrnna-energeticka-bilance-statu-v-metodice-eurostatu-za-leta-2010_2020--265192/)
Ministry of Industry and Trade. (2021). *Regional energy balance of the czech republic.* (Retrieved September, 2023, from https://www.mpo.cz/cz/energetika/statistika/energeticke-bilance/krajske-energeticke-bilance--260319)
Mone, C., Hand, M., Bolinger, M., Rand, J., Heimiller, D., & Ho, J. (2017). *2015 Cost of Wind Energy Review.* Golden, CO 80401: National Renewable Energy Laboratory.
Mone, C., Smith, A., Maples, B., & Hand, M. (2015). *2013 Cost of Wind Energy Review* (Tech. Rep.). National Renewable Energy Laboratory (NREL), Golden, CO (United States).
Monforti, F., Huld, T., Bódis, K., Vitali, L., D'isidoro, M., & Lacal-Arántegui, R. (2014). Assessing complementarity of wind and solar resources for energy production in italy. a monte carlo approach. *Renewable Energy*, *63*, 576–586.
Natural Resources Canada. (2014). *Learn the facts: Emissions from your vehicle.* (Retrieved JuLy, 2023, from https://natural-resources.canada.ca/sites/www.nrcan.gc.ca/files/oee/pdf/transportation/fuel-efficient-technologies/autosmart_factsheet_9_e.pdf)
NREL. (2011-2018). *Cost of Wind Energy Review.* US Department of Energy.
NREL. (2015a). *AEP Model.* National Renewable Energy Laboratory. GitHub. (Retrieved February, 2019, from https://github.com/WISDEM/nrel_csm)
NREL. (2015b). *BOS model.* GitHub. (Retrieved February, 2019, from https://github.com/WISDEM/Plant_CostsSE)
OPEC. (2023a). 2023 world oil outlook 2045. Retrieved March, 2023, from https://woo.opec.org/
OPEC. (2023b). *Several opec+ countries announce additional voluntary cuts to the total of 2.2 million barrels per day.* Retrieved March, 2024, from https://www.opec.org/pr-detail/39-30-nov-2023.html (Press releases)
Open Energy Information. (2019). *Energy generation facilities.* (Retrieved April, 2019, from https://openei.org/wiki/Category:Energy_Generation_Facilities)
Pfenninger, S., & Staffell, I. (2016). Long-term patterns of european pv output using 30 years of validated hourly reanalysis and satellite data. *Energy*, *114*, 1251–1265.
Pierru, A., Smith, J., & Zamrik, T. (2018). Opec's impact on oil price volatility: The role of spare capacity. *The Energy Journal*, *39*(2), 173–196.
Pierru, A., Smith, J. L., & Almutairi, H. (2020). Opec's pursuit of market stability. *Economics of Energy & Environmental Policy*, *9*(2), 51–70.
Poore, R., & Lettenmaier, T. (2000-2002). *Alternative Design Study Report: WindPACT Advanced Wind Turbine Drive Train Designs Study.* Golden, CO, 5: National Renewable Energy Laboratory, NREL/SR-500-33196.
Qiu, Y., & Anadon, L. D. (2012). The price of wind power in China during its expansion: Technology adoption, learning-by-doing, economies of scale, and manufacturing localization. *Energy Economics*, *34*(3), 772-785.

Ramadhan, M., & Naseeb, A. (2011). The cost benefit analysis of implementing photovoltaic solar system in the state of Kuwait. *Renewable Energy*, *36*(4), 1272–1276.

Ramirez Camargo, L., & Stoeglehner, G. (2018). Spatiotemporal modelling for integrated spatial and energy planning. *Energy, Sustainability and Society*, *8*, 1–29.

Rečka, L., Máca, V., & Ščasnỳ, M. (2023). Green deal and carbon neutrality assessment of czechia. *Energies*, *16*(5), 2152.

Rečka, L., & Ščasnỳ, M. (2016). Impacts of carbon pricing, brown coal availability and gas cost on czech energy system up to 2050. *Energy*, *108*, 19–33.

Rečka, L., & Ščasnỳ, M. (2017). Impacts of reclassified brown coal reserves on the energy system and deep decarbonisation target in the czech republic. *Energies*, *10*(12), 1947.

Rečka, L., & Ščasnỳ, M. (2018). Brown coal and nuclear energy deployment: Effects on fuel-mix, carbon targets, and external costs in the czech republic up to 2050. *Fuel*, *216*, 494–502.

Resch, B., Sagl, G., Törnros, T., Bachmaier, A., Eggers, J.-B., Herkel, S., ... Gündra, H. (2014). Gis-based planning and modeling for renewable energy: Challenges and future research avenues. *ISPRS International Journal of Geo-Information*, *3*(2), 662–692.

Roques, F., Hiroux, C., & Saguan, M. (2010). Optimal wind power deployment in europe—a portfolio approach. *Energy policy*, *38*(7), 3245–3256.

Rystad Energy. (2023). Claims of underinvestment in the global oil and gas industry are overblown amid efficiency gains. Retrieved August, 2024, from https://www.rystadenergy.com/news/underinvestment-global-oil-gas-industry-overblown-efficiency-prices

Sarfarazi, S., Sasanpour, S., & Cao, K.-K. (2023). Improving energy system design with optimization models by quantifying the economic granularity gap: The case of prosumer self-consumption in germany. *Energy Reports*, *9*, 1859–1874.

Sorrell, S., Speirs, J., Bentley, R., Brandt, A., & Miller, R. (2010). Global oil depletion: A review of the evidence. *Energy Policy*, *38*(9), 5290–5295.

Stehly, T. J., Beiter, P. C., Heimiller, D. M., & Scott, G. N. (2018). *2017 Cost of Wind Energy Review* (Tech. Rep.). National Renewable Energy Lab.(NREL), Golden, CO (United States).

Stolarski, M. J., Stachowicz, P., Sieniawski, W., Krzyżaniak, M., & Olba-Zięty, E. (2021). Quality and delivery costs of wood chips by railway vs. road transport. *Energies*, *14*(21), 6877.

Tang, T., & Popp, D. (2016). The learning process and technological change in wind power: evidence from China's CDM wind projects. *Journal of Policy Analysis and Management*, *35*(1), 195-222.

Technical University of Denmark. (2017). *Global Wind Atlas 2.0.* (Retrieved August, 2019, from https://globalwindatlas.info/)

The US Geological Survey, the Berkeley Lab, & the American Wind Energy Association. (2016). *The United States Wind Turbine Database.* (Retrieved May, 2019, from https://eerscmap.usgs.gov/uswtdb/data/)

The Wind Power. (2019). *USA Wind Farms.* (Retrieved April, 2019, from https://www.thewindpower.net/windfarms_list_en.php)

Tran, T. T., & Smith, A. D. (2017). fevaluation of renewable energy technologies and their potential for technical integration and cost-effective use within the us energy sector.

Renewable and Sustainable Energy Reviews, *80*, 1372–1388.

Tullow Oil plc. (2024, April). *Oil life cycle.* Retrieved April, 2024, from https://www.tullowoil.com/about-us/oil-life-cycle/

TZB-info. (2022). *Přehled energetických plodin, jejich vlastnosti a přepočty jednotek.* (Retrieved June, 2022, from https://www.tzb-info.cz/tabulky-a-vypocty/98-prehled-energetickych-plodin-jejich-vlastnosti-a-prepocty-jednotek)

U.S. Bureau of Economic Analysis. (2018). *Gross domestic product (implicit price deflator).* (Retrieved March, 2018, from https://fred.stlouisfed.org/series/A191RD3A086NBEA)

U.S. Energy Information Administration. (1998-2017). *Form EIA-860 database.* (Retrieved May, 2019, from https://www.eia.gov/electricity/data/eia860/)

Vytečka, L. (2016). *Logistika výrobního procesu zaměřeno na skladování nákladu a přepravu dřevní Štěpky.* (Dřevošrot a.s. Retrieved July, 2023, from https://docplayer.cz/3301723-Logistika-vyrobniho-procesu-zamereno-na-skladovani-nakladku-a-prepravu-drevni-stepky-drevosrot-a-s.html)

Wachtmeister, H., & Höök, M. (2020). Investment and production dynamics of conventional oil and unconventional tight oil: Implications for oil markets and climate strategies. *Energy and Climate Change*, *1*, 100010.

Wang, J., & Rakha, H. A. (2017). Fuel consumption model for heavy duty diesel trucks: Model development and testing. *Transportation Research Part D: Transport and Environment*, *55*, 127–141.

White, W. (2023). *The new age of scarcity: How we can adapt.* Retrieved January, 2025, from https://williamwhite.ca/2023/12/10/the-new-age-of-scarcity-how-we-can-adapt/ (Published on the author's personal website)

Wiebe, K. S., & Lutz, C. (2016). Endogenous technological change and the policy mix in renewable power generation. *Renewable and Sustainable Energy Reviews*, *60*, 739-751.

Wiser, R., & Bolinger, M. (2008-2018). *Wind technologies market report.*

Wiser, R., & Bolinger, M. (2018). 2017 wind technologies market report. *US Department of Energy.*. (Retrieved October, 2018, from https://www.energy.gov/eere/wind/downloads/2017-wind-technologies-market-report)

Yang, Q., Huang, T., Wang, S., Li, J., Dai, S., Wright, S., ... Peng, H. (2019). A gis-based high spatial resolution assessment of large-scale pv generation potential in china. *Applied Energy*, *247*, 254–269.

Yu, Y., Li, H., Che, Y., & Zheng, Q. (2017). The price evolution of wind turbines in China: A study based on the modified multi-factor learning curve. *Renewable Energy*, *103*, 522-536.

Zhang, B., Hastings, A., Clifton-Brown, J. C., Jiang, D., & Faaij, A. P. (2020). Modeled spatial assessment of biomass productivity and technical potential of miscanthus× giganteus, panicum virgatum l., and jatropha on marginal land in china. *GCB Bioenergy*, *12*(5), 328–345.